

THE ROLES OF CELLULAR INHIBITOR OF APOPTOSIS PROTEINS 1 AND 2 IN  
THE POLARIZATION OF M1 AND M2 MACROPHAGES

by

Alixandra J. Lammie

Submitted in partial fulfilment of the requirements  
for the degree of Master of Science

at

Dalhousie University  
Halifax, Nova Scotia  
August 2017

© Copyright by Alixandra J. Lammie, 2017

*For my Family.*

# TABLE OF CONTENTS

<b>LIST OF TABLES .....</b>	<b>vii</b>
<b>LIST OF FIGURES .....</b>	<b>viii</b>
<b>ABSTRACT .....</b>	<b>xi</b>
<b>LIST OF ABBREVIATIONS USED.....</b>	<b>xii</b>
<b>ACKNOWLEDGEMENTS .....</b>	<b>xvii</b>
<b>CHAPTER 1: INTRODUCTION.....</b>	<b>1</b>
1.1 Macrophage function in health and disease .....	1
1.2 M1 and M2 macrophage polarization .....	2
1.3 M1 and M2 macrophage markers .....	3
1.4 Cellular inhibitor of apoptosis 2 (cIAP2) and second mitochondria-derived activator of caspases (SMAC) .....	4
1.5 cIAP1/2 promote macrophage survival .....	6
1.6 Pro-survival and pro-death signaling by the canonical and non-canonical NF- $\kappa$ B pathways .....	7
1.7 Experimental autoimmune encephalomyelitis mouse model of multiple sclerosis.....	11
1.8 Rationale: Use of genetic cIAP2 ablation or LCL161-induced cIAP1/2 suppression to understand the roles of these anti-apoptotic proteins in M1 and M2 macrophage polarization .....	12
1.9 Central hypothesis.....	14
1.10 Research aims .....	14
<b>CHAPTER 2: MATERIAL &amp; METHODS.....</b>	<b>16</b>
2.1 Bone marrow extraction and cytokine treatments to promote mild or strong M1 or M2 macrophage polarization .....	16
2.2 Treatment of bone marrow derived macrophages with the SMAC mimetic LCL161 .....	19

2.3 LPS-induced cell death .....	19
2.4 Immunopanning .....	19
2.5 Quantitative Real Time Polymerase Chain Reaction (qRT-PCR).....	22
2.6 Flow Cytometry .....	24
2.7 Western Blotting.....	25
2.8 Experimental Autoimmune Encephalomyelitis (EAE).....	26
2.9 Care of EAE mice.....	27
2.10 Tissue Collection and Analysis.....	27
2.11 Multiplexed enzyme-linked immunosorbent assays.....	28
<b>CHAPTER 3: RESULTS .....</b>	<b>29</b>
3.1 cIAP2 ablation reduced macrophage generation from BMDMs cultured under mild M1 polarizing conditions.....	29
3.2 cIAP2 null BMDMs exposed to strong M2 polarizing conditions displayed reduced macrophage generation relative to WT cultures .....	29
3.3 cIAP2 ablation increased BMDM apoptosis under strong M2 polarizing conditions.....	33
3.4 cIAP2 deficiency impaired BMDM differentiation by strong M1 and M2 polarizing conditions.....	35
3.5 Macrophage selection of BMDM cultures by immunopanning .....	38
3.6 cIAP2 null mpBMDMs displayed enhanced M1 and M2 marker expression under M2 polarizing conditions.....	41
3.7 cIAP1 and cIAP2 protein levels were reduced in WT BMDMs treated with LCL161 .....	44
3.8 Immunopanning also reduced macrophage percentages in the supernatants of cultures treated with LCL161 .....	46
3.9 Acute suppression of cIAP1/2 levels with LCL161 induced a bias towards M1 polarization.....	48

3.10 Acute suppression of cIAP1/2 levels with LCL161 enhanced apoptosis in BMDMs cultured under strong M2 polarizing conditions .....	50
3.11 EAE mice dosed with LCL161 exhibited increased disease severity.....	52
3.12 LCL161 administration enhanced CD38 expression in the spinal cords of EAE mice.....	54
3.13 LCL161 suppressed both Th1 and Th2 cytokine concentrations in EAE mice.....	57
3.14 LCL161 treatment increased Ly6C <sup>Lo</sup> monocytes in EAE mice .....	62
3.15 Treatment with LCL161 increased BMDM necrosis in cultures exposed to a lethal concentration of LPS.....	64
<b>CHAPTER 4: DISCUSSION .....</b>	<b>66</b>
4.1 Determining the effects of cIAP2 suppression on M1 and M2 macrophage polarization .....	66
4.2 cIAP2 deficiency impaired the generation of macrophages in BMDMs cultured under mild M1 or strong M2 polarizing conditions.....	67
4.3 Ablation of cIAP2 biases the polarization of BMDMs to an M2-like state .....	68
4.4 Immunopanning of BMDM cultures to isolate macrophages.....	68
4.5 Strong M1 or M2 polarizing conditions have distinct effects on M1 and M2 mRNA expression profiles in non-immunopanned and immunopanned BMDMs .....	69
4.6 Suppression of cIAP1/2 protein levels in BMDMs with the SMAC mimetic LCL161 induced an M1 macrophage polarization bias.....	71
4.7 LCL161 massively increased the apoptosis of macrophages in BMDMs cultured under strong M2 polarizing conditions.....	72
4.8 Oral administration of LCL161 increased EAE disease severity .....	73
4.9 LCL161 increased CD38 expression in the spinal cords and suppressed plasma Th1 and Th2 cytokine concentrations for EAE mice .....	73
4.10 LCL161 treatment did not alter levels of Ly6C <sup>Hi</sup> monocytes but increased Ly6C <sup>Lo</sup> monocytes in EAE mice.....	75

4.11 Suppression of cIAP1/2 levels with LCL161 converted the mode of cell death for LPS-treated BMDMs from apoptosis to necrosis.....	76
4.12 NF- $\kappa$ B pathway involvement in macrophage polarization and survival .....	77
4.13 Regulation of dendritic cell and neutrophil cell function by cIAP1/2 .....	79
4.14 The potential role of cIAP1/2 in oligodendrocyte cell survival.....	80
4.15 Conclusions.....	81
<b>REFERENCES.....</b>	<b>84</b>

## LIST OF TABLES

<b>TABLE 1:</b> Forward and reverse primer sequences for M1/M2 markers, reference genes and others.....	23
---	----

## LIST OF FIGURES

<b>FIGURE 1:</b> Regulation by cIAP1/2 of TNRF1-mediated activation of complex I and complexes IIa and IIb.....	10
<b>FIGURE 2:</b> Schematic representation of the cell culture protocol.....	18
<b>FIGURE 3:</b> Experimental protocol to select for macrophages in BMDMs cultures by immunopanning with the F4/80 antibody.....	21
<b>FIGURE 4:</b> Flow cytometry analyses of WT and cIAP2 null BMDMs double-labelled with antibodies against CD11b and F4/80 that were cultured under mild M1 (GM-CSF) or M2 (M-CSF) polarizing conditions.....	31
<b>FIGURE 5:</b> Flow cytometry analyses of WT and cIAP2 null BMDMs double-labelled with antibodies against CD11b and F4/80 that were cultured under strong M1 (GM-CSF+LPS) or M2 (M-CSF+IL-4) polarizing conditions.....	32
<b>FIGURE 6:</b> Flow cytometry analyses of Annexin V positive WT and cIAP2 null macrophages detected in BMDMs cultured under mild M1 (GM-CSF), strong M1 (GM-CSF+LPS), mild M2 (M-CSF) or strong M2 (M-CSF+IL-4) polarizing conditions.....	34
<b>FIGURE 7:</b> M1 (A and C) and M2 (B, D and E) marker mRNA levels for WT and cIAP2 null BMDMs cultured under strong M1 (GM-CSF+LPS) or M2 (M-CSF+IL-4) polarizing conditions expressed relative to BMDMs exposed to mild M1 (GM-CSF) or M2 (M-CSF) polarizing conditions, respectively.....	36
<b>FIGURE 8:</b> cIAP2 mRNA levels for BMDMs grown under strong M1 (GM-CSF+LPS) or M2 (M-CSF+IL-4) polarizing conditions expressed relative to cultures maintained under mild M1 (GM-CSF) or M2 (M-CSF) polarizing condition, respectively.....	37
<b>FIGURE 9:</b> Flow cytometry analyses of macrophages double-positive for CD11b and F4/80 in the supernatant of non-immunopanned and immunopanned BMDMs.....	40
<b>FIGURE 10:</b> M1 marker (A, C and E), M2 marker (B, D, and F) and cIAP2 (G) mRNA levels for WT and cIAP2 null mpBMDMs selected by immunopanning from BMDM cultures grown under strong M1 (GM-CSF+LPS) or M2 (M-CSF+IL-4) polarizing conditions expressed relative to mpBMDMs exposed to mild M1 (GM-CSF) or M2 (M-CSF) polarizing conditions, respectively.....	43
<b>FIGURE 11:</b> Effects of treatment with the SMAC-mimetic LCL161 (10 $\mu$ M) for 24 hr on cIAP1/2 levels in BMDMs.....	45

<b>FIGURE 12:</b> Flow cytometry analyses of macrophages double-positive for CD11b and F4/80 in the supernatant of non-immunopanned and immunopanned WT BMDMs treated with LCL161 (10 $\mu$ M) for 24 hr .....	47
<b>FIGURE 13:</b> M1 marker (A, C and E), M2 marker (B, D, and F) and cIAP2 (G) mRNA levels for vehicle and LCL161 treated mpBMDMs obtained from cultures grown under strong M1 (GM-CSF+LPS) or M2 (M-CSF+IL-4) polarizing conditions.....	49
<b>FIGURE 14:</b> The apoptosis marker Annexin V was used to assess the effects of treatment for 24 hr with the SMAC-mimetic LCL161 (10 $\mu$ M) on WT BMDMs cultured under mild M1, strong M1, mild M2 or strong M2 polarizing conditions .....	51
<b>FIGURE 15:</b> Clinical scores for EAE mice orally gavaged with vehicle (100 $\mu$ l) or LCL161 (50 mg/kg) once every 3 days from DPI 1-15 (A) or DPI 8-30 (B), n=9-12/group.....	53
<b>FIGURE 16:</b> Effects of oral administration of vehicle (blue bars) or LCL161 (green bars) on spinal cord M1 marker mRNA levels (A-F) for CFA and EAE mice at DPI 15 .....	55
<b>FIGURE 17:</b> Effects of oral administration of vehicle (blue bars) or LCL161 (green bars) on spinal cord M2 marker (A-C) and chemoattractant MCP-1 (D) mRNA levels in CFA and EAE mice at DPI 15 .....	56
<b>FIGURE 18:</b> Effects of oral administration of vehicle (blue bars) or LCL161 (green bars) on plasma concentrations for the pro-inflammatory Th1 cytokines TNF- $\alpha$ , IFN- $\gamma$ , IL-1 $\alpha$ , IL-1 $\beta$ , IL-12p40, IL-12p70 and IL-17A (A-G) in CFA and EAE mice at DPI 15.....	58
<b>FIGURE 19:</b> Effects of oral administration of vehicle (blue bars) or LCL161 (green bars) on plasma concentrations for the Th2 anti-inflammatory cytokines IL-10, IL-13 and IL-5 (A-C) in CFA and EAE mice at DPI 15 .....	59
<b>Figure 20:</b> Effects of oral administration of vehicle (blue bars) or LCL161 (green bars) on plasma concentrations for the growth and differentiation cytokines IL-6, IL-3 and GM-CSF (A-C) in CFA and EAE mice at DPI 15.....	60
<b>Figure 21:</b> Effects of oral administration of vehicle (green bars) or LCL161 (blue bars) on plasma concentrations for the for CXCL1, CCL2, CCL3, CCL4, CCL5 and Eotaxin (A-F) in CFA and EAE mice at DPI 15.....	61
<b>Figure 22:</b> A) Flow cytometry protocol for the detection of Ly6CHi and Ly6CLO monocytes isolated from the spleens of EAE mice treated with vehicle or LCL161 .....	63

**FIGURE 23:** Effects of exposure to a lethal concentration of LPS (10 µg/ml) for 4 hr on the apoptosis and necrosis of BMDMs cultured under mild M1, strong M1, mild M2 or strong M2 polarizing conditions that were treated with vehicle or LCL161 ..... 65

## ABSTRACT

This thesis examined the effects of genetic ablation of the anti-apoptotic protein cIAP2 and SMAC mimetic (LCL161)-induced cIAP1 and cIAP2 suppression on the polarization of pro-inflammatory (M1) and anti-inflammatory (M2) macrophages. Quantitative RT-PCR was employed to measure M1 and M2 mRNA markers in bone marrow derived macrophages (BMDMs) cultured under mild or strong M1 or M2 polarizing conditions. These measurements indicated that cIAP2 loss impaired both M1 and M2 polarization. Macrophage isolation by immunopanning suggested that cIAP2 loss also impaired dendritic cell polarization. LCL161 increased M1 mRNA marker levels in strongly M1 polarized macrophages. By contrast, LCL161 induced the massive apoptosis of strongly M2 polarized macrophages. Hence, cIAP1/2 suppression biased macrophage polarization *in vitro* towards a pro-inflammatory M1 state. LCL161 increased the severity of experimental autoimmune encephalomyelitis and suppressed both Th1 and Th2 cytokine plasma concentrations suggestive of impaired M1 and M2 polarization. SMAC mimetics may therefore worsen multiple sclerosis.

## LIST OF ABBREVIATIONS USED

7-AAD	7-Aminoactinomycin D
Ala-Val-Pro-Ile	Alanine-Valine-Proline-Isoleucine
ANI	Apoptotic Necrotic Index
APCs	Antigen Presenting Cells
Arg-1	Arginase-1
B2M	Beta-2-Microglobulin
BBB	Blood Brain Barrier
BIR	Baculoviral IAP Repeat
BIRC	Baculoviral IAP Repeat-Containing Protein
BMDMs	Bone Marrow Derived Macrophages
BRUCE	BIR Repeat-Containing Ubiquitin-Conjugating Enzyme
c-Myc	Myelocytomatosis viral oncogene homolog
CARD	Caspase Activation and Recruitment Domains
CCL	Chemokine (C-C motif) Ligand
CD	Cluster of Differentiation
cDNA	Complementary Deoxyribonucleic Acid
CFA	Complete Freud's Adjuvant
cIAP	Cellular Inhibitor of Apoptosis
CNS	Central Nervous System
Cq	Quantification Cycle
CSF-1R	Colony Stimulating Factor-1 Receptor
CXCL	Chemokine (C-X-C motif) Ligand

DC	Dendritic Cells
DIABLO	Direct Inhibitor of Apoptosis-Binding Protein with low pl
DKO	Double Knock Out
DMSO	Dimethyl Sulfoxide
DMT	Disease Modifying Therapies
DPI	Days Post Immunization
EAE	Experimental Autoimmune Encephalomyelitis
EDTA	Ethylenediaminetetraacetic Acid
EGF	Epidermal Growth Factor
ELISA	Enzyme-Linked Immunosorbent Assay
Erg2	Early Growth Response Protein 2
FACS	Fluorescence-Activated Cell Sorting
FADD	Fas Associated Death Domain
FBS	Fetal Bovine Serum
FLIP	FLICE-like Inhibitory Protein
Fpr2	Formyl Peptide Receptor 2
g	Grams
G-CSF	Granulocyte Colony Stimulating Factor
GAPDH	Glyceraldehyde 3-Phosphate Dehydrogenase
GM-CSF	Granulocyte Monocyte Colony Stimulating Factor
Gpr18	G-protein Coupled Receptor 18
HPRT	Hypoxanthine-Guanine Phosphoribosyltransferase
hr	Hour

HSCs	Hematopoietic Progenitor Cells
IAP	Inhibitor of Apoptosis
IFN- $\gamma$	Interferon-gamma
IKK	I $\kappa$ B Kinase
IL	Interleukin
ILP	IAP-like Protein
I $\kappa$ B	Inhibitor of kappa B
kb	Kilobase
KC	Keratinocyte Chemoattractant
kDa	Kilodalton
kg	Kilograms
KO	Knock Out
LPS	Lipopolysaccharide
M-CSF	Monocyte Colony Stimulating Factor
mA	Milliamps
MCP	Monocyte Chemoattractant Protein
mg	Miligrams
MHCII	Histocompatibility Complex Class II
min	Minute
MIP	Macrophage Inflammatory Protein
ml	Milliliters
mM	Millimole
MOG	Myelin Oligodendrocyte Glycoprotein

mpBMDMs	macrophage-purified BMDMs
MS	Multiple Sclerosis
n	Sample Size
NAIP	Neuronal Apoptosis Inhibitory Protein
NF H <sub>2</sub> O	Nuclease Free Water
NF-κB	Nuclear Factor kappa-light-chain-enhancer of activated B cells
ng	Nanograms
NIK	NF-kappa-B-Inducing Kinase
NOS	Nitric Oxide Synthase
OPC	Oligodendrocyte Progenitor Cells
PBS	Phosphate Buffered Saline
PTX	Pertussis toxin
qRT-PCR	Quantitative Real-Time Polymerase Chain Reaction
RANTES	Regulated on Activation, Normal T-cell Expressed and Secreted
RING	Really Interesting New Gene
RIP	Receptor-Interacting Protein
RNA	Ribonucleic Acid
ROCK	Rho-associated Protein Kinase
RPMI	Roswell Park Memorial Institute
RQI	RNA Quality Indicator
s	Seconds
sc	Subcutaneous
SMAC	Second Mitochondrial Activator of Caspases

TBS-T	Tris-Buffered Saline-Tween
TGF- $\beta$	Transforming growth factor beta
TLR	Toll Like Receptors
TNF- $\alpha$	Tumour Necrosis Factor-alpha
TNFR	Tumour Necrosis Factor Receptor
TRADD	TNF Receptor type 1-Associated Death Domain
TRAF	TNF Receptor-Associated Factor
WT	Wild-Type
xg	Times Gravity
XIAP	X-linked Inhibitor of Apoptosis Protein
$\mu\text{g}$	Micrograms
$\mu\text{l}$	Microliters
$\mu\text{M}$	Micromole
$\mu\text{m}$	Micrometer (Micron)
~	Approximately
$\Delta$	Delta
%	Percent

## ACKNOWLEDGEMENTS

First and foremost, I would like to thank my supervisor Dr. George S. Roberson for all the time he's dedicated to guiding me through my Masters, and in the writing of this thesis. Working in his lab for the last two years has been an amazing experience that I will never forget.

I would also like to extend a huge thank you to all members of the Robertson lab, past and present, for providing their continued support; both as colleagues and as friends. A special thank you goes out to Max and Matt, who helped get me started in the lab and were always available to discuss my research. I would also like to thank Mathew and Anna-Claire for their continued friendship and support. To Elizabeth, thank you for always being someone I can turn to for advice and guidance.

I would also like to acknowledge all the encouragement and aid I received from everyone in the Department of Pharmacology, especially the members of my advisory committee Dr. Keith Brunt and Dr. Chris Sinal. Also, thank you to all the graduate students from other departments that have been there for me. Without the support of everyone, I would not be here today.

I would also like to thank members of my Defense Committee, Dr. Scott Grandy and Dr. Denis Dupré, for reviewing of this thesis.

Finally, I would like to extend an enormous thank you to all my friends and family. I know I will always have people to turn to for encouragement, advice and inspiration. To my parents, thank you for always providing me with your unwavering support and pushing me to do my best. I truly appreciate everything you have done for me. I do not know where I would be without you. THANK YOU!

# CHAPTER 1: INTRODUCTION

## 1.1 Macrophage function in health and disease

Macrophages are phagocytic immune cells that play a vital role in both innate and adaptive immunity<sup>1-3</sup>. Although there are a variety of macrophage subtypes, the focus of this thesis will be on those arising from bone marrow hematopoietic progenitor cells (HSCs). Macrophages generated from HSCs, or circulating monocytes, are diverse and highly plastic cells. This diversity and plasticity is dependent on the microenvironment in which these cells are located<sup>2-4</sup>. This allows macrophages to serve both pro- and anti-inflammatory functions thus enabling them to play important roles in homeostatic processes such as tissue remodeling, recycling of erythrocytes and removal of cellular debris<sup>1,5</sup>. Macrophage fidelity is therefore critical for good health while their dysregulation can lead to the promotion and progression of many diseases. Examples of diseases that are influenced by macrophage dysregulation include cancer, arthritis, inflammatory bowel disease and multiple sclerosis. These disorders are often accompanied by the impaired polarization of macrophages between pro-inflammatory and anti-inflammatory states. To understand how impaired macrophage polarization may contribute to immune dysfunction, it is first necessary to describe the mechanisms that regulate macrophage polarization.

## **1.2 M1 and M2 macrophage polarization**

Although macrophages are broadly defined as either M1 (pro-inflammatory) or M2 (anti-inflammatory), this classification system is simplistic. More accurately, these cells exist within a spectrum of functional states enabling them to become M1-like or M2-like, depending on the polarizing conditions<sup>1,2,4-6</sup>. The criteria for classification of M1 and M2 macrophages have been hotly debated. Established researchers in the field have thus yet to agree on the precise nomenclature or standards to define them<sup>7</sup>. One method to assign these features is based on the characteristics of macrophages obtained by stimulating HSCs with the cytokine combinations of Granulocyte Macrophage-Colony Stimulating Factor (GM-CSF) + lipopolysaccharide (LPS) or Macrophage-Colony Stimulating Factor (M-CSF) + interleukin-4 (IL-4)<sup>8</sup>. Exposure to GM-CSF+LPS stimulates the "classical activation" of macrophages. These macrophages are termed M1 cells because their polarization is associated with activation of the Th1 immune response<sup>8</sup>. Exposure to M-CSF+IL-4 causes "alternative activation" that gives rise to macrophages termed M2 cells because of their association with the Th2 immune response<sup>8</sup>. For the purposes of my thesis, macrophages that encourage inflammation are termed M1 macrophages, whereas those that reduce inflammation and promote tissue repair are called M2 macrophages.

### 1.3 M1 and M2 macrophage markers

In mice, macrophages generally display cluster of differentiation molecule 11b (CD11b), EGF-like module-containing mucin-like hormone receptor-like 1 (F4/80) and Colony Stimulating Factor-1 Receptor (CSF-1R) of their cell surface<sup>3,5</sup>. A variety of receptor and cytokine markers have been employed to identify specific macrophage subtypes. Those macrophages categorized as being M1-like have pro-inflammatory characteristics, as well as, microbicidal and tumouricidal activity<sup>3,9</sup>. These cells are activated by ligands for Toll Like Receptor 3 and 4 (TLR-3/4) or exposure to interferon-gamma (IFN- $\gamma$ ), that triggers the expression of the CD86 on the cell surface and their increased production of pro-inflammatory mediators including: tumour necrosis factor-alpha (TNF- $\alpha$ ), interleukin-1beta (IL-1 $\beta$ ), IL-12, IFN- $\gamma$  and superoxide anions<sup>3,9,10</sup>. Conversely, macrophages of the M2 lineage are anti-inflammatory in nature and are chiefly associated with parasitic infections, tumour progression, immunoregulatory functions and angiogenesis<sup>3,9</sup>. M2 polarization promoted by IL-4 and IL-13 results in the cell surface expression of CD206 and major histocompatibility complex class II (MHCII) molecules, as well as, the elevated production of IL-4, IL-10, Arg-1 (Arginase-1), Ym1 and nitric oxide synthase 2 (NOS2)<sup>3,9,10</sup>. However, many of these markers are not always specific for M1 or M2 macrophages. This is because macrophages are polarized within a dynamic M1-M2 spectrum and often display both M1 and M2 markers, thus making it difficult to define the absolute degree of M1 and M2 polarization<sup>11</sup>. New findings, however, have identified markers that appear to discriminate M1 from M2 macrophages. Jablonski *et al.* (2015) performed a comprehensive analysis of the transcriptional signature of murine M0 (non-polarized), M1 and M2 macrophages to identify markers that are exclusive to each of

these cell sub-types. These investigators found that increased CD38, G-protein coupled receptor 18 (Gpr18) and formyl peptide receptor 2 (Fpr2) expression was M1-exclusive, while the induction of early growth response protein 2 (Egr2) and avian myelocytomatosis viral oncogene homolog (c-Myc) was M2-exclusive<sup>11</sup>. Use of these markers thus offers the opportunity to define the relative contribution of M1 and M2 macrophages in the progression and resolution of inflammation. Moreover, information derived from such studies may assist the development of drugs designed to promote the optimal balance of M1 and M2 macrophage function necessary for the improved treatment of inflammatory disorders.

#### **1.4 Cellular inhibitor of apoptosis 2 (cIAP2) and second mitochondria-derived activator of caspases (SMAC)**

Members of the Inhibitors of Apoptosis (IAP) family play pivotal roles in the regulation of cell death and survival<sup>12</sup>. The first IAP was discovered in baculoviruses, with subsequent cloning studies in human cells resulting in the identification the IAP family members cIAP1 (BIRC2), cIAP2 (BIRC3), NAIP, XIAP, ILP2, BRUCE and survivin<sup>13-17</sup>. IAPs share a conserved region of 70-80 amino acids known as the Baculoviral IAP repeat (BIR) domain with all members except NAIP, BRUCE and survivin also containing a carboxy-RING zinc finger with E3 ligase activity<sup>12</sup>. XIAP blocks apoptotic cell death by directly inhibiting the cysteinyl protease activity of caspase-3<sup>18</sup>. Unlike XIAP, cIAP1 and cIAP2 (cIAP1/2) are inefficient at directly inhibiting caspase activity<sup>19</sup>. Instead, cIAP1/2 suppresses TNF- $\alpha$  receptor 1 (TNFR1)-mediated apoptosis by inhibiting formation of the death-inducing 'complex-II', that is the activation platform for caspase-

8. which induces cell death by the extrinsic pathway<sup>12,20</sup>. cIAP1 and cIAP2 have redundant functions with cIAP2 considered to be a duplication event of cIAP1 that occurred in recent evolutionary history<sup>21</sup>. The constitutive presence of cIAP1 in conjunction with the adaptor proteins TNF receptor-associated factor 1 and 2 (TRAF1/2) mediates the E3-ligase induced ubiquitination followed by the degradation of cIAP2<sup>12,20</sup>. Genetic ablation of cIAP1 elevates cIAP2 levels, however, cIAP2 ablation does not alter cIAP1 levels<sup>22</sup>. Cellular stress (hypoxia) as well as the stimulation of the Toll-4 receptor or TNFR1 produces the transcriptional activation of cIAP2 enabling this anti-apoptotic protein to exert dynamic control over apoptotic resistance<sup>22-24</sup>.

IAPs are regulated by proteins that oppose their anti-apoptotic activities. One such IAP inhibitor is the second mitochondria-derived activators of caspase (SMAC) which is a natural IAP inhibitor released by mitochondria. In recent years, small molecule SMAC mimetics have been developed that sensitize cancer cells to apoptosis by suppressing cIAP1/2 levels<sup>25</sup>. SMAC (a.k.a. DIABLO) is a 29 kDa protein which moves from the mitochondrion to the cytoplasm after exposure to an apoptotic trigger<sup>26,27</sup>. SMAC mimetics are based on the structure of the four-amino acid terminus of SMAC (Ala-Val-Pro-Ile). X-ray crystallography studies first suggested that SMAC mimetics would activate caspase-3 by releasing this death protease from XIAP binding sites<sup>12,27,28</sup>. However, subsequent studies showed that SMAC mimetics trigger apoptosis by facilitating cIAP1/2 dimerization which enables their E3-ligase activities to produce the hetero- and auto- ubiquitination and subsequent degradation of these proteins by the proteasome<sup>20,25</sup>.

## 1.5 cIAP1/2 promote macrophage survival

Evidence that cIAP1/2 regulate the survival of both normal and transformed (cancerous) cells have fueled intense interest in the relative anti-apoptotic roles of these proteins<sup>20,26</sup>. Single cIAP1 or cIAP2 nulls are viable. However, because the mouse genes encoding cIAP1 and cIAP2 are only ~15 kb apart on chromosome 9A2<sup>29</sup>, they operate as a single locus (murine chromosomal location 9qA1), so it has not been possible to generate cIAP1/cIAP2 double-knockout (DKO) mice by crossing single-KO strains<sup>20,30</sup>. Recently developed transgenic mice in which critical exons of cIAP1 and cIAP2 are flanked by distinct recombinase recognition sites (cIAP1<sup>lox/lox</sup> and cIAP2<sup>Frt/Frt</sup>) have been used to study the effects of global or cell-specific manipulation of cIAP1, cIAP2 or cIAP1/2 on immune function<sup>20,30</sup>. Use of these mice has shown that global cIAP1/2 deletion caused embryonic lethality between E10.5 and E11.5<sup>30</sup>. The death of cIAP1/2 DKO mice was rescued to birth by deletion of TNFR1, but not TNFR2, indicating that these anti-apoptotic proteins restrain the pro-death effects of TNFR1 activation<sup>30</sup>. Treatment of primary cultures of bone marrow derived macrophages (BMDMs), differentiated with L929 conditioned medium, with a SMAC mimetic showed that cIAP1/2 suppression produced a transient elevation of TNF- $\alpha$  which triggered TNFR1-induced cell death<sup>31</sup>. The importance of cIAP1/2 in conferring the resistance of macrophages to apoptosis is further supported by two other lines of evidence. First, systemic administration of a SMAC mimetic depletes these cells in mice<sup>32</sup>. Second, elevation of TNF- $\alpha$  levels by injection of an oncolytic virus dramatically increased the ability of oral administration of the SMAC mimetic LCL161 to kill cancer cells in a mouse tumor model<sup>33</sup>. These studies further support a pivotal role for cIAP1/2 in maintaining macrophage viability in the

presence of elevated TNF- $\alpha$  levels and the utility of a SMAC mimetic to investigate the effects of cIAP1/2 inhibition on macrophage function<sup>20</sup>. Lastly, L929 conditioned medium is used as a source of M-CSF suggesting that cIAP1/2 suppression impairs the survival of mildly-M1 polarized macrophages. However, treatment of BMDMs with specific cytokine combinations necessary to promote M1 or M2 macrophage polarization is required to determine the effect of cIAP1/2 suppression on these processes.

One of the key functions of macrophages is their ability to produce pro-inflammatory cytokines that mobilize immune events necessary to kill invading pathogens<sup>34</sup>. However, the presence of IAPs are required to protect macrophages from cytokine-induced cell death. For instance, cIAP2 ablation renders macrophages highly-susceptible to cell death by LPS. This enabled cIAP2 nulls to survive a toxic dose of LPS because macrophages that propagate a “lethal cytokine storm” undergo massive apoptosis<sup>23</sup>. In the absence of cIAP2, macrophages still produced a transient increase of TNF- $\alpha$  following stimulation with LPS<sup>23</sup>. This finding suggests that ablation of just cIAP2 is sufficient to promote macrophage apoptosis by increased TNFR1 activation<sup>23</sup>.

## **1.6 Pro-survival and pro-death signaling by the canonical and non-canonical NF- $\kappa$ B pathways**

The pro-survival effects of TNFR1 activation are mediated by activation of the canonical NF- $\kappa$ B pathway which leads to the upregulation of pro-survival genes [cIAP2, FLICE-like inhibitory protein (FLIP-2)] that oppose caspase-8 activation by blocking formation of death-inducing complex II<sup>12,20</sup>. The heightened sensitivity of cIAP2 nulls to LPS-induced

macrophage cell death therefore suggests that cIAP2 deficiency is sufficient to permit TNFR1-induced formation of the death-inducing complex II. Additionally, it has been shown that inhibition of the NF- $\kappa$ B pathway alone does not lead to the release of SMAC from mitochondria. Only in the presence of TNF- $\alpha$  is SMAC released that triggers caspase-dependent death<sup>35</sup>. Based on these studies, it appears that cIAP2 deletion in the presence of inflammatory conditions, or SMAC-mimetic-induced cIAP1/2 suppression and TNF- $\alpha$  production, dysregulate the canonical NF- $\kappa$ B pathway resulting in formation of death-inducing complex II<sup>23,26,36,37</sup>. Hence in the absence of cIAP2, TNF- $\alpha$  fails to increase the expression of pro-survival genes by the canonical NF- $\kappa$ B pathway (complex I) and instead activates cell death via complex II signalling<sup>23,26,36,37</sup>.

In association with TRAF1/2, cIAP1/2 mediate the pro-survival effects of canonical NF- $\kappa$ B signaling by preventing release of RIP1 from the TNFR1 complex by ubiquitinating this kinase (Figure 1A)<sup>38</sup>. When cIAP1/2 levels are reduced, complex II canonical NF- $\kappa$ B signaling is induced by the release of receptor-interacting protein kinase (RIP) that associates with Fas-associated protein with death domain (FADD) and caspase-8 to form complex IIa (ripotosome) to activate caspase-mediated apoptosis (Figure 1B)<sup>12,32,38</sup>.

However, RIP1 can also form a complex with RIP3 that induces necroptosis (complex IIb or necrosome) which is unmasked by treatment with a caspase-8 inhibitor (Figure 1B)<sup>39</sup>.

Formation of the RIP1/3 complex IIb appears to be the main regulator of death in cIAP1/2 null macrophages because deletion of RIP3 confers macrophages resistance to SMAC-induced cell death<sup>32</sup>.

In the non-canonical NF- $\kappa$ B pathway, cIAP1/2 in association with TRAF2/3 promotes the ubiquitination of NF- $\kappa$ B-inducing kinase (NIK), preventing p100 to p52 conversion<sup>12,39,40</sup>. Under cIAP1/2 null conditions, NIK accumulates, leading to p100 to p52 conversion and activation of the non-canonical NF- $\kappa$ B pathway<sup>12,20,38</sup>. The non-canonical NF- $\kappa$ B can influence cell survival as up-regulation of TNF- $\alpha$  occurs upon activation. Subsequently, TNF- $\alpha$  can then activate TNFR1 in an autocrine/paracrine manner<sup>41</sup>. As previously mentioned, in the absence of cIAP1/2 proper canonical NF- $\kappa$ B signalling through TNFR1 does not occur. Instead the pro-apoptotic complex II is activated, causing cellular death. In these ways, cIAP1/2 are strategically positioned to exert exquisite control over both canonical and non-canonical NF- $\kappa$ B signalling.

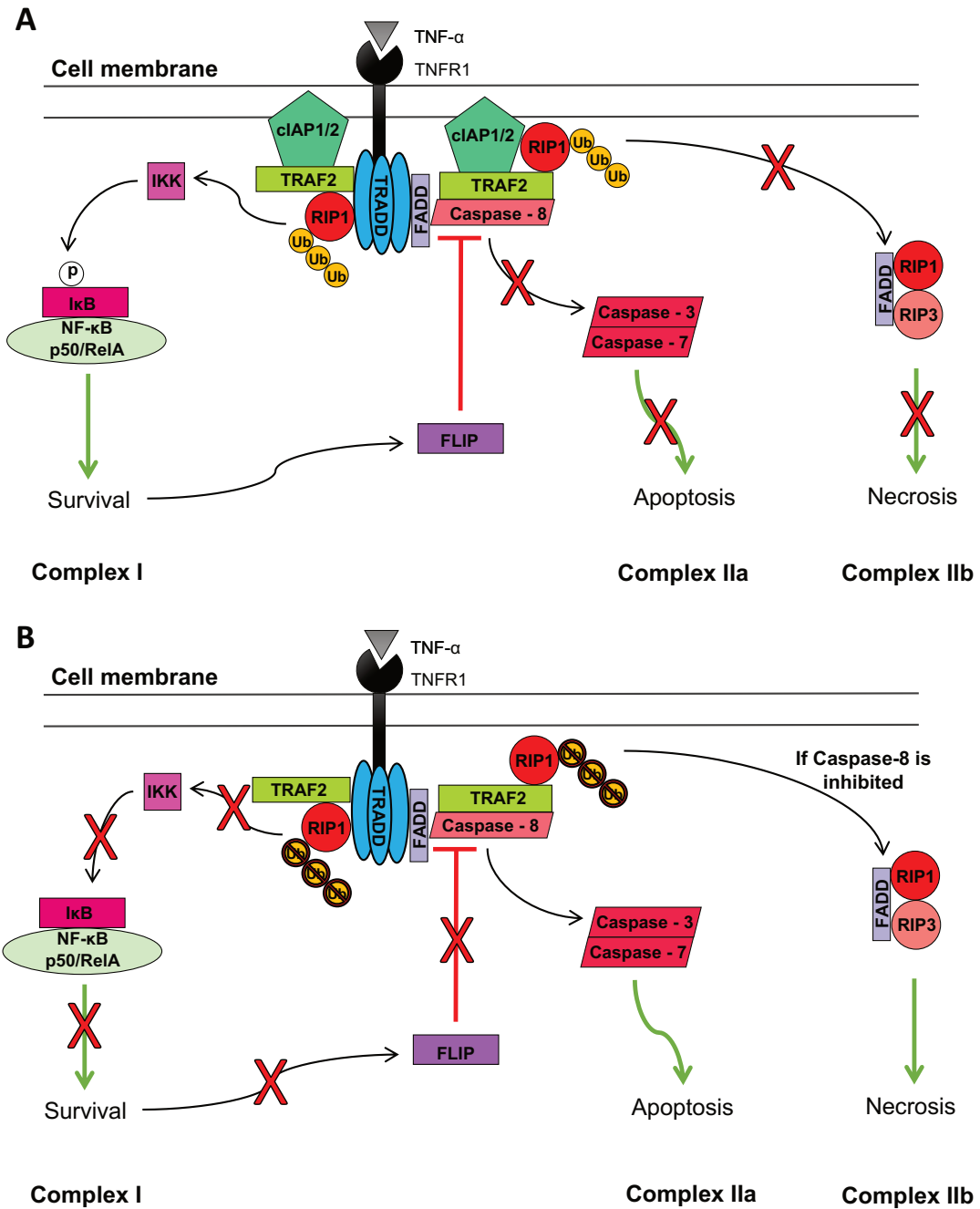


**Figure 1:** Regulation by cIAP1/2 of TNFR1-mediated activation of complex I and complexes IIa and IIb. A) Under survival conditions, cIAP1/2 mediates the activation of complex I by ubiquitinating RIP1 enabling this kinase to phosphorylate I $\kappa$ B resulting in the degradation of this NK- $\kappa$ B inhibitor. The loss of I $\kappa$ B enables p50/RelA subunits to translocate to the nucleus and upregulate the expression of pro-survival genes such as FLIP that inhibit caspase-8. The presence of cIAP1/2 also prevents the formation and activation of death-inducing complexes IIa (apoptosis) and IIb (necrosis). B) In the absence of cIAP1/2, RIP1 is not ubiquitinated that blocks phosphorylation of I $\kappa$ B and the release of p50/RelA necessary for pro-survival signaling. The reduced production of FLIP combined with loss of cIAP1/2 allows caspase-8 to associate with FADD and activate complex IIa-induced apoptosis. Necrotic death may also occur via formation of complex IIb (FADD+RIP1+RIP3) that is enhanced by caspase-8 inhibition.

## **1.7 Experimental autoimmune encephalomyelitis mouse model of multiple sclerosis**

Multiple sclerosis (MS) is characterized by the autoimmune-mediated destruction of myelin that surrounds axons in the central nervous system (CNS)<sup>42</sup>. Remyelination failure with disease progression results in irreversible axon damage that causes permanent neurological deficits<sup>43,44</sup>. While the exact causes of MS are unknown, a combination of genetic and environment factors have been implicated<sup>42</sup>. Neuropathology features of MS include disruption of the blood brain barrier (BBB), immune infiltration, demyelination and axon damage that involves the activation of cells that comprise both the innate (neutrophils, macrophages and dendritic cells) and adaptive (T-cells, B-cells) immune systems<sup>45</sup>. The infiltration of innate immune cells is thought to be an early event that primes-myelin reactive T cells responsible for autoimmune-mediated demyelination<sup>46</sup>. Remyelination enables functional recovery, however, with repeated cycles of autoimmune-mediated demyelination, remyelination fails resulting in axon damage and persistent neurological impairments<sup>42</sup>. M1 macrophages release pro-inflammatory mediators (nitric oxide and TNF- $\alpha$ ) that damage myelin-producing oligodendrocytes and oligodendrocyte progenitor cells essential for remyelination<sup>47</sup> while M2 macrophages clear cellular debris and release anti-inflammatory cytokines [IL-10, transforming growth factor-beta (TGF- $\beta$ )] that support remyelination<sup>48</sup>. Understanding the signalling events that regulate the polarization and survival of M1 and M2 macrophages may therefore have profound therapeutic implications for MS<sup>49</sup>.

Experimental autoimmune encephalomyelitis (EAE) is a widely used animal model for MS<sup>50</sup>. EAE is induced in mice by immunization with a 21-amino acid portion of myelin

oligodendrocyte glycoprotein (MOG<sub>35-55</sub> peptide) in complete Freund's adjuvant in combination with injections of pertussis toxin to promote opening of the BBB that results in autoimmune-mediated demyelination, paralysis and motor deficits resembling MS<sup>45,50</sup>. Although no single animal model fully recapitulates the complex etiology of MS, mouse EAE models have been shown to reproduce immune events implicated in MS and proven useful in the identification of clinically effective MS therapeutics<sup>50,51</sup>. Like MS, EAE causes BBB disruptions, immune infiltration and CD4<sup>+</sup> T cell-mediated demyelination resulting in axonal damage<sup>45,50,52</sup>. Antigen presenting cells (APCs), such as macrophages and dendritic cells, also play important roles in the initiation, progression and resolution of EAE<sup>50</sup>. I therefore employed a mouse model of MOG<sub>35-55</sub>-induced EAE to study the effects of suppression of cIAP1/2 by oral administration of the SMAC mimetic LCL161 on disease severity, spinal cord M1 and M2 cytokine expression and plasma concentrations of Th1 and Th2 cytokines and chemoattractants.

### **1.8 Rationale: Use of genetic cIAP2 ablation or LCL161-induced cIAP1/2 suppression to understand the roles of these anti-apoptotic proteins in M1 and M2 macrophage polarization**

Many of the disease modifying therapies (DMT) that have been developed to treat MS are immunomodulatory drugs that target peripheral events which contribute to neuroinflammation<sup>53,54</sup>. In MS, macrophages promote myelin damage and facilitate the activation of T cells that drive autoimmunity. Although the activation of resident macrophages (microglia) may contribute to the induction of neuroinflammation and the subsequent resolution of neuroinflammation, the importance of infiltrating peripheral

macrophages in promoting CNS damage and repair necessary for remyelination in MS is better established<sup>55-59</sup>. Understanding how M1 and M2 macrophage polarization is regulated is therefore a major goal in MS research.

Early studies with the EAE model of MS demonstrated that macrophage depletion delayed the onset and reduced the severity of clinical disease signs<sup>60</sup>. More recent studies suggest these benefits resulted from the loss pro-inflammatory M1-like macrophages and have shown that enhancing the natural progression of macrophages from an M1-like to M2-like state reduced inflammation and enhanced recovery in EAE mice<sup>56-58,60,61</sup>. One drug that shifts macrophage polarization in this direction is fasudil, a selective Rho-associated kinase inhibitor<sup>62</sup>. Treatment of EAE mice with fasudil significantly delayed disease onset and attenuated EAE progression by decreasing BBB permeability and shifting macrophage polarization from an M1-like to M2-like state<sup>62</sup>. This work lends credence to the notion that altering macrophage polarization may be beneficial in reducing EAE disease severity, and by extension, the treatment of MS.

As mentioned earlier, Conte et al. (2006) showed that cIAP2 null mice were resistant to LPS-induced sepsis because pro-inflammatory macrophages were rendered highly susceptible to TNFR1-induced cell death. In support of this finding, LPS-induced increases in plasma pro-inflammatory cytokines and chemokines are blocked in cIAP2 nulls and suppression of cIAP1/2 levels with a SMAC mimetic attenuates the induction of mRNAs encoding these proteins in BMDMs by LPS<sup>23,63</sup>. These effects have been attributed to induction of macrophage cell death by the activation of TNFR1-mediated

death-inducing complex II in the absence of cIAP1/2<sup>36,37</sup>. Elevated TNF- $\alpha$  production also activates and recruits macrophages to the CNS in both EAE and MS<sup>64</sup>. The absence of cIAP2 might thus reduce EAE severity by reducing the resistance of pro-inflammatory M1 macrophages to TNF- $\alpha$ -induced cell death<sup>65</sup>. However, our laboratory has observed that cIAP2 nulls displayed increased rather than reduced EAE severity (Chedrawe et al. 2016; <https://endms.confex.com/endms/2016/meetingapp.cgi/Paper/11113>). I propose that this finding reflects a more complex mechanism whereby cIAP2 loss elevates EAE severity by impairing the balance between M1 and M2 macrophage function that both exacerbates pro-inflammatory and disrupts anti-inflammatory processes. To address this hypothesis, I have assessed the effects of genetic ablation of cIAP2 or SMAC mimetic-induced cIAP1/2 suppression on M1 and M2 macrophage polarization and survival in BMDMs and macrophages isolated from these cultures by immunopanning. These studies were complemented by comparing disease severity, spinal cord M1 and M2 marker mRNA levels and plasma cytokine and chemoattract concentrations for EAE mice treated orally with either vehicle or the SMAC mimetic LCL161.

### **1.9 Central hypothesis**

Genetic ablation of cIAP2 or LCL161-induced cIAP1/2 suppression will impair M1 and M2 macrophage polarization resulting in elevated disease severity for LCL161-treated EAE mice.

### **1.10 Research aims**

This central hypothesis was tested by completion of the following 5 research aims:

***Aim 1:*** Comparisons of the generation, differentiation and survival of macrophages and dendritic cells in WT and cIAP2 null BMDMs cultured under mild or strong M1 or M2 polarizing conditions.

***Aim 2:*** Comparisons of the generation and differentiation of macrophages isolated by immunopanning from WT and cIAP2 null BMDMs cultured under mild or strong M1 or M2 polarizing conditions.

***Aim 3:*** Comparisons of the generation, differentiation and survival of macrophages isolated by immunopanning from BMDMs cultured under mild or strong M1 or M2 polarizing conditions and treated with either vehicle or LCL161.

***Aim 4:*** Comparisons of disease severity, liver cIAP1/2 levels, spinal cord M1 and M2 marker mRNA levels and plasma cytokine and chemoattract concentrations for EAE mice treated orally with either vehicle or LCL161.

***Aim 5:*** Comparisons of the percentages of classical and non-classical monocytes isolated from the spleens of EAE mice treated with either vehicle or LCL161

## CHAPTER 2: MATERIAL & METHODS

### 2.1 Bone marrow extraction and cytokine treatments to promote mild or strong M1 or M2 macrophage polarization

Wild-type (WT) C57BL/6 or cIAP2 null mice were euthanized with an over-dose injection of pentobarbital (150 mg/kg) according to a protocol approved by the University Committee on Laboratory Animals. Bone marrow was then rapidly extracted from the femur and tibia by washing out the bone marrow with phosphate buffered saline containing 0.2% ethylenediaminetetraacetic Acid (PBS-EDTA; Life Technologies). The bone marrow was then vortexed, filtered through a 40  $\mu\text{m}$  nylon mesh and centrifuged at 400  $\times g$  for 8 min. The supernatant was removed and the resulting pellet was re-suspended with 4 ml of sterile red cell lysis buffer for 15–20 min at room temperature.

Subsequently, PBS-EDTA (3 ml) was added and the cells were centrifuged as before.

Finally, the resulting pellet was re-suspended in 10 ml of Roswell Park Memorial Institute medium (RPMI)-complete [RPMI media 1640; 10% FBS (Fetal Bovine Serum); 1% streptomycin - penicillin, 1% MEM Non-Essential Amino Acid, 1% Sodium Pyruvate and 1% GlutaMax; Life Technologies]. Cells were plated on 6-well plates at a density of  $1 \times 10^6$  cells/well for the flow cytometry and qRT-PCR studies or on 10 cm plates at a density of  $6 \times 10^6$  cells/plate to obtain sufficient amounts of protein for western blotting. Mild M1 or M2 polarizing conditions were produced by culturing the cells with either RPMI-complete media + GM-CSF (200 ng/ml; Shenandoah Biotechnology Inc.) or RPMI-complete media + M-CSF (100 ng/ml; Shenandoah Biotechnology Inc.), respectively. Strong M1 and M2 macrophage polarization conditions were produced by culturing the cells with RPMI-complete media + GM-CSF (20 ng/ml) + LPS (100 ng/ml;

Sigma-Aldrich) or RPMI-complete media + M-CSF (100 ng/ml) + IL-4 (20 ng/ml; Peptotech). Cells were cultured for 7 days (maturity), with half the media and cytokines topped up on day 4. Once at maturity, the cells were stained immediately for flow cytometry or stored at  $-80^{\circ}\text{C}$  until qRT-PCR or western blot analyses. Statistical analysis was performed using the Mann-Whitney U test to compare differences in macrophage generation.

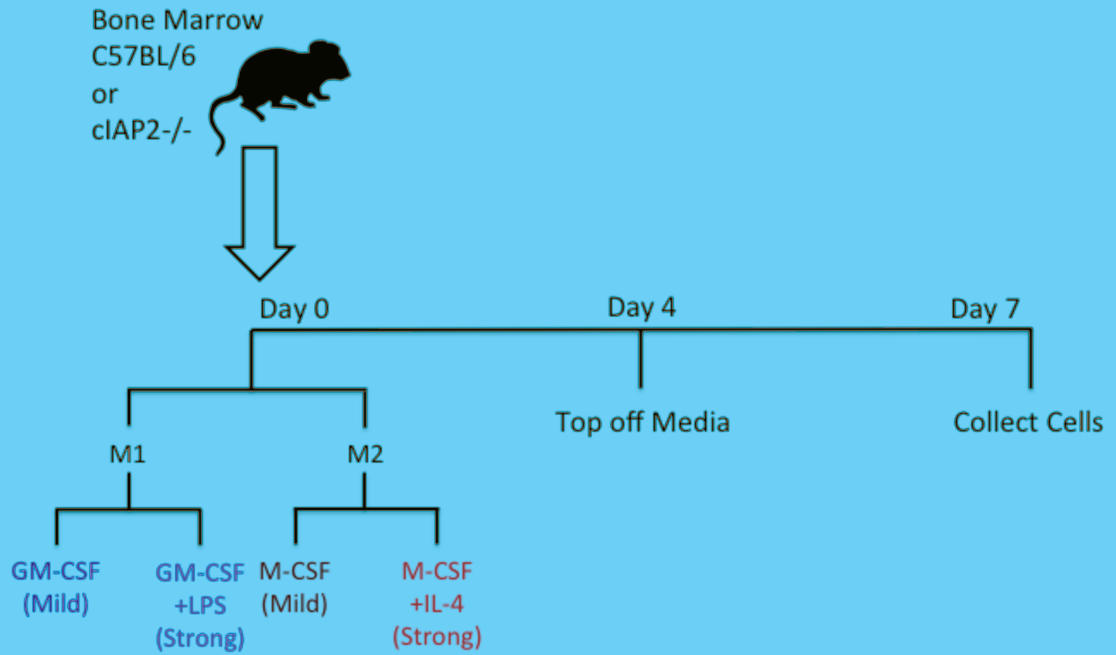


**Figure 2:** Schematic representation of the cell culture protocol. Bone marrow was extracted from the femur and tibia of WT C57BL/6 or cIAP2 null mice, purified, and plated. Cells were plated with RPMI-complete containing either GM-CSF or M-CSF or GM-CSF+LPS or M-CSF+IL-4 followed flow cytometry, qRT-PCR or western blotting analyses 7 days later.

## **2.2 Treatment of bone marrow derived macrophages with the SMAC mimetic LCL161**

To further explore the effects of cIAP2 deficiency on the polarization of bone marrow derived macrophages (BMDMs), a subset of WT BMDM cells were treated with vehicle (DMSO; 0.01%) or the SMAC mimetic LCL161 (10  $\mu$ M; Novartis) for 24 hours (hr) before collection. The SMAC mimetic was added on day 6 and cells were collected on day 7 (maturity) for subsequent analyses.

## **2.3 LPS-induced cell death**

To determine the effects of cIAP2 deficiency on the polarization of bone marrow macrophages (BMDMs), a subset of WT BMDM cells treat with vehicle (DMSO; 0.01%) or the SMAC mimetic LCL161 (10  $\mu$ M; Novartis) were exposed to LPS (3  $\mu$ M) for 4 hr. Cells were then collected and stained immediately for flow cytometry as described below. Statistical analysis was performed by Mann-Whitney U test to compare changes in cellular death with significance at  $p < 0.05$ .

## **2.4 Immunopanning**

Immunopanning was performed using the F4/80 antibody to select for macrophages. On culture Day 6, 10 cm petri dishes (Falcon) were prepared. The bottom of each dish was coated by the addition of Tris (10 ml; 50 mM, pH 9.5) with F4/80 antibody (10  $\mu$ g/ml; eBioscience). The dishes were then sealed with parafilm and left at 4°C on a flat surface for 24 hr. The Tris-F4/80 antibody solution was then removed and the plates washed 3 times with PBS (~1 ml/wash). On culture Day 7, cells were prepared for panning.

Supernatants from 3 wells (~ 9 ml) were first removed and transferred to a polystyrene tube (50 ml; Falcon). The remaining attached cells were dissociated from the cells by incubation with TrypLE (1 ml/well; Life Technologies) at 37°C for ~10 min. The loosened cells were then collected and combined with their respective supernatants. The cells were then spun-down at 400 xg for 8 min, re-suspend in 4 ml RMPI-complete and cell numbers counted using a hemocytometer and Trypan Blue Satin (Life Technologies). The re-suspend cells were then added to the panning plates and allowed to incubate for 1 hr (swirling halfway through) at 37°C. Following this step, the supernatant was transferred to a polystyrene tube (15 ml; Falcon) and the plate was washed with PBS (5-8 times). Each wash was combined with the supernatant. After performing a cell count, the supernatant was spun down at 400 xg for 8 min, re-suspended in ~ 4 ml FACs buffer and stained for flow cytometry. Adherent macrophages were removed from the F4/80 antibody coated-plates by the addition of Aurum<sup>TM</sup> lysis solution (Bio-Rad) and stored at -80°C until qRT-PCR analysis.

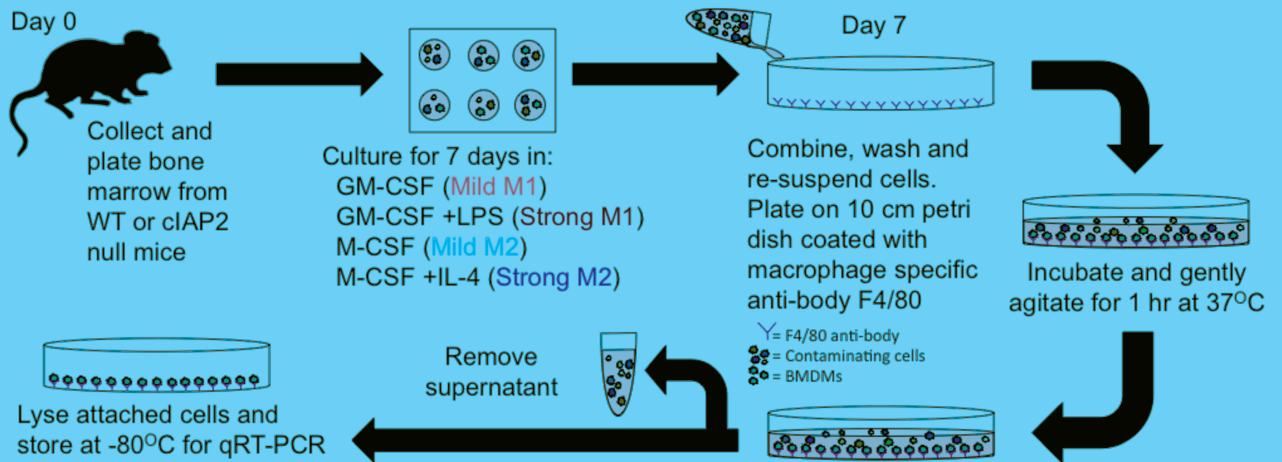


**Figure 3:** Experimental protocol to select for macrophages in BMDMs cultures by immunopanning with the F4/80 antibody. After 7 days in culture, cells from 3 wells of a 6-well plate were collected and combined. The cells were then plated on a 10 cm petri dishes that were coated with the F4/80 antibody. After a 1 hr incubation at 37°C the supernatant was removed and the adherent cell macrophages were lysed and collected for qRT-PCR analyses.

## **2.5 Quantitative Real Time Polymerase Chain Reaction (qRT-PCR)**

Total RNA was extracted using the Aurum™ Total RNA Mini Kit (Bio-Rad) according to the manufacture's "Spin Protocol" instructions. Integrity of the resulting RNA was then tested using the RNA StdSns analysis kit and the Experion™ Automated Electrophoresis System (Bio-Rad). RNA with a passing (>7.5) RNA quality indicator (RQI) was then tested for purity and concentration using an Epoch Microplate Spectrophotometer (BioTek Instruments) or NanoDrop (Thermo Scientific).

After determining the RNA concentration, each sample was normalized to a concentration of 500 ng or 750 ng of RNA per 16 µl volume (mix of RNA and NF H<sub>2</sub>O). These normalized samples were then brought to a final volume of 20 µl with iScript™ Reverse Transcription Supermix for qRT-PCR (Bio-Rad) and cDNA synthesis was performed according to instructions by the manufacture.

Finally, qRT-PCR was performed with SsoFast EvaGreen Supermix kit (Bio-Rad). Individual genes (Table 1) were optimized for both annealing temperature and concentration using the Bio-Rad CFX 96 real time system C1000 Touch thermal cycler. A typical qRT-PCR program was 95°C × 30 s + (95°C × 5 s + 58°C × 5 s + plate reading) × 40 cycles + melting curve (2 s stop with plate readings for every 0.5°C increase from 65 °C to 95 °C). All qRT-PCR protocols were done in accordance with the MIQE guidelines<sup>66</sup>. Analysis was performed with the Bio-Rad CFX Manager 3.1 software using the ΔC<sub>q</sub> method. Each experiment was performed at least three times with triplicate determinations from each sample. Statistical comparisons of fold changes in mRNA levels were performed using unpaired t-tests with significance at p<0.05.

**Table 1:** Forward and reverse primer sequences for M1/M2 markers, reference genes and others.

M1	M2
<b>CD38</b> F: TCTCTAGGAAAGCCCAGATCG R: GTCCACACCAGGAGTGAGC	<b>CD206</b> F: TCAGCTATTGGACGCGAGGCA R: TCCGGGTTGCAAGTTGCCGT
<b>CD86</b> F: ACGATGGACCCCAGATGCACCA R: GCGTCTCCACGGAAACAGCA	<b>c-Myc</b> F: ACCCGCTCAACGACAGCAGC R: CCGTGGGGAGGACTCGGAGG
<b>Fpr2</b> F: TCTACCATCTCCAGAGTTCTGTGG R: TTACATCTACCACAATGTGAACTA	<b>Erg2</b> F: AGTTGTGGAGAGAGAAACAATC R: ACACCATAGTCAATAAGCCATC
<b>Gpr18</b> F: TGAAGCCCAAGGTCAAGGAGAAGT R: TTCATGAGGAA GGTGGTGAAGGCT	<b>IL-10</b> F: ACAGCCGGGAAGACAATAACT R: GCAGCTCTAGGAGCATGTGG
<b>NOS2</b> F: GTTCTCAGCCCAACAATACAAGA R: GTGGACGGGTCGATGTCAC	<b>P2Y12</b> F: GTGTTGACACCAGGCACATC R: TCCCGGAGACACTCATATCC
<b>TNF-<math>\alpha</math></b> F: CAGGCGGTGCCTATGTCTC R: CGATCACCCGAAGTTCAGTAG	
<b>House Keeping (reference)</b>	<b>Other</b>
<b>GAPDH</b> F: AGGTCGGTGTGAACGGATTTG R: GGGGTCGTTGATGGCAACA	<b>cIAP-2</b> F: TGAAGAGTGCTGACACCTTTG R: GGAAAAGCTGAATACGTGGACAA
<b><math>\beta</math>-actin</b> F: GTGACGTTGACATCCGTAAAGA R: GCCGGACTCATCGTACTC	<b>MCP-1</b> F: TCTGGGCCTGCTGTTTCA R: GCGTTAACTGCATCTGGCT
<b>HPRT1</b> F: TCAGTCAACGGGGGACATAAA R: GGGGCTGTACTGCTTAACCAG	
<b>B2M</b> F: TTCTGGTGCTTGTCTCACTGA R: GGGGCTGTACTGCTTAACCAG	

## 2.6 Flow Cytometry

The media from each well was removed and placed in a polystyrene tube (5 ml; Falcon). Adherent cells were removed by incubation with TrypLE (1 ml; Life Technologies) for ~10 min at 37°C. These cells were then collected and combined with the corresponding media. The tubes were brought to a final volume of 2 ml by the addition of FACS buffer (PBS + 5 ml EDTA + 5 ml FBS) before being spun down at 500 xg for 5 min at 4°C (wash step). The resulting supernatant was removed and Fc block (eBioscience) was added. The tubes were vortexed and left to incubate for 30 min at 4°C, followed by a wash step. The cells were then stained extracellularly with antibodies for CD11b (eBioscience) and F4/80 (eBioscience). Subsets of spleen samples were also stained with antibodies against Ly6C (eBioscience) and Ly6G (eBioscience). Next, the cells were incubated with fixation buffer (eBioscience) for 30 min and washed a final time. The tubes were then brought to a final volume of 400 µl with FACS buffer and analyzed. Some cells were also stained with the apoptosis marker Annexin V (PE Annexin V Apoptosis Detection Kit I (BD Pharmingen)) and the viability marker 7-AAD and analyzed without fixation within 1 hr. Samples were read using the BD FACSAria III and analyzed using FCS Express software. Non-stained samples were used as controls. For all samples 10 000 events (aka. single cells) were analyzed by dot plot or histogram analysis. Dot plot analysis sorts cells based on the expression levels of two specific markers where, cells located higher on the y-axis or further along the x-axis express more of the marker of interest. Histogram analysis sorts cells based on cell count and one marker of interest. All statistical analysis for flow cytometry results were performed using Mann-Whitney U test with significance at  $p < 0.05$ .

## 2.7 Western Blotting

Western blotting was performed using a slightly-modified version of the General Protocol for Western Blotting (Bio-Rad). Protein was collected from cells lysed with RIPA buffer (SigmaFAST & Phenylmethanesulfonyl fluoride protein inhibitors; Sigma-Aldrich). Protein concentrations were then determined with the Bio-Rad Protein Assay according to the manufacturer's instructions using an Epoch Microplate Spectrophotometer (BioTek Instruments).

Each lane of the gel was loaded with 20  $\mu\text{g}$  of protein. Gels were then run at 55 V for about 4 hr in Laemmli sample buffer (Bio-Rad) followed by transfer to a nylon membrane (350 mA for  $\sim$ 1.5 hr). Following protein transfer, the membrane was blocked with 5% milk protein (dissolved in TBS-T) on a shaker for 1 hr, washed with TBS-T and then incubated overnight at 4°C with antibody against anti-BIRC3 (aka, cIAP2; 0.5  $\mu\text{g}/\text{ml}$ , LifeSpan BioScience). After a wash with TBS-T, the membrane was incubated with the 2° antibody (0.5  $\mu\text{g}/\text{ml}$  Peroxidase Anti-mouse IgG (H+L); Vector Laboratories) at room temperature for 1hr. Following the final wash with TBS-T, the membrane was incubated with Amersham™ ECL™ Prime Western Blotting Detection Reagent (GE healthcare) solution A and B (1:1 ration; 1 ml/sample) for 5 min room temperature and then imaged using the ChemiDoc™ Touch imaging system (Bio-Rad). After imaging the membrane, it was washed in TBS-T then incubated overnight (4°C) with 0.5  $\mu\text{g}/\text{ml}$  Monoclonal Anti- $\beta$ -Actin antibody (Sigma-Aldrich). The same 2° antibody was used to visualize  $\beta$ -Actin the following day.

## **2.8 Experimental Autoimmune Encephalomyelitis (EAE)**

The EAE protocol was approved by the University Committee on Laboratory Animal. C57BL/6 mice were obtained from Charles River and allowed to habituate to the facility for seven days before experiments commenced. The cIAP2 null colony was maintained in house. EAE was induced in these mice as previously described<sup>67</sup>. Adult female mice (20 g) were injected with amino acids 35–55 (MEVGWYRSPFS- RVVHLYRNGK) of myelin oligodendrocyte glycoprotein (MOG<sub>35-55</sub>; Gen Script) to induce EAE. Animals injected with complete Freund's adjuvant (CFA) served as antigen controls. CFA was prepared by mixing incomplete Freund's adjuvant (Difco Laboratories) with heat-killed *Mycobacterium tuberculosis* H37RA (Difco Laboratories) at a 10 mg/ml concentration. MOG<sub>35-55</sub> was dissolved in sterile PBS at a concentration of 3 mg/ml and emulsified in a 1:1 ratio with complete Freund's adjuvant (CFA). The MOG<sub>35-55</sub>/CFA emulsion was delivered via two subcutaneous (sc) injections (100 µl/injection) on both sides of the base of the tail so that each mouse received a total of 300 µg of MOG<sub>35-55</sub>. For the antigen controls, CFA was injected in the same manner. All mice were injected intraperitoneally with 300 ng of (1.5 µg/ml) pertussis toxin (PTX; Sigma) on day 0 and 2 post-immunization (DPI 0 and 2). LCL161 treated-mice were orally gavaged with this SMAC mimetic (50 mg/kg) starting at post-immunization day 1 (DPI 1) and again every third day until the end the end of the experiment (DPI 30). LCL161 was suspended in in NEOBEE<sup>®</sup> 1053 (Stepan Company) and delivered in volume of 100 µl. Control mice received only NEOBEE. Statistical comparisons of clinical score were performed using the Wilcoxon Test (significance at p<0.05), which compares the mean clinical scores of EAE mice treated with vehicle to those treated with LCL161.

## **2.9 Care of EAE mice**

Upon disease onset, all mice were given access to mash, hand-fed with DietGel Boost (ClearH2O) and given injections of 0.9% sodium chloride solution (sc) as necessary to maintain hydration. A humane end-point was reached when: 1) weight loss exceeded 20% of the starting weight; 2) if a clinical score of 5 was reached; 3) if a mouse was unable to right itself; or 4) unable to access food and water for 24 hr. Clinical scores for each mouse was determined by changes in motor function using an 11-point ordinal scale: 0, no motor deficits; 0.5, hooked tail; 1.0, fully flaccid tail; 1.5, bilateral hind limb splay; 2.0, minor walking deficits; 2.5, major walking deficits; 3.0, dropped pelvis; 3.5, unilateral hind limb paralysis; 4.0, bilateral hind limb paralysis; 4.5, forelimb paralysis; and 5.0, moribund. Those assessing the mice were blinded to the treatment groups.

## **2.10 Tissue Collection and Analysis**

Mice were humanely killed at DPI 15 or 30 by intraperitoneal injection of an overdose of pentobarbital (150 mg/kg). Blood was then collected via cardiac heart puncture and centrifuged at 1000 rpm for 10 min at 4°C to isolate the plasma which was stored at -80°C. The spleen was also removed and weighed. Each spleen was washed with PBS to collect the splenocytes that were then centrifuged at 400 xg for 8 min. After removing the supernatant, red cell lysis buffer (4 ml) was added for 15-20 min at room temperature. Subsequently, PBS-EDTA (3 ml) was added and the cells were centrifuged as before. The cells were then lysed in Aurum<sup>TM</sup> lysis solution (Bio-Rad) and stored at -80°C until performing qRT-PCR. Additionally, subsets of spleens were collected for flow cytometry. These spleens were mashed and filtered through a 40 µm nylon mesh,

centrifuged at 400 xg for 8 min, then suspended in red blood cell lysis buffer (4 ml). Twenty minutes later, the cells were washed and stained for flow cytometry as described above. Protein was also extracted from liver samples. Livers were homogenized to a single cell suspension with the BeadBug™ Microtube Homogenizer (ThermoFisher) using 1 ml PBS (Bio-Rad) and silicone beads. The resulting suspension was then transferred to a 1.5 ml micro-centrifuge tube and stored at -80°C until western blotting. Finally, the marrow from spinal cords was collected and homogenized to a single cell suspension with the BeadBug™ Microtube Homogenizer (ThermoFisher) using 1 ml Trizol (Bio-Rad) and silicone beads. mRNA was extracted with the Aurum™ Total RNA Fatty and Fibrous Tissue Kit (Bio-Rad) for qRT-PCR analysis as described above.

### **2.11 Multiplexed enzyme-linked immunosorbent assays**

A multiplex enzyme-linked immunosorbent assay (ELISA) was performed using the Bio-Plex Pro™ Mouse Cytokine Group1 Panel 23-plex (Bio-Rad) kit to measure the relative concentrations (pg/ml) of 23 cytokines: IL-1 $\alpha$ , IL-1 $\beta$ , IL-2, IL-3, IL-4, IL-5, IL-6, IL-9, IL-10, IL-12p40, IL-12p70, IL-13, IL-17A, Eotaxin, G-CSF, GM-CSF, IFN- $\gamma$ , KC, MCP-1, MIP-1 $\alpha$ , MIP-1 $\beta$ , RANTES and TNF-  $\alpha$ . Blood plasma was collected from mice at DPI 15 for the following 4 treatment conditions: CFA + vehicle, CFA + LCL161, EAE + vehicle and EAE + LCL161. All procedures were done in accordance with the manufacturer's instructions and analyzed using a Bio-Plex® 200 system. Statistical analysis was performed by unpaired t-test to assess changes in cytokine concentration.

## CHAPTER 3: RESULTS

### **3.1 cIAP2 ablation reduced macrophage generation from BMDMs cultured under mild M1 polarizing conditions**

The percentages of macrophages generated by either mild M1 (GM-CSF) or mild M2 (M-CSF) polarizing conditions in BMDM cultures derived from both wild-type (WT) C57BL/6 mice or cIAP2 nulls were compared (Figure 4). Representative flow cytometry analyses (dot plots) show the gating used to count M1 (pink boxes) and M2 (light blue boxes) macrophages detected by double-labeling with antibodies against CD11b (general myeloid marker) and F4/80 (macrophage specific marker; Figure 4A). The x-axis (CD11b) and y-axis (F4/80) applies to each individual dot plot. The percentages of macrophage in BMDMs cultured under either mild M1 or mild M2 polarizing conditions were determined from the dot plots (Figure 4B). Under mild M1 polarizing conditions, a lower percentage of macrophages was generated from cIAP2 null (~20%) than WT (~30%) cultures (Figure 4B). By comparison, higher percentages of macrophages were observed in both WT and cIAP2 nulls BMDMs cultured under mild M2 polarizing conditions with just over 95% double-positive cells detected for these two genotypes (Figure 4B).

### **3.2 cIAP2 null BMDMs exposed to strong M2 polarizing conditions displayed reduced macrophage generation relative to WT cultures**

Subsequently, the percentages of macrophages generated by either strong M1 (GM-CSF+LPS) or strong M2 (M-CSF+IL-4) polarizing conditions in WT BMDM and cIAP2 null cultures were compared (Figure 5). Representative flow cytometry analyses (dot

plots) show the gating for M1 (red boxes) and M2 (blue boxes) macrophages detected by double-labeling with antibodies against CD11b and F4/80 (Figure 5A). The x-axis (CD11b) and y-axis (F4/80) applies to each individual dot plot. The percentages of double-positive cells in the BMDM cultures are presented in Figure 5B. By comparison to mild M1 or M2 polarizing conditions, higher percentages of macrophages were generated by strong M1 or M2 polarizing conditions. Unlike mild M1 polarization conditions for which fewer macrophages were produced in cIAP2 null than WT BMDMs, comparable percentages of double-positive cells were observed in WT (~68%) and cIAP2 null (~64%) BMDMs cultured under strong M1 polarizing conditions (Figure 5B). However, under strong M2 polarizing conditions a lower percentage of macrophages was generated in cIAP2 null (~87%) than WT BMDM cultures (~96%; Figure 5B).

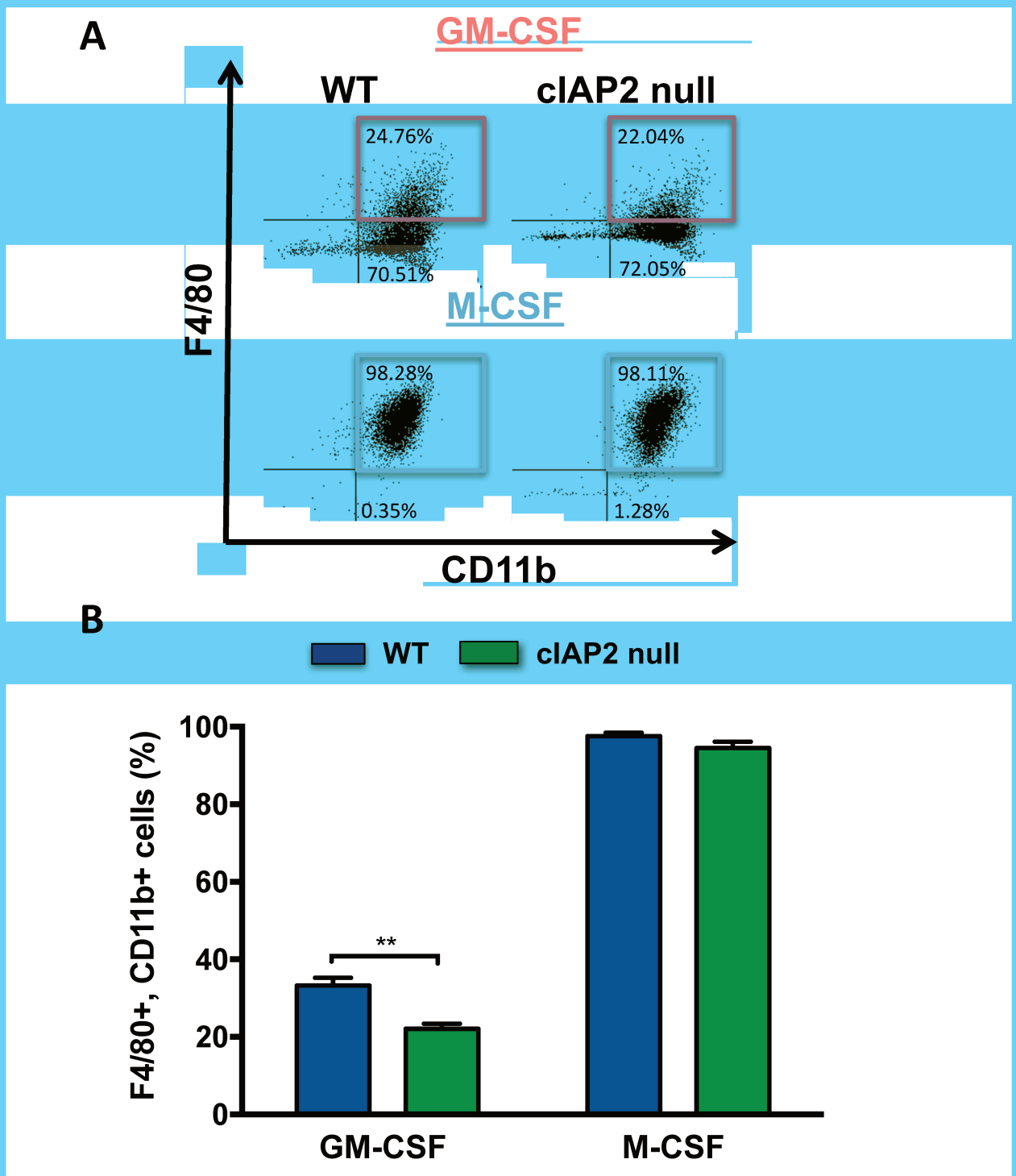


**Figure 4:** Flow cytometry analyses of WT and cIAP2 null BMDMs double-labelled with antibodies against CD11b and F4/80 that were cultured under mild M1 (GM-CSF) or M2 (M-CSF) polarizing conditions. A) Representative flow cytometry analyses (dot plots) showing the gating for M1 (pink boxes) and M2 (light blue boxes) double-positive macrophages. Percentages in lower right quadrants correspond to cells immunopositive for just CD11b. B) Percentages of double-positive cells generated from WT or cIAP2 null BMDMs cultured under mild M1 or M2 polarizing conditions. \*\* $p < 0.01$ , Mann-Whitney U test (n=4).

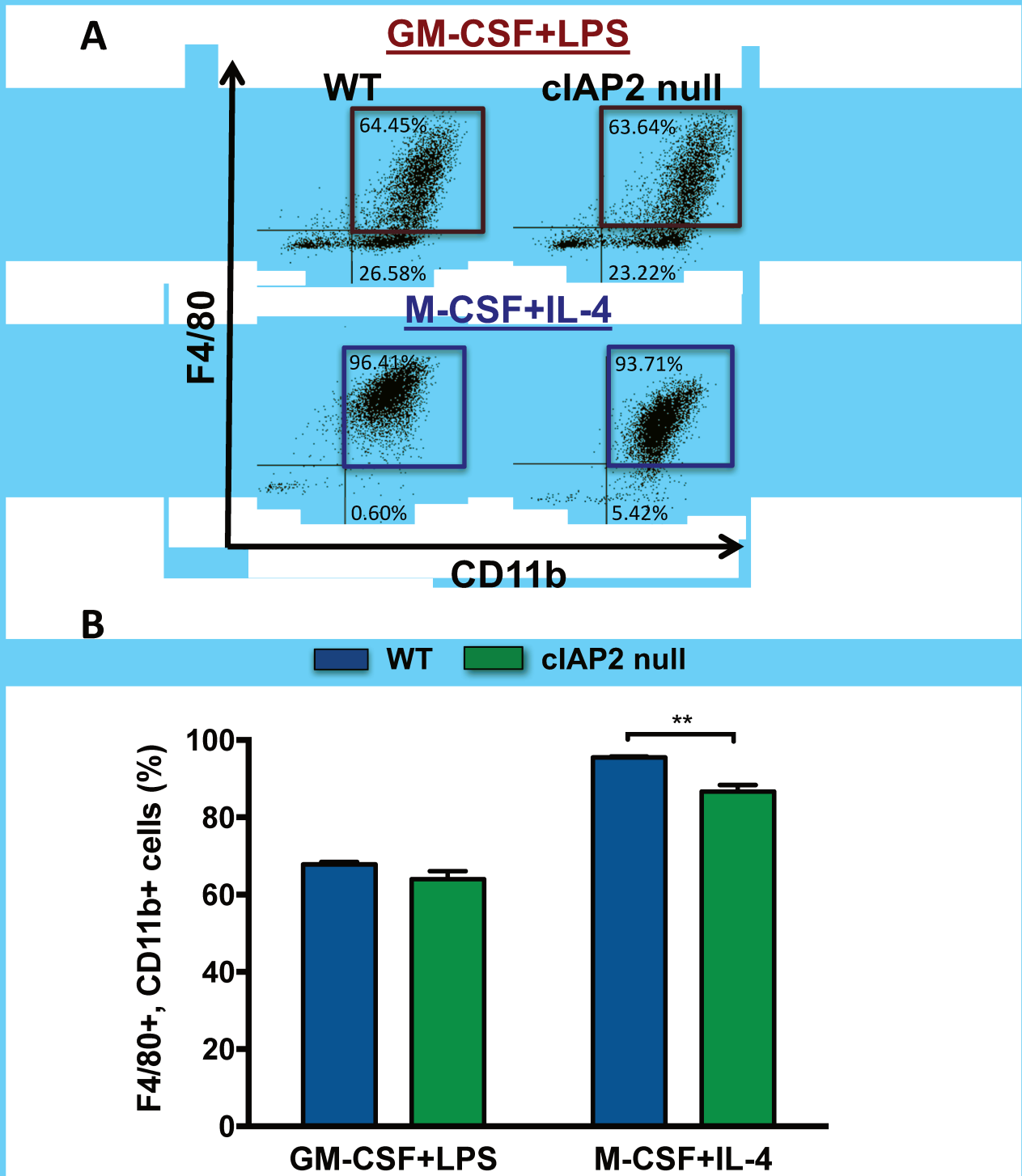


**Figure 5:** Flow cytometry analyses of WT and cIAP2 null BMDMs double-labelled with antibodies against CD11b and F4/80 that were cultured under strong M1 (GM-CSF+LPS) or M2 (M-CSF+IL-4) polarizing conditions. A) Representative flow cytometry analyses (dot plots) showing the gating for M1 (red boxes) and M2 (blue boxes) double-positive macrophages. Percentages in lower right quadrants correspond to cells immunopositive for just CD11b. B) Percentages of double-positive cells generated from WT or cIAP2 null BMDMs cultured under strong M1 (GM-CSF+LPS) or M2 (M-CSF+IL-4) polarizing conditions. \*\* $p < 0.01$ , Mann-Whitney U test ( $n = 4$ )

### **3.3 cIAP2 ablation increased BMDM apoptosis under strong M2 polarizing conditions**

The loss of cIAP2 may have increased apoptotic cell death, thus contributing to the decreased generation of macrophages in BMDMs cultured under mild M1 (Figure 4B) and strong M2 (Figure 5B) polarizing conditions. BMDM cultures derived from WT and cIAP2 null mice were stained with Annexin V to detect apoptotic cells (Figure 6). The percentages of Annexin V positive cells were similar for WT and cIAP2 null BMDMs cultured under mild M1 (GM-CSF; ~8-15%), strong M1 (GM-CSF+LPS; ~15%) or mild M2 (M-CSF; ~10%) polarizing conditions. However, under strong M2 polarizing conditions (M-CSF+IL-4) the percentages of Annexin V positive cells were increased for cIAP2 null (~18%) relative to WT BMDM cultures (~8%).

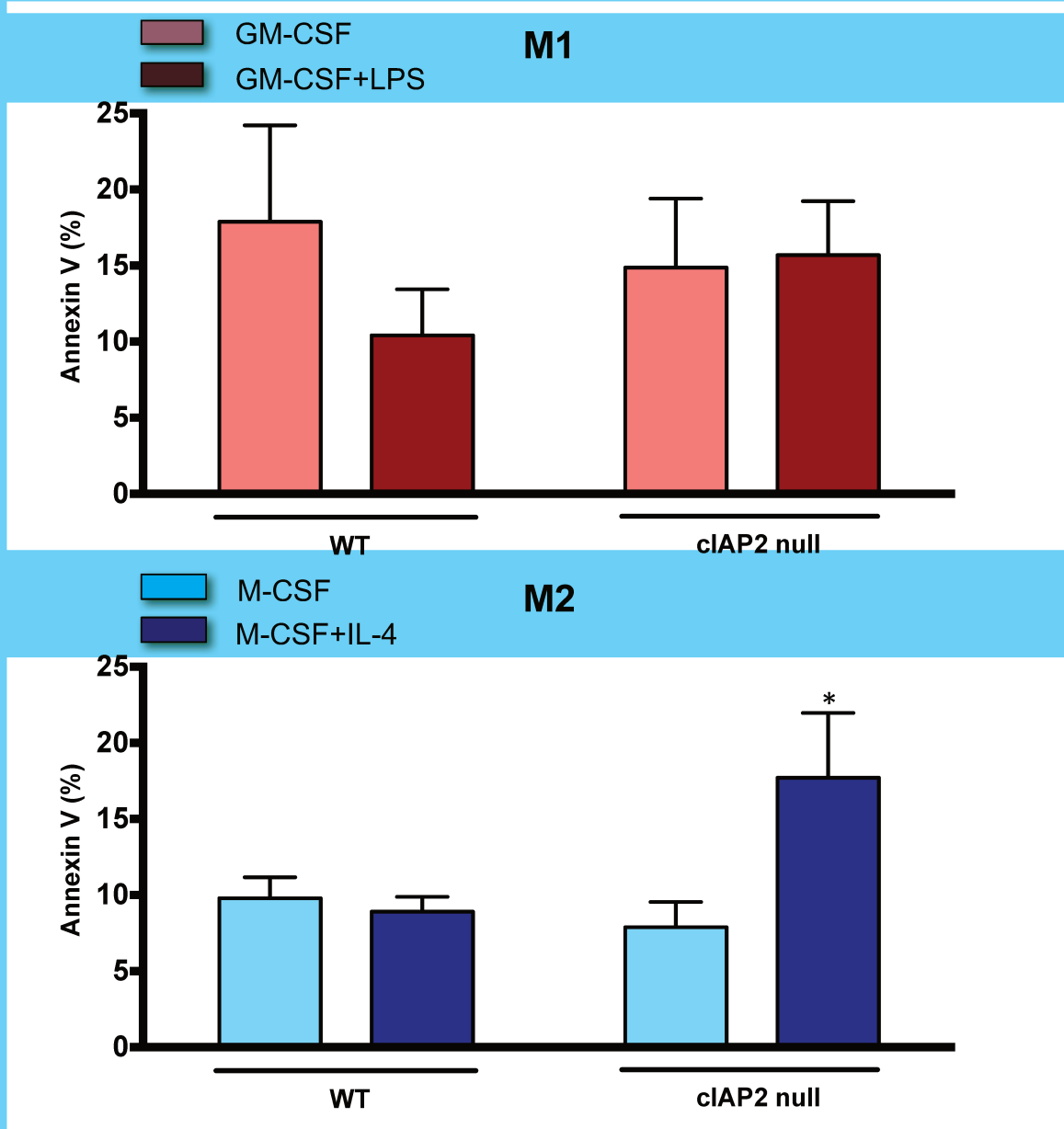


**Figure 6:** Flow cytometry analyses of Annexin V positive WT and cIAP2 null macrophages detected in BMDMs cultured under mild M1 (GM-CSF), strong M1 (GM-CSF+LPS), mild M2 (M-CSF) or strong M2 (M-CSF+IL-4) polarizing conditions. After gating for double-positive macrophage cells (CD11b<sup>+</sup>, F4/80<sup>+</sup>), the percentages of Annexin V positive cells were determined. \*p<0.05, Mann-Whitney U test (n=4).

### **3.4 cIAP2 deficiency impaired BMDM differentiation by strong M1 and M2**

#### **polarizing conditions**

After 7 days in culture, BMDMs cultured under strong M1 or M2 polarizing conditions were collected and analyzed for levels of M1 and M2 mRNA markers by qRT-PCR. Differences in TNF- $\alpha$ , CD86, P2Y12, IL-10 and CD206 expression under strong M1 (GM-CSF+LPS) or M2 (M-CSF+IL-4) polarizing conditions are expressed relative to mRNA levels for cultures maintained under mild M1 (GM-CSF) or M2 (M-CSF) polarizing conditions, respectively. Statistical comparisons were only made between WT and cIAP2 null BMDMs cultured under either strong M1 or M2 polarizing conditions. Under strong M1 polarizing conditions, cIAP2 null cells displayed reduced M1 (TNF- $\alpha$  and CD86) marker mRNA levels relative to WT cultures (Figure 7A and C). By contrast, mRNA levels for the M2 markers P2Y12, IL-10 and CD206 were elevated for cIAP2 null compared to WT BMDMs (Figure 7B, D and E). Under strong M2 polarizing conditions, cIAP2 null BMDMs showed reduced mRNA levels for CD86 (M1 marker) as well as P2Y12 and IL-10 (M2 markers), relative to WT cultures, suggesting a failure of both M1 and M2 polarization. The expression of cIAP2 in WT cells under M1 and M2 polarizing conditions was also examined (Figure 8). cIAP2 mRNA levels were similar under strong M1 and M2 polarizing conditions.

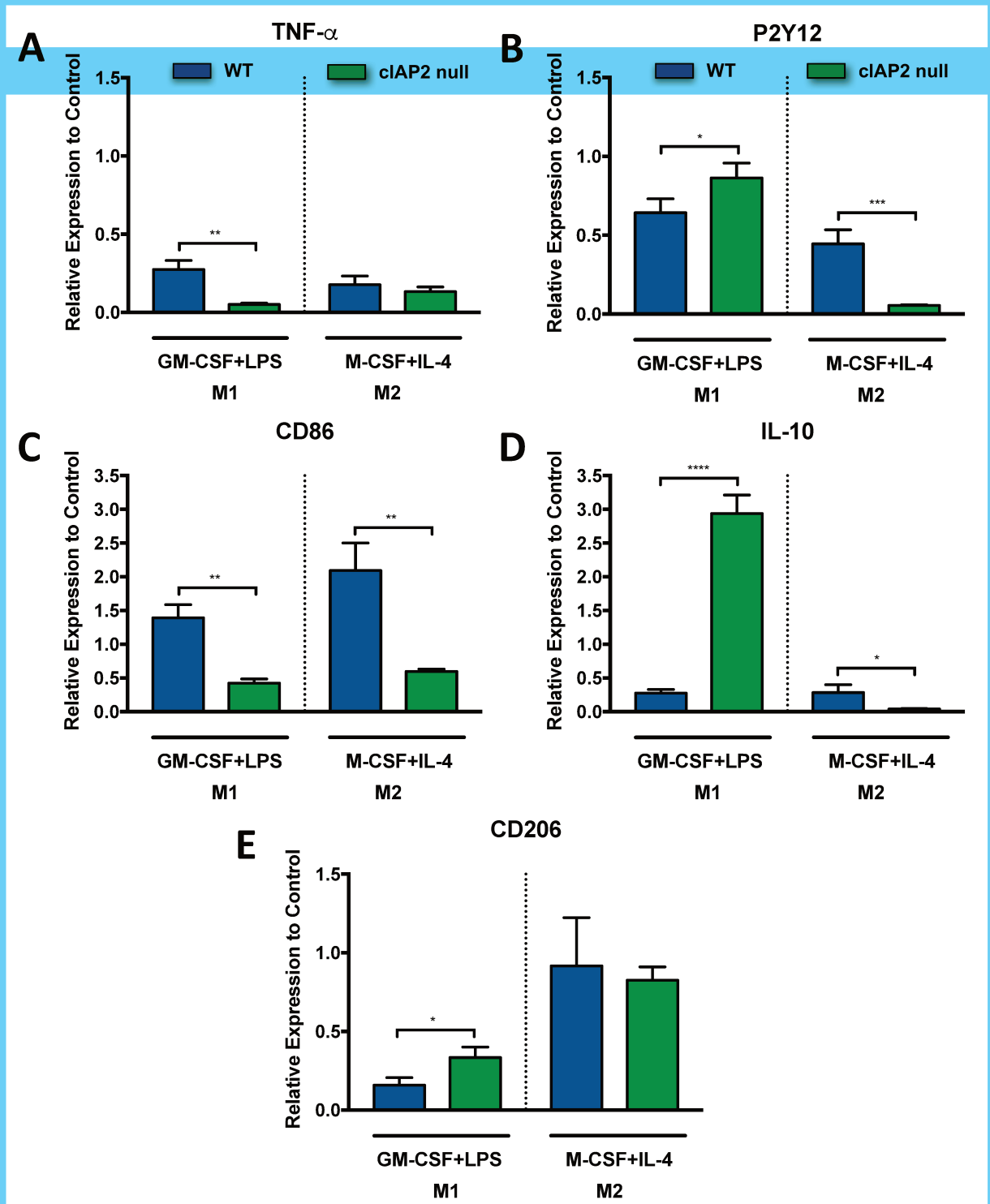


**Figure 7:** M1 (A and C) and M2 (B, D and E) marker mRNA levels for WT and cIAP2 null BMDMs cultured under strong M1 (GM-CSF+LPS) or M2 (M-CSF+IL-4) polarizing conditions expressed relative to BMDMs exposed to mild M1 (GM-CSF) or M2 (M-CSF) polarizing conditions, respectively. \* $p < 0.05$ , \*\* $p < 0.01$ , \*\*\* $p < 0.001$ , \*\*\*\* $p < 0.0001$ , unpaired t-test ( $n=3$ ).

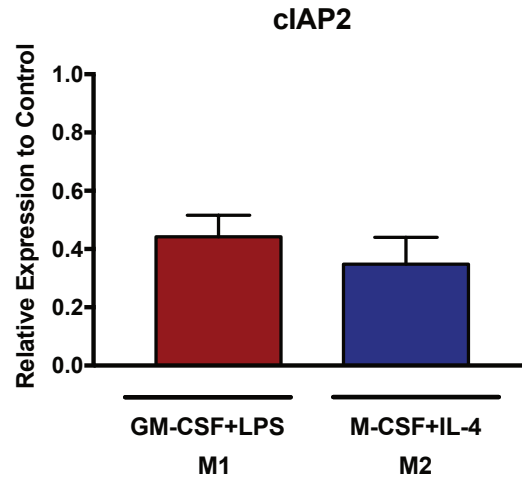


**Figure 8:** cIAP2 mRNA levels for BMDMs grown under strong M1 (GM-CSF+LPS) or M2 (M-CSF+IL-4) polarizing conditions expressed relative to cultures maintained under mild M1 (GM-CSF) or M2 (M-CSF) polarizing condition, respectively. Unpaired t-test (n=3).

### **3.5 Macrophage selection of BMDM cultures by immunopanning**

To select for macrophages, BMDM cultures were immunopanned with the F4/80 antibody that binds the macrophage-specific EGF-like module-containing mucin-like hormone receptor-like 1<sup>68</sup>. After 7 days of culture, BMDMs were collected and plated on petri dishes coated with the F4/80 antibody to isolate macrophage cells. After 1 hr, non-adherent cells located in the supernatant were removed, stained with antibodies against CD11b and F4/80 and analyzed by flow cytometry for double-positive cells (macrophages). Figure 9 shows representative flow cytometry analyses (dot plots) of double-positive (CD11b and F4/80) macrophages in the supernatant of non-immunopanned and immunopanned BMDMs cultures. Gating used to measure macrophages produced by mildly M1 or M2 polarizing conditions are indicated by pink and light blue boxes, respectively (Figure 9A). Gating used to quantify macrophages generated by strong M1 or M2 polarizing conditions are represented by red and blue boxes, respectively (Figure 9B). The x-axis (CD11b) and y-axis (F4/80) applies to each individual dot plot (Figure 9A and B). Relative to the percentages of macrophages in the supernatants of non-immunopanned BMDMs, immunopanned BMDM cultures showed reduced supernatant macrophage percentages: mild M1 (29.04%-17.75%), mild M2 (84.35%-78.13%), strong M1 (52.70%-24.82%) and strong M2 (92.69%-84.35%). The relative smaller decreases in the macrophage percentages produced by immunopanning for mild M2 and strong M2 polarized cultures may reflect the higher numbers of macrophages in these cultures that saturated F4/80 binding sites thus leaving more macrophages in the supernatant. These findings indirectly support the effectiveness of my immunopanning technique by showing that the adherence of macrophages to F4/80

coated-dishes depleted macrophage percentages in the supernatant. These macrophage-purified BMDMs will be termed mpBMDMs.

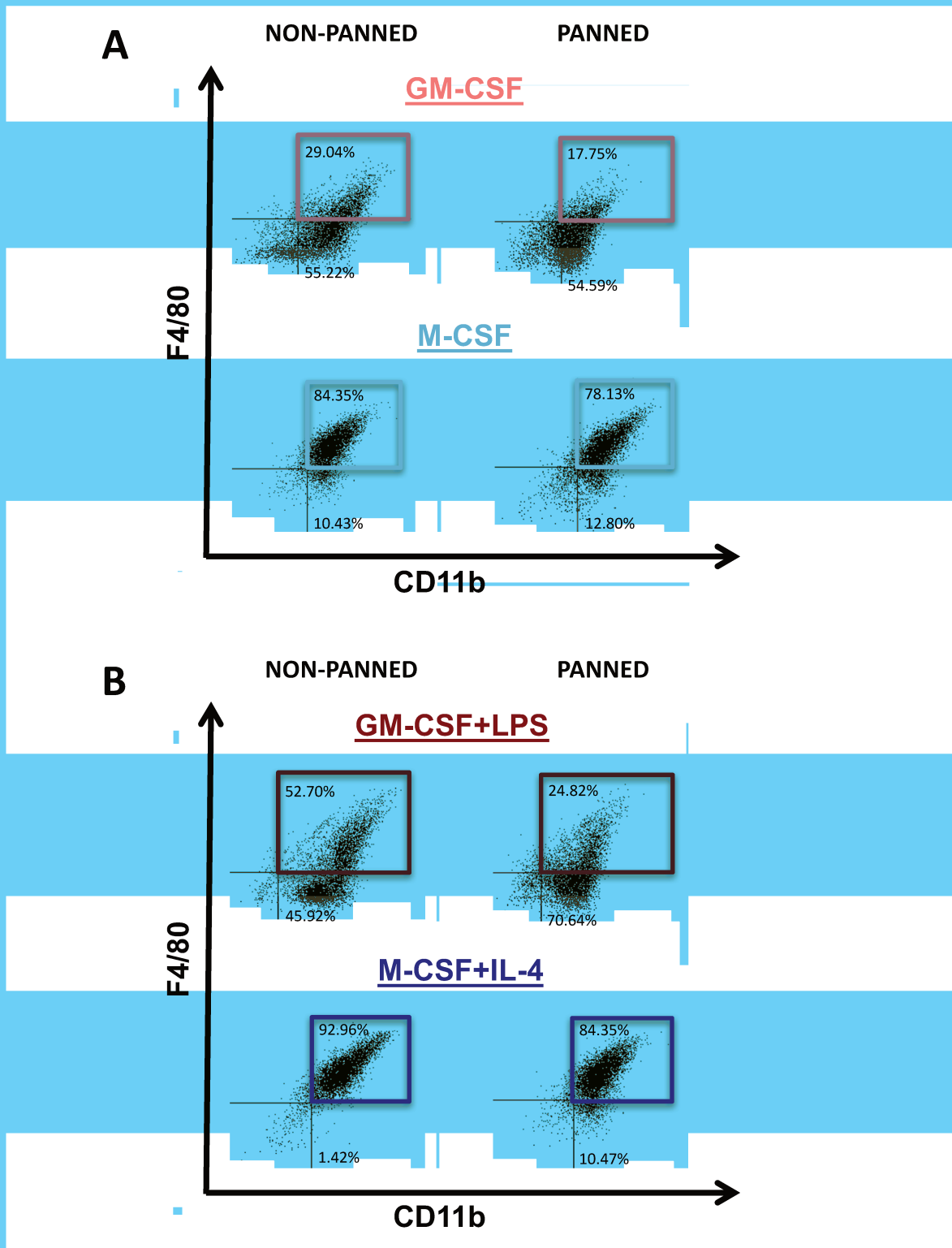


**Figure 9:** Flow cytometry analyses of macrophages double-positive for CD11b and F4/80 in the supernatant of non-immunopanned and immunopanned BMDMs. A) Flow cytometry analyses (dot plots) for BMDMs cultured under M1 mild (pink) and M2 (light blue) polarizing conditions. B) Flow cytometry analysis (dot plots) for BMDMs cultured under strong M1 (red) or strong M2 (blue) polarizing conditions. Percentages in lower right quadrants correspond to cells immunopositive for just CD11b.

### **3.6 cIAP2 null mpBMDMs displayed enhanced M1 and M2 marker expression under M2 polarizing conditions**

In the next series of studies, the effects of cIAP2 loss on M1 and M2 polarization for mpBMDMs was determined. Following 7 days in culture under strong M1 or M2 polarizing conditions, mpBMDMs were generated by immunopanning and analyzed for M1 and M2 marker mRNA levels by qRT-PCR (Figure 10). As in the previous experiments, M1 and M2 mRNA levels for strongly M1 or M2 polarized cultures are expressed as changes relative to values for cultures maintained under mild M1 (GM-CSF) or M2 (M-CSF) polarizing conditions, respectively. Additional M1 (CD38, Gpr18) and M2 (c-Myc, Erg2) markers were used to improve the detection of M1 and M2 mpBMDMs. Unlike non-immunopanned BMDMs (Figure 7), the levels of M1 marker mRNAs (TNF- $\alpha$ , Gpr18, CD38) were similar for WT and cIAP2 null mpBMDMs following strong M1 polarizing conditions (Figure 10A, C and E). This suggests that contamination by non-macrophage immune cell populations, such as dendritic cells, may have contributed to the reductions in M1 marker mRNA levels observed in non-immunopanned BMDMs derived from cIAP2 nulls. In stark contrast to non-immunopanned BMDMs for which strong M2 polarization reduced the expression of both M1 (CD86; Figure 7C) and M2 (P2Y12 and IL-10; Figure 7B and D) markers in cIAP2 null relative to WT BMDMs, both M1 (TNF- $\alpha$ , Gpr18 and CD38) and M2 (c-Myc, IL-10 and Egr-2) markers were elevated in cIAP2 null compared to WT mpBMDMs (Figure 10A-F). The overall expression for M1 markers (TNF- $\alpha$ , 3.9; Gpr18, 9.7; CD 38, 19.3) was higher than that for M2 markers (c-Myc, 6.4; IL-10, 4.0; Erg2, 1.8) suggesting that cIAP2 null macrophages adopted a more M1 than M2 state under strong

M2 polarization conditions. Lastly, WT cells displayed higher cIAP2 levels when cultured under strong M1 than M2 polarizing conditions.

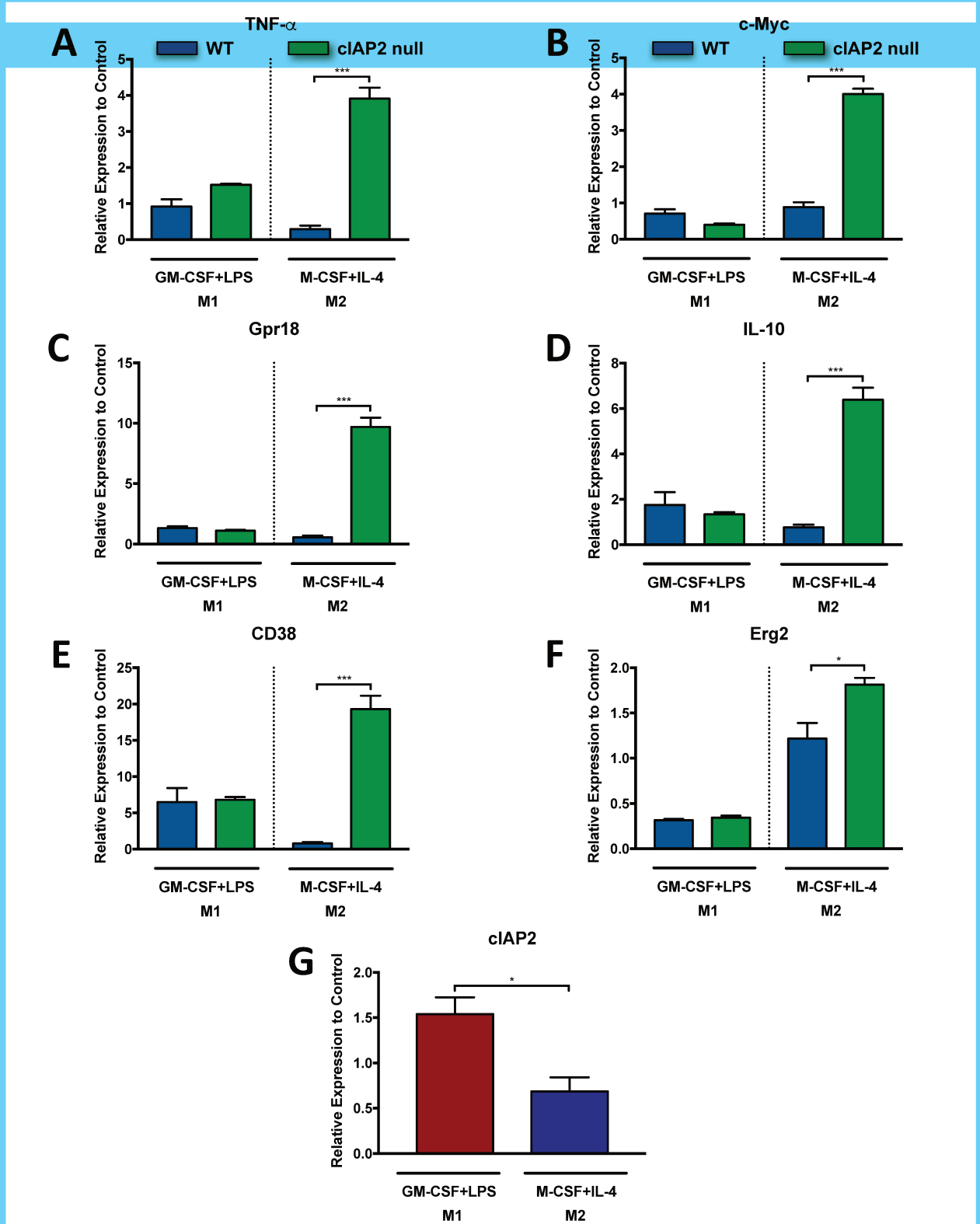


**Figure 10:** M1 marker (A, C and E), M2 marker (B, D, and F) and cIAP2 (G) mRNA levels for WT and cIAP2 null mpBMDMs selected by immunopanning from BMDM cultures grown under strong M1 (GM-CSF+LPS) or M2 (M-CSF+IL-4) polarizing conditions expressed relative to mpBMDMs exposed to mild M1 (GM-CSF) or M2 (M-CSF) polarizing conditions, respectively. \* $p < 0.05$ , \*\*\* $p < 0.001$ , unpaired t-test ( $n = 3$ ).

### **3.7 cIAP1 and cIAP2 protein levels were reduced in WT BMDMs treated with LCL161**

To test the ability of the SMAC mimetic LCL161 to reduce cIAP1 and cIAP2 (cIAP1/2) protein levels, WT BMDM cultures were treated with LCL161 and analyzed by western blotting. Vehicle (DMSO, 0.01%) or LCL161 (10  $\mu$ M) was added to WT BMDM on culture day 6 for 24 hr. On culture day 7, BMDMs were collected for protein extraction. Relative to WT cultures exposed to strong M1 polarizing conditions, LCL161 reduced both cIAP1/2 protein levels in BMDMs cultured under mild M1, mild M2, and strong M1 polarizing conditions (Figure 11). Sufficient protein levels could not be collected for LCL161 treated BMDMs cultured under strong M2 polarizing conditions.

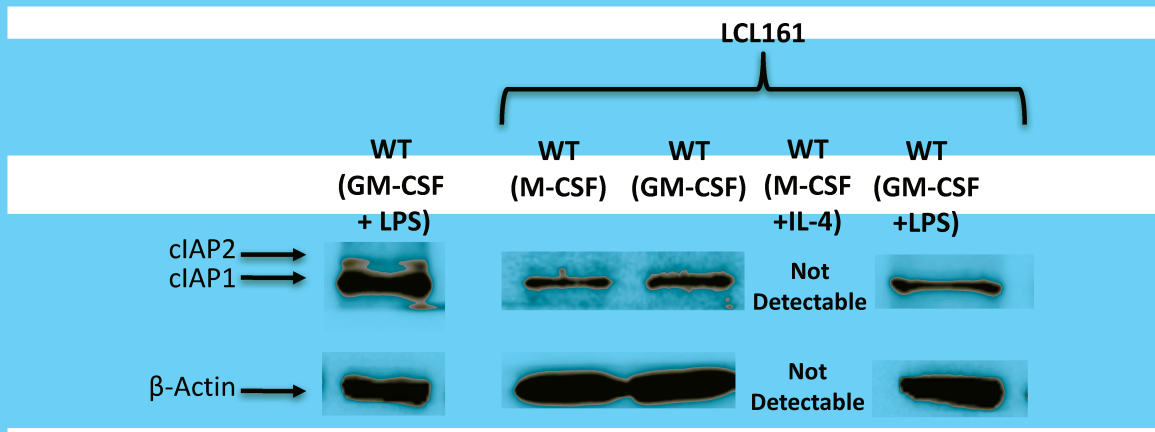


**Figure 11:** Effects of treatment with the SMAC-mimetic LCL161 (10  $\mu$ M) for 24 hr on cIAP1/2 levels in BMDMs. Western blots for cIAP1/2 levels in WT BMDMs + vehicle cultured under strong M1 conditions, WT BMDMs + LCL161 cultured under mild M1, mild M2 or strong M1 conditions.  $\beta$ -Actin served as the loading control.

### **3.8 Immunopanning also reduced macrophage percentages in the supernatants of cultures treated with LCL161**

The SMAC mimetic LCL161 was used to acutely suppress both cIAP1 and cIAP2 (cIAP1/2) levels in WT BMDMs. WT BMDMs were cultured in the presence of vehicle (DMSO, 0.01%) or LCL161 (10  $\mu$ M) for 24 hr, immunopanned and the supernatant collected for flow cytometry analyses. Figure 12 shows representative flow cytometry analyses (dot plots) of double-positive (CD11b and F4/80) macrophages in the supernatants of non-immunopanned and immunopanned BMDMs cultures treated with LCL161. Macrophage gating for mildly polarizing M1 and M2 conditions are represented by pink and light blue boxes, respectively (Figure 12A). Macrophage gating for strong M1 and M2 polarizing conditions are represented by red and blue boxes, respectively (Figure 12B). The x-axis (CD11b) and y-axis (F4/80) applies to each individual dot plot (Figure 12A and B). Relative to non-immunopanned cultures, the percentages of double-positive cells were reduced in the supernatants for all immunopanned cultures: mild M1 (23.82%-14.89%), mild M2 (64.48%-35.59%), strong M1 (50.71%-25.75%), strong M2 (63.70%-29.07%).

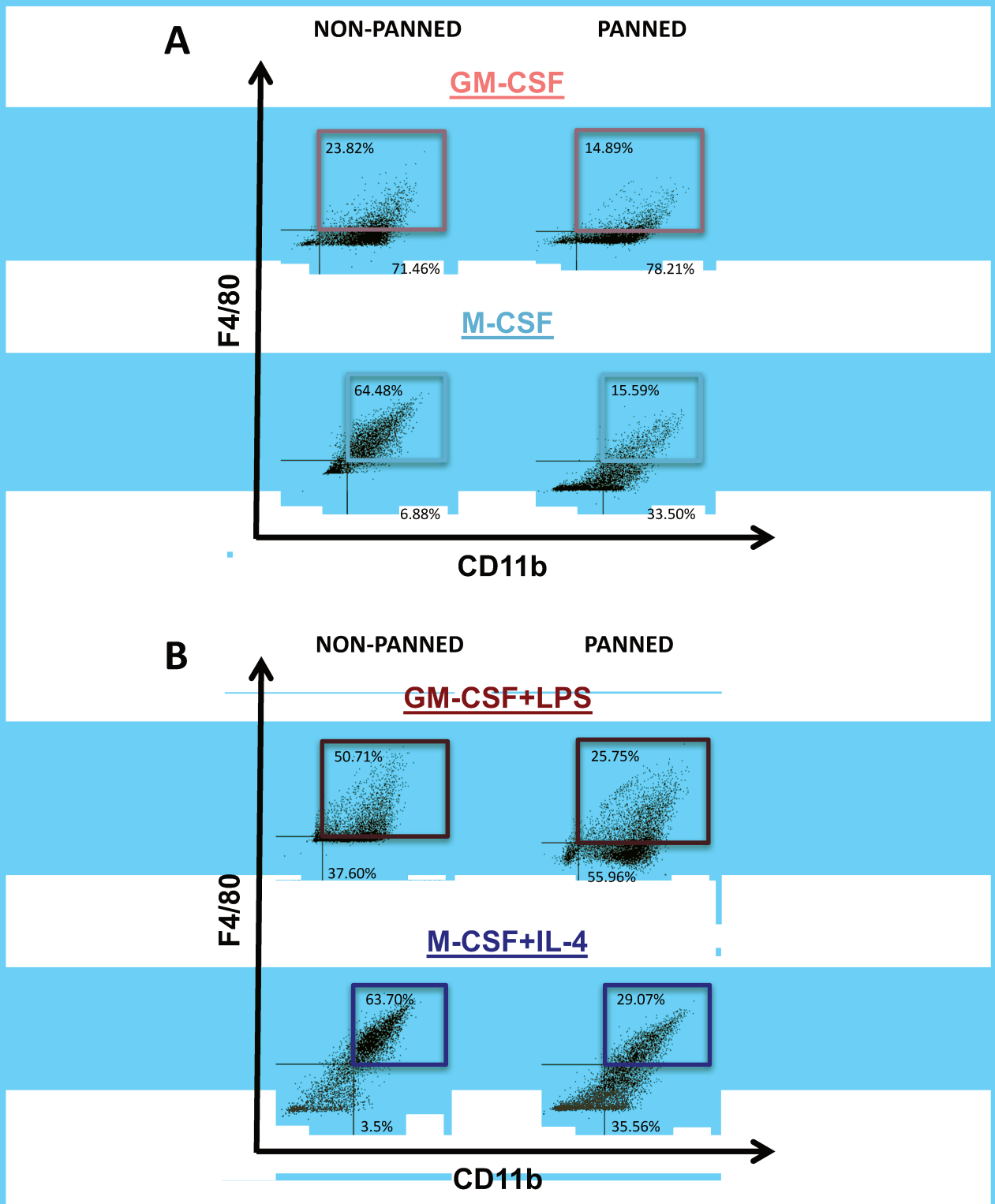


**Figure 12:** Flow cytometry analyses of macrophages double-positive for CD11b and F4/80 in the supernatant of non-immunopanned and immunopanned WT BMDMs treated with LCL161 (10  $\mu$ M) for 24 hr. A) Flow cytometry analysis (dot plots) for BMDMs cultured under mild M1 (pink) and M2 (light blue) polarizing conditions. B) Flow cytometry analysis (dot plots) for BMDMs cultured under strong M1 (red) or strong M2 (blue) polarizing conditions. Percentages in lower right quadrants correspond to cells immunopositive for just CD11b.

### **3.9 Acute suppression of cIAP1/2 levels with LCL161 induced a bias towards M1 polarization**

Following immunopanning, the effects LCL161 (10  $\mu$ M for 24 hr) on the polarization of mpBMDMs were determined by qRT-PCR measurements of M1 and M2 marker mRNA levels. Under strong M1 polarizing conditions, treatment with LCL161 enhanced M1 marker expression (TNF- $\alpha$  and CD38; Figure 13A and E), compared to vehicle-treated mpBMDMs. Although not statistically significant, mRNA levels for the M1 marker Gpr18 also showed a trend for increased levels ( $p=0.066$ ; Figure 13C). By contrast, mRNA levels for the M2 marker c-Myc were decreased in LCL161-treated cultures grown under strong M1 polarization conditions (Figure 13B). Collectively, these changes in M1 and M2 mRNA expression support a bias towards M1 following the acute inhibition of cIAP1/2 levels by LCL161. Lastly, under strong M1 polarization conditions, cIAP2 mRNA levels were enhanced by LCL161 suggestive of a compensatory increase in transcription resulting from the enhanced proteasomal-mediated degradation of cIAP2 induced by this SMAC mimetic<sup>12,20</sup>. Under strong M2 polarizing conditions sufficient mRNA could not be collected from LCL161 treated cells. Therefore, how LCL161 treatment affects macrophage polarization, compared to vehicle treated cells, could not be determined.

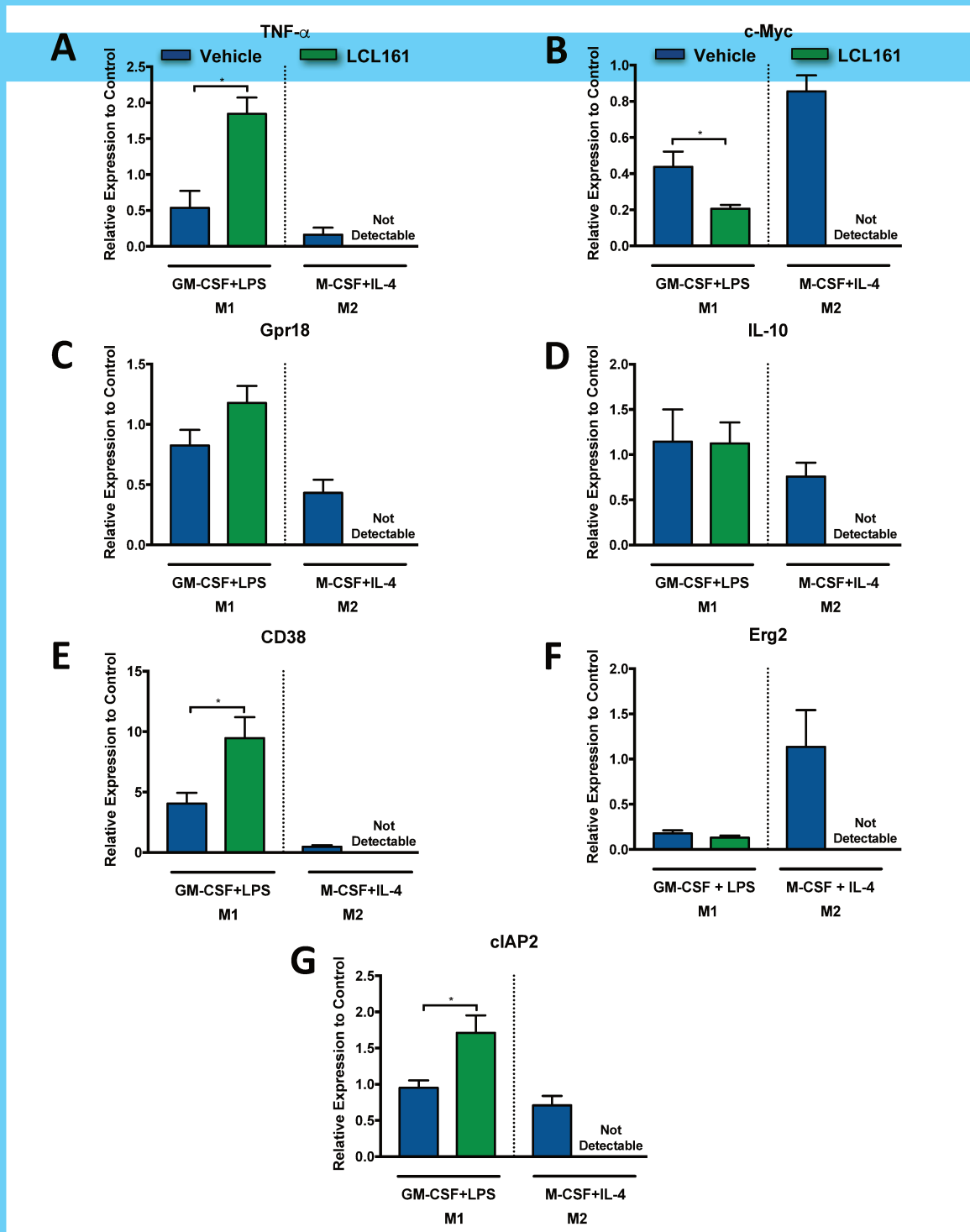


**Figure 13:** M1 marker (A, C and E), M2 marker (B, D, and F) and cIAP2 (G) mRNA levels for vehicle and LCL161 treated mpBMDMs obtained from cultures grown under strong M1 (GM-CSF+LPS) or M2 (M-CSF+IL-4) polarizing conditions. M1 and M2 mRNA levels are expressed relative to mpBMDMs derived from cultures exposed to mild M1 (GM-CSF) or M2 (M-CSF) polarizing conditions, respectively. \* $p < 0.05$ , \*\*\* $p < 0.001$ , unpaired t-test ( $n=3$ ).

### **3.10 Acute suppression of cIAP1/2 levels with LCL161 enhanced apoptosis in BMDMs cultured under strong M2 polarizing conditions**

Elevated apoptotic death was detected in cIAP2 null BMDMs exposed to strong M2 polarization conditions (Figure 6). Since both cIAP1 and cIAP2 levels are suppressed by LCL161 (Figure 11), the dual reduction in these proteins may have promoted massive apoptotic cell death resulting in the failure to detect M1 and M2 marker mRNA levels in mpBMDMs obtained from cultures grown under strong M2 polarizing conditions (Figure 13). To determine the apoptotic status of LCL161-treated cultures, WT BMDMs were treated with LCL161 (10  $\mu$ M) for 24 hr then analyzed by flow cytometry for Annexin V (apoptosis marker). The percentages of Annexin V positive BMDMs (CD11b<sup>+</sup>, F4/80<sup>+</sup>) were elevated in LCL161-treated cultures grown under mild M1, strong M1 or mild M2 conditions (~30-40%; Figure 14) compared to untreated WT BMDMs (~10-15%; Figure 6). Moreover, under strong M2 polarizing conditions the percentage of apoptotic cells (~76%) in BMDMs treated with LCL161 was dramatically elevated compared to untreated-WT BMDMs (~8%) and cIAP2 null (~18%) BMDMs (Figure 6). Finally, LCL161 treatment elevated the percentage of apoptotic macrophages in BMDMs cultured under strong M2 (~76%) relative to mild M2 (~40%) polarizing conditions (Figure 14). Hence, the massive death of macrophages detected in cultures growth under strong M2 conditions appeared to account for the failure to detect M1 and M2 marker mRNAs under strong M2 polarizing conditions (Figure 13A-F).

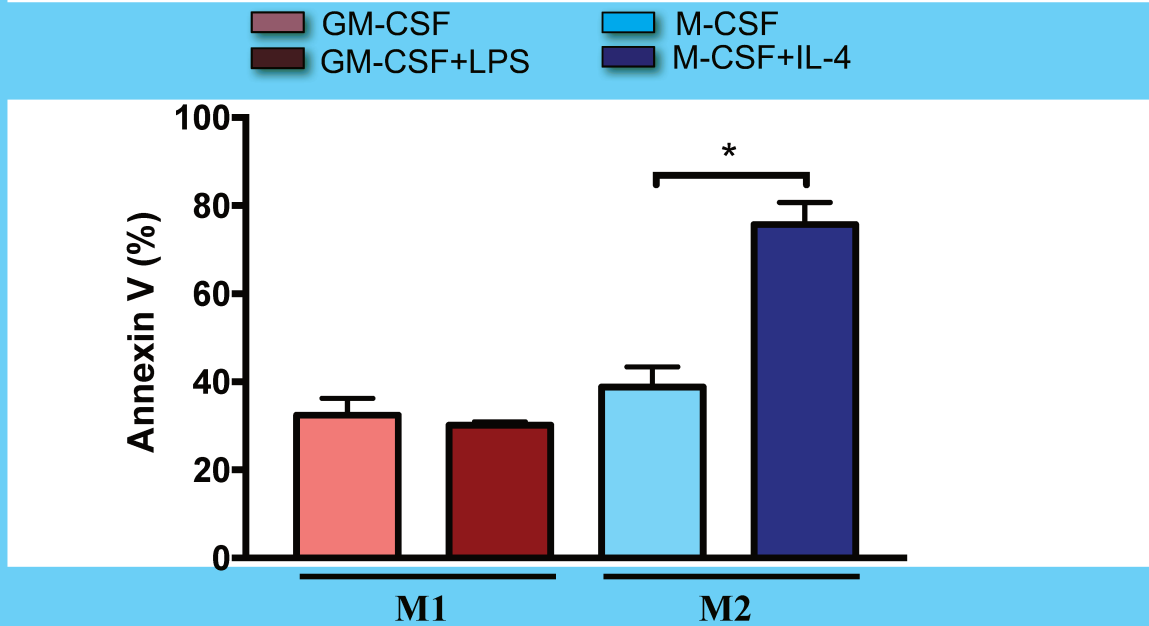


**Figure 14:** The apoptosis marker Annexin V was used to assess the effects of treatment for 24 hr with the SMAC-mimetic LCL161 (10  $\mu$ M) on WT BMDMs cultured under mild M1, strong M1, mild M2 or strong M2 polarizing conditions. After gating for double-positive macrophage cells (CD11b+, F4/80+), the percentages of Annexin V positive cells were determined. \* $p < 0.05$ , Mann-Whitney U test (n=3).

### **3.11 EAE mice dosed with LCL161 exhibited increased disease severity**

EAE was induced in WT female C57BL/6 mice by immunization with MOG<sub>35-55</sub> followed one day later (day-post immunization 1; DPI 1) by the start of oral dosing with either vehicle (100  $\mu$ l, NEOBEE) or LCL161 (50 mg/kg) that were administered every third day thereafter. The effects of LCL161 on the expression of M1 and M2 markers in the spinal cord and circulating cytokine levels were examined at peak disease (DPI 15). Relative to vehicle-treated mice, LCL161 elevated clinical scores from DPI 12-15 (Figure 15A). Liver, spinal cords, blood and spleens from these mice were harvested at DPI 15 to assess cIAP1/2 levels and immune status at peak disease. To determine the effect of LCL161 on EAE disease progression beyond DPI 15, a second series of EAE mice were treated with vehicle or LCL161 and monitored until DPI 30. In this experiment, LCL161-treated EAE mice displayed earlier disease onset and more severe clinical signs from DPI 11-30 than vehicle-treated EAE mice (Figure 15B). Western blotting of liver samples taken from these mice confirmed a reduction in cIAP1/2 protein levels by LCL161 treatment (Figure 15C). Immunization controls that received just CFA followed by treatment with either vehicle or LCL161 did not develop EAE and maintained a clinical score of 0 for the entire time course (data not shown).

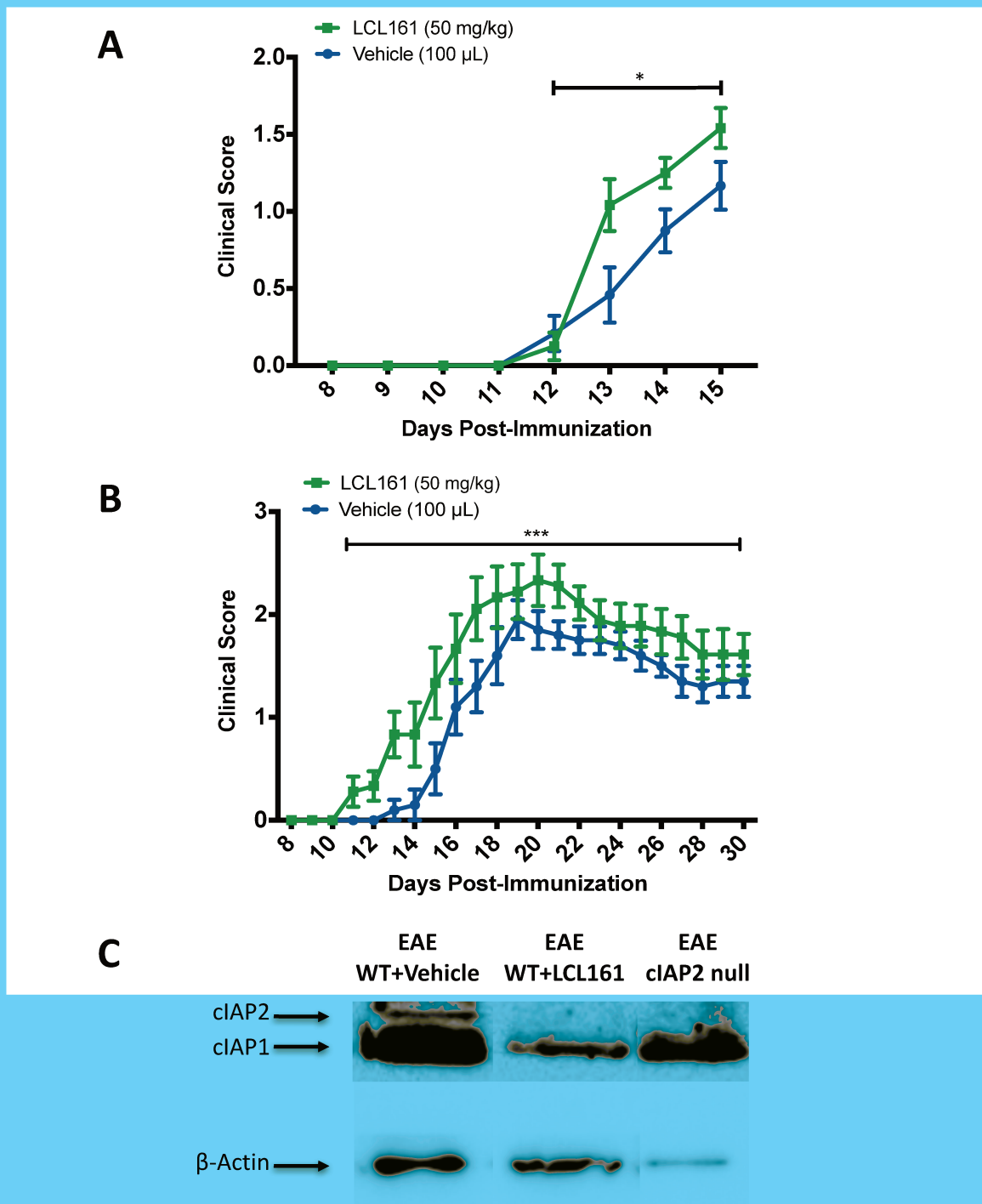


**Figure 15:** Clinical scores for EAE mice orally gavaged with vehicle (100  $\mu$ l) or LCL161 (50 mg/kg) once every 3 days from DPI 1-15 (A) or DPI 8-30 (B), n=9-12/group. \* $p$ <0.05, \*\*\* $p$ <0.001, Wilcoxon Test. C) Liver cIAP1/2 protein levels in EAE mice treated with vehicle or LCL161 or untreated EAE cIAP2 nulls.  $\beta$ -Actin antibody was used as a loading control.

### **3.12 LCL161 administration enhanced CD38 expression in the spinal cords of EAE mice**

The spinal cords from mice sacrificed at DPI 15 were collected and analyzed for M1 and M2 marker mRNA levels by qRT-PCR. CFA-treated mice served as MOG<sub>35-55</sub> antigen controls. For CFA controls, LCL161 reduced TNF $\alpha$  and elevated GPR18 relative to vehicle-treated mice (Figure 16B and F). For EAE mice, LCL161 increased CD38 (M1 marker) mRNA levels relative to vehicle-treated animals (Figure 16A). There were no differences between mRNA levels for all other M1 markers (TNF- $\alpha$ , Fpr2, CD86, NOS2 and Gpr18) between LCL161- and vehicle-treated EAE mice (Figure 16B-F). There were also no differences in mRNA levels for M2 markers (Erg2, P2Y12, and c-Myc; Figure 17A-C) mRNA and the chemoattractant MCP-1 (Figure 17D) between EAE mice that received vehicle or LCL161. However, mRNA levels for the M2 markers Erg2 and c-Myc were elevated in CFA mice treated with LCL161 compared to CFA animals given vehicle (Figure 17A and B).

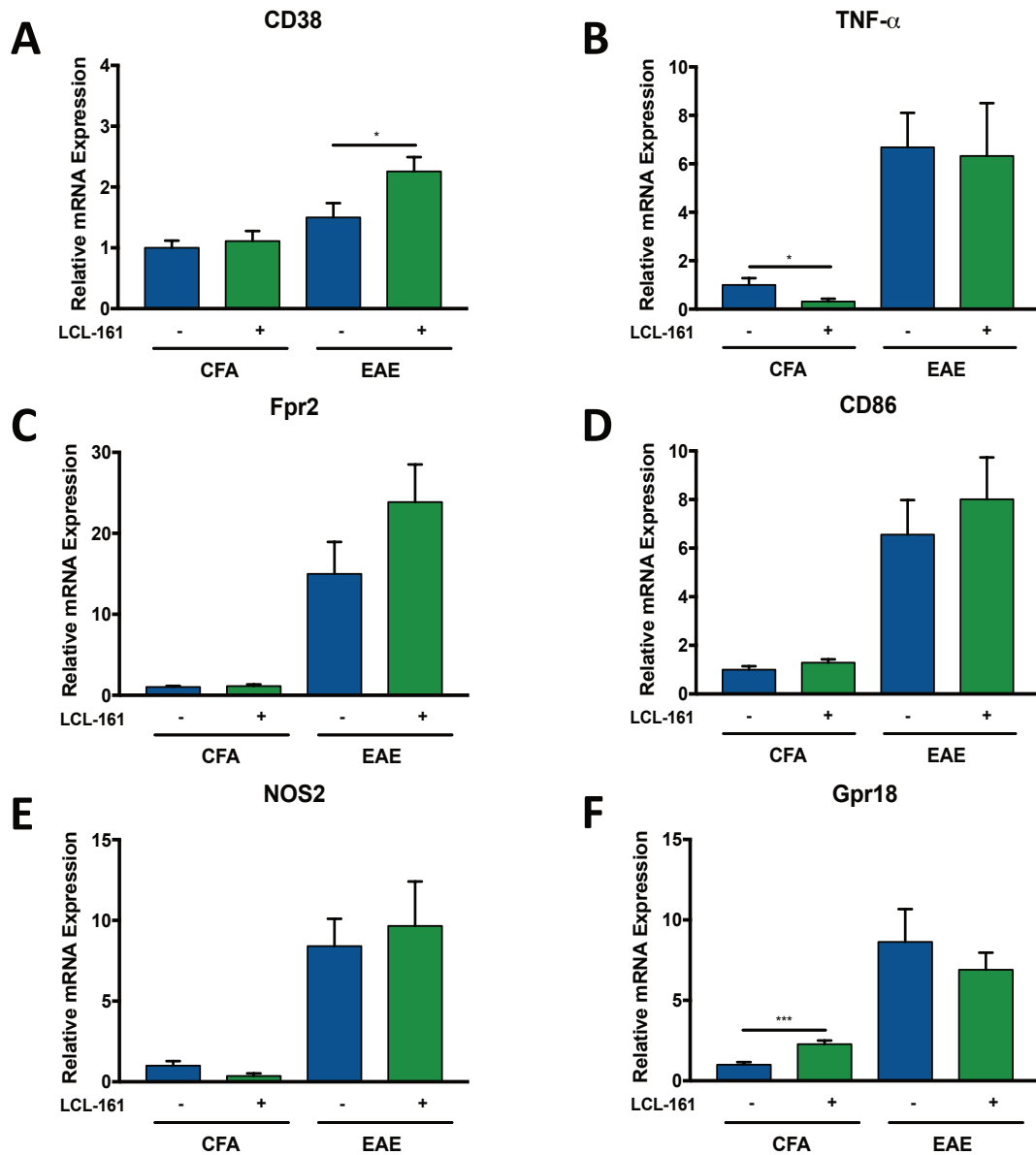


**Figure 16:** Effects of oral administration of vehicle (blue bars) or LCL161 (green bars) on spinal cord M1 marker mRNA levels (A-F) for CFA and EAE mice at DPI 15. \* $p < 0.05$ , \*\*\* $p < 0.001$ , unpaired t-test (n=8-10).

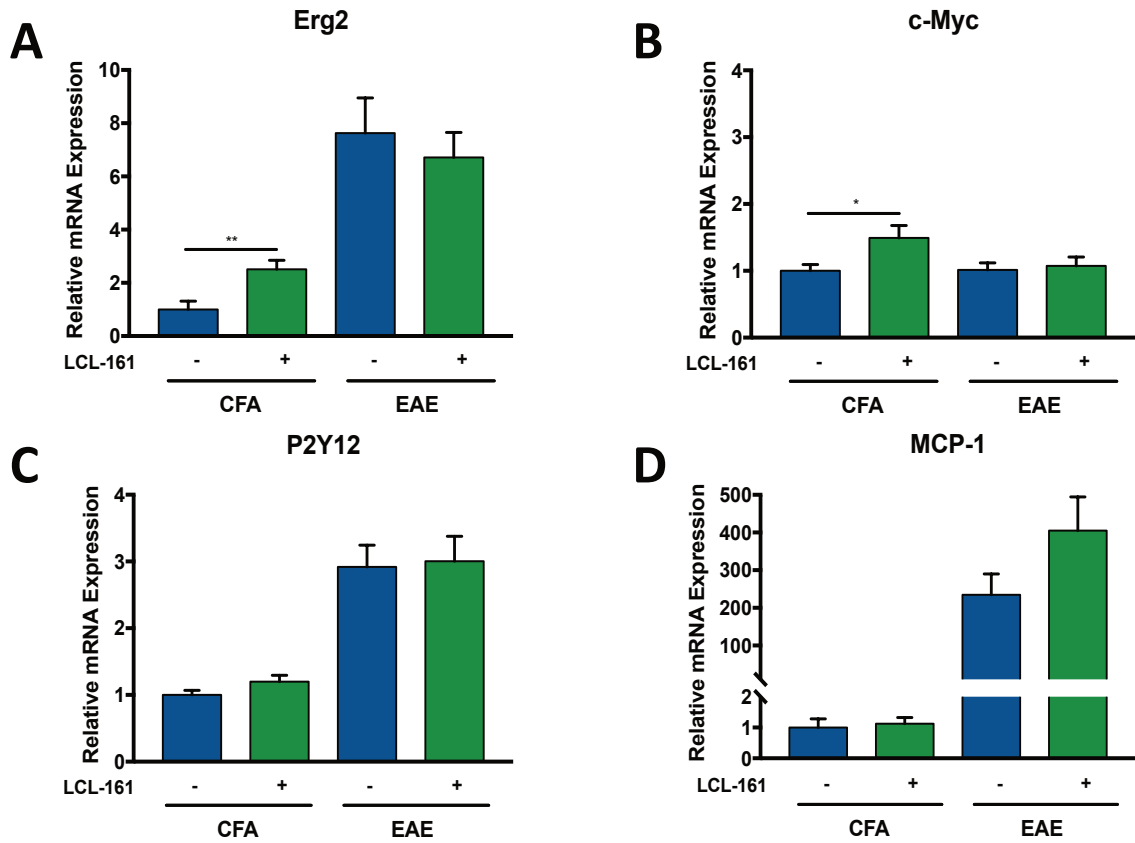


**Figure 17:** Effects of oral administration of vehicle (blue bars) or LCL161 (green bars) on spinal cord M2 marker (A-C) and chemoattractant MCP-1 (D) mRNA levels in CFA and EAE mice at DPI 15. \* $p < 0.05$ , \*\* $p < 0.01$ , unpaired t-test ( $n = 8-10$ ).

### **3.13 LCL161 suppressed both Th1 and Th2 cytokine concentrations in EAE mice**

Blood was also collected at DPI 15 to assess plasma cytokine concentrations by multiplexed ELISAs. The cytokines analyses were broadly classified into four categories: Th1 cytokines, Th2 cytokines, growth and differentiation cytokines and chemoattractant markers. Statistical comparisons were only made between vehicle and LCL161 treated animals for both CFA and EAE disease conditions. Concentrations of the pro-inflammatory (Th1) cytokines TNF- $\alpha$ , IFN- $\gamma$  and IL-1 $\beta$  (Figure 18; A, B and D) were reduced in EAE mice dosed with LCL161 compared to EAE mice that received vehicle. Interestingly, IL-12p40 concentrations were elevated in vehicle-treated relative to LCL161-treated CFA mice while LCL161 had the reverse effects on EAE mice (Figure 18E). By contrast, the opposite trends were observed for IL-12p70 (Figure 18F). These results may be explained by the antagonistic action of IL-12p40 on activation of the IL-12 receptor by IL-12p70<sup>69</sup>. LCL161 did not alter concentrations for the remaining Th1 cytokines IL-1 $\alpha$  and IL-17A (Figure 18C and G). LCL161-treated EAE mice also displayed reduced concentrations of the anti-inflammatory (Th2) cytokines IL-10, IL-13 and IL-5 (Figure 19A-C). These findings indicate that LCL161 disrupted both pro- and anti-inflammatory immune responses in EAE animals. Additionally, the concentrations of both IL-6 and IL-3, cytokines related to growth and differentiation, were reduced by LCL161 treatment in EAE mice (Figure 20A and B). However, GM-CSF concentrations were not changed by LCL161 (Figure 20C). Finally, plasma concentrations of the chemoattractants CXCL1, CCL2, CCL3, CCL4, CCL5 and Eotaxin were measured (Figure 21A-F). Only CXCL1 and CCL4 concentrations were reduced in LCL161-treated relative to vehicle-treated EAE mice (Figure 21A and D).

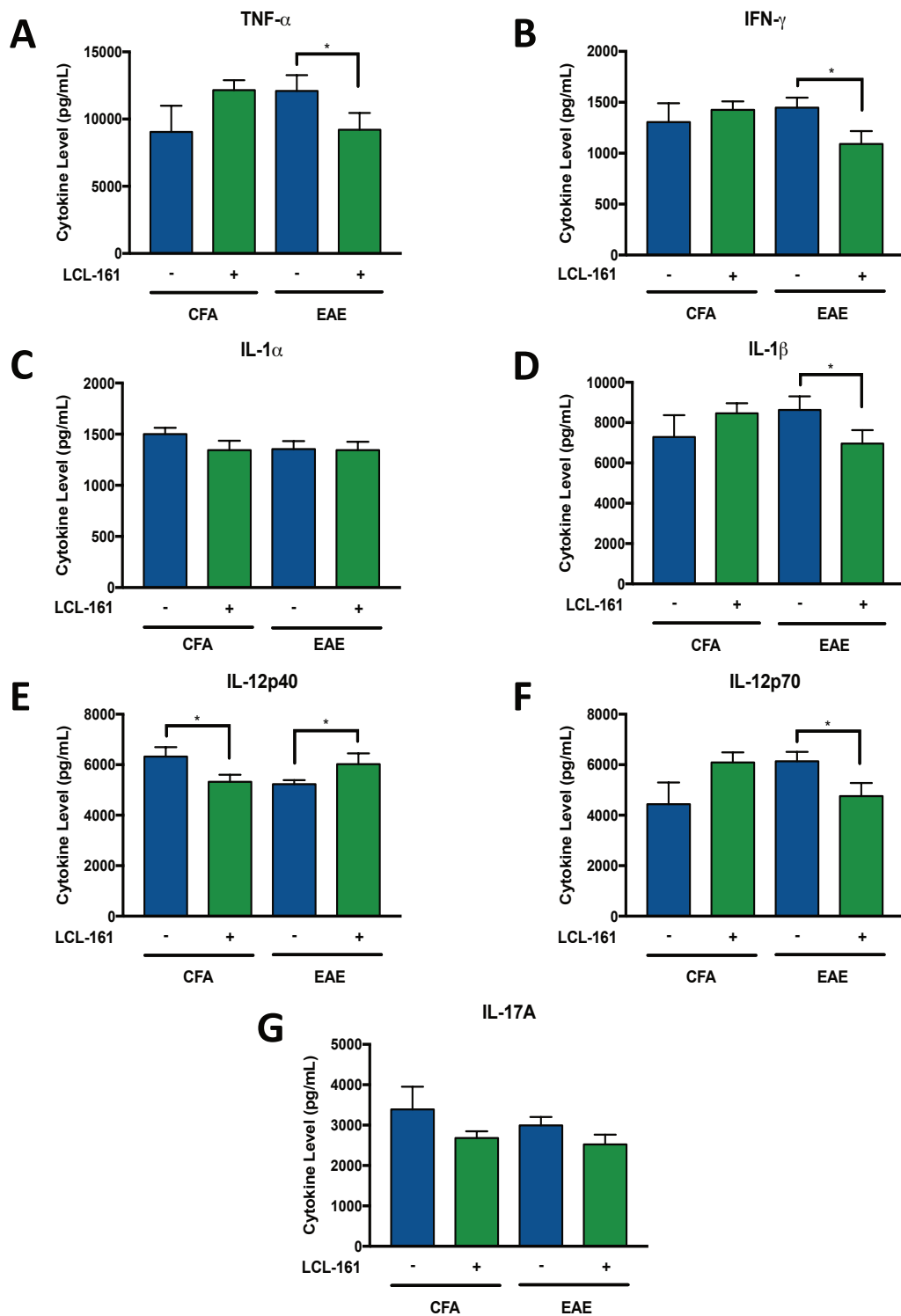


**Figure 18:** Effects of oral administration of vehicle (blue bars) or LCL161 (green bars) on plasma concentrations for the pro-inflammatory Th1 cytokines TNF- $\alpha$ , IFN- $\gamma$ , IL-1 $\alpha$ , IL-1 $\beta$ , IL-12p40, IL-12p70 and IL-17A (A-G) in CFA and EAE mice at DPI 15. \* $p < 0.05$ , unpaired t-test (n=8-10).

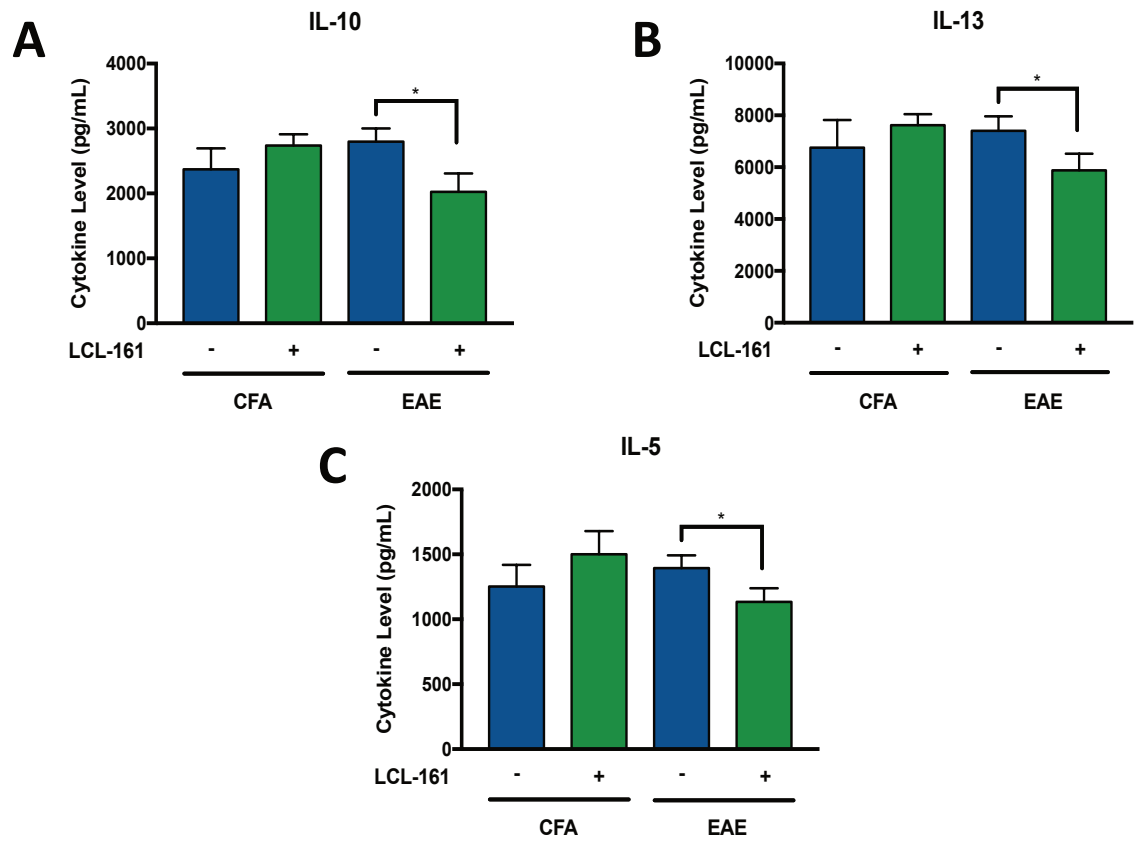


**Figure 19:** Effects of oral administration of vehicle (blue bars) or LCL161 (green bars) on plasma concentrations for the Th2 anti-inflammatory cytokines IL-10, IL-13 and IL-5 (A-C) in CFA and EAE mice at DPI 15. \* $p < 0.05$ , unpaired t-test, (n=8-10).

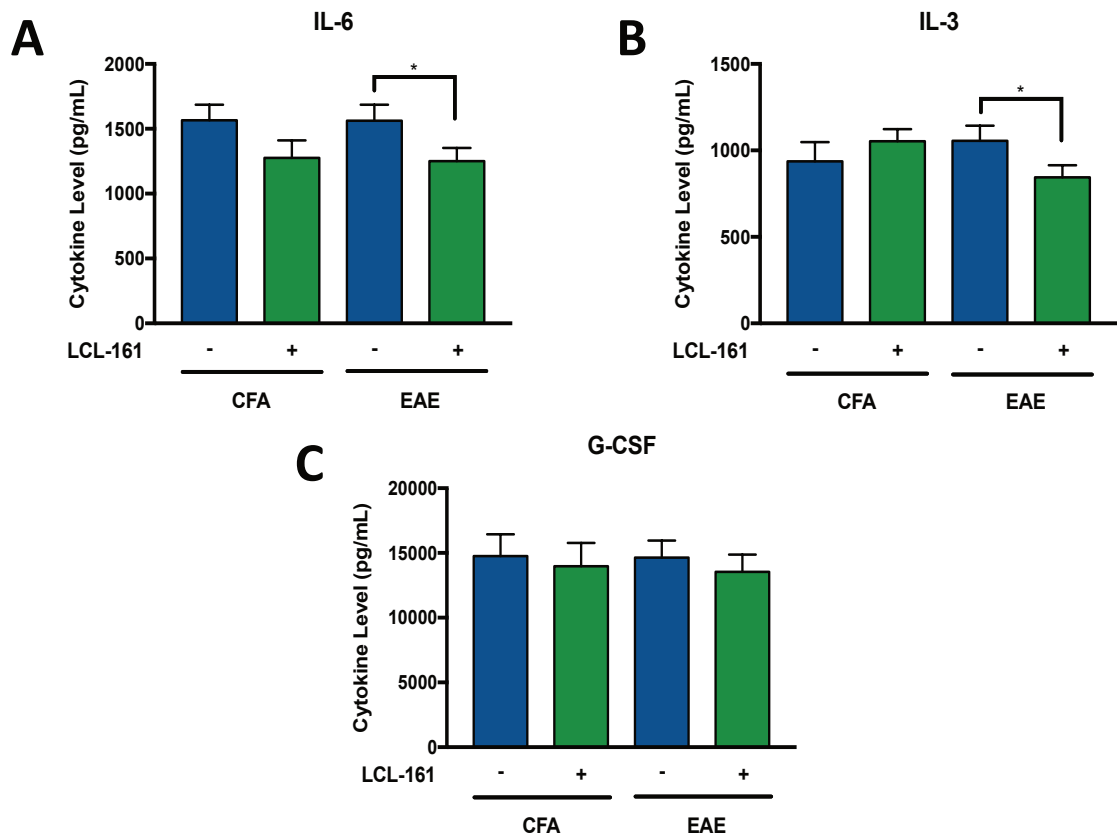


**Figure 20:** Effects of oral administration of vehicle (blue bars) or LCL161 (green bars) on plasma concentrations for the growth and differentiation cytokines IL-6, IL-3 and GM-CSF (A-C) in CFA and EAE mice at DPI 15. \* $p < 0.05$ , unpaired t-test ( $n = 8-10$ ).

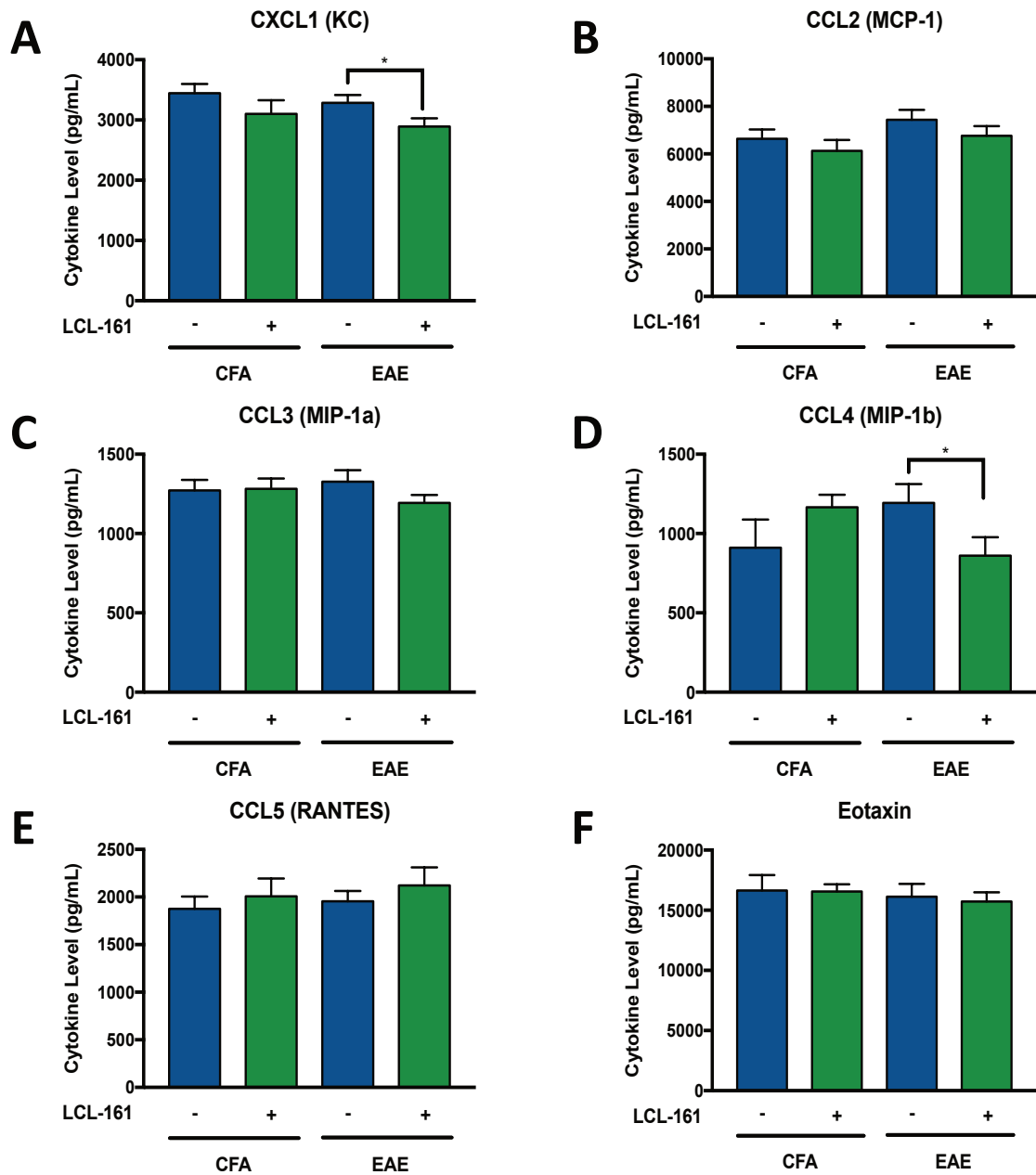


**Figure 21:** Effects of oral administration of vehicle (green bars) or LCL161 (blue bars) on plasma concentrations for the for CXCL1, CCL2, CCL3, CCL4, CCL5 and Eotaxin (A-F) in CFA and EAE mice at DPI 15. \*p<0.05, unpaired t-test (n=8-10).

### 3.14 LCL161 treatment increased Ly6C<sup>Lo</sup> monocytes in EAE mice

Spleens from EAE mice treated with either vehicle or LCL161 were collected on DPI 15 and processed into single-cell suspensions. These cells were then stained with antibodies against CD11b, Ly6G and Ly6C and analyzed by flow cytometry to determine if the percentages of monocyte subsets in EAE mice were influenced by LCL161 treatment.

Ly6G and Ly6C are two members of the Ly6 family of type V glycosphosphatidylinositol anchored cell surface proteins that comprise the GR1 (granulocyte marker) complex.

These markers are frequently used to identify various classes of peripheral immune cells such as neutrophils, eosinophils and monocytes. There are two main subtypes of

monocytes (classical and non-classical) which can mature into macrophages. Since both of classical and non-classical monocytes are involved in the initiation and resolution of

inflammation<sup>70,71</sup>, flow cytometry was used to determine the relative the percentages for each of these monocyte subsets (Figure 22A). First, dead cells were gated out using FSC

(forward scatter) vs. SSC (side scatter) sorting which separates cells by size and

complexity, respectively. Neutrophils were excluded by gating on CD11b<sup>Pos</sup>, Ly6G<sup>Neg</sup>

cells. These CD11b<sup>Pos</sup>, Ly6G<sup>Neg</sup> cells were then further separated into Ly6C<sup>Pos</sup> and SSC<sup>Lo</sup> populations using Ly6C vs. SSC sorting to exclude eosinophils. The percentages of each

monocyte subtype [classical (CD11b<sup>Pos</sup>, Ly6G<sup>Neg</sup>, Ly6C<sup>Hi</sup>, SSC<sup>Lo</sup>); non-classical (CD11b<sup>Pos</sup>, Ly6G<sup>Neg</sup>, Ly6C<sup>Lo</sup>, SSC<sup>Lo</sup> Ly6C<sup>Hi</sup> and Ly6C<sup>Lo</sup>)] were then determined (Figure 22B). The

percentages of classical monocytes were similar for EAE mice that received LCL161 or vehicle (Figure 22B). However, non-classical monocytes were elevated in LCL161-

relative to vehicle-treated EAE mice (Figure 22B).

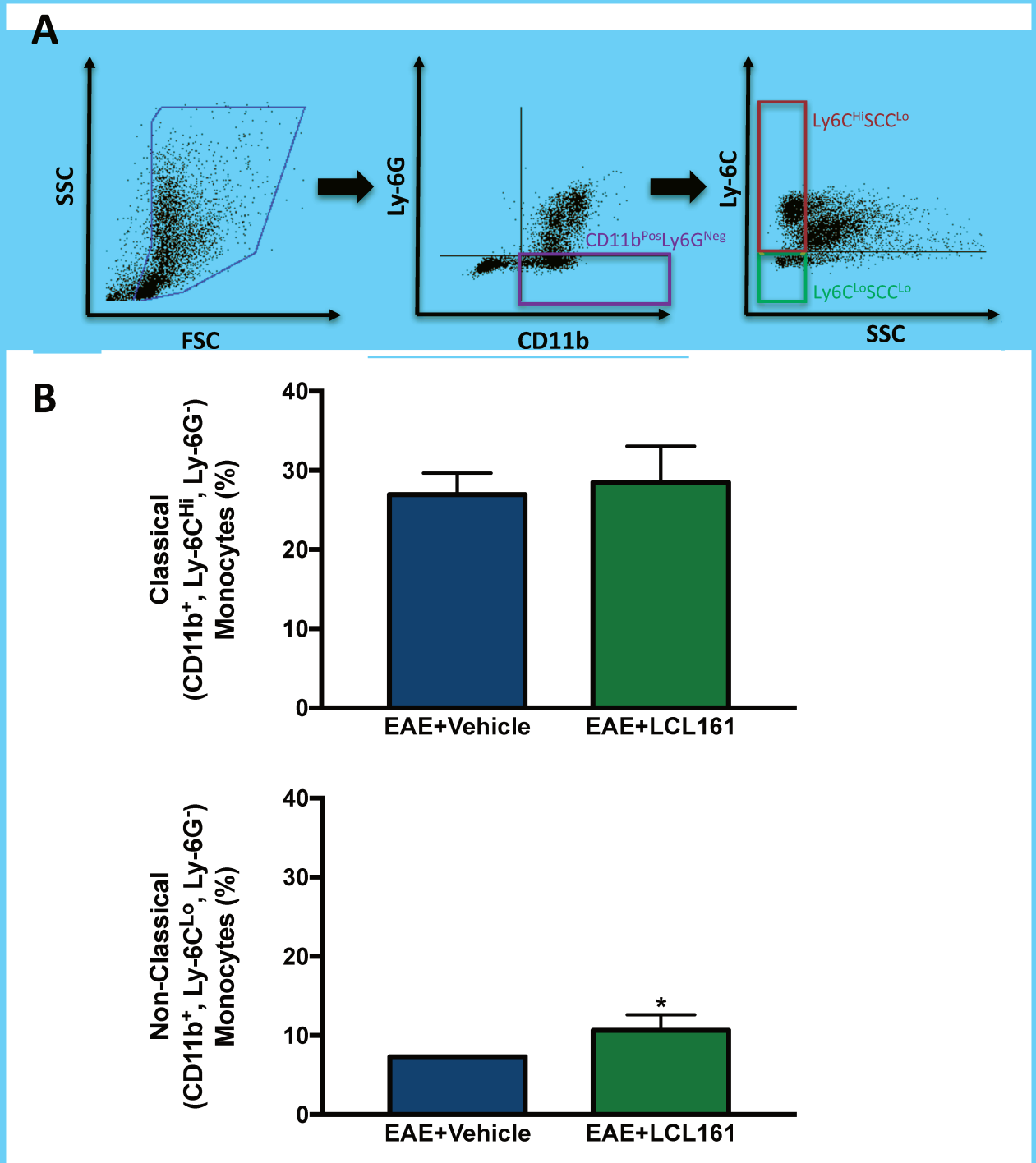


**Figure 22:** A) Flow cytometry protocol for the detection of Ly6C<sup>Hi</sup> and Ly6C<sup>Lo</sup> monocytes isolated from the spleens of EAE mice treated with vehicle or LCL161. On DPI 15 spleens were collected from LCL161 and vehicle mice, stained with antibodies against CD11b, Ly6G and Ly6C and analyzed by flow cytometry. B) Percentages of classical and non-classical macrophages in EAE mice treated with vehicle or LCL161. \*p<0.05, Mann-Whitney U test (n=4).

### **3.15 Treatment with LCL161 increased BMDM necrosis in cultures exposed to a lethal concentration of LPS**

In a final experiment, the potential ability of LCL161 to shift cell death produced by exposure to a lethal concentration of LPS from apoptosis to necrosis was investigated. BMDMs, extracted from WT C57BL/6 mice, were cultured for 7 days under mild M1, strong M1, mild M2 or strong M2 polarizing conditions. Half the cultures were treated with either vehicle (0.01% DMSO) or LCL161 (10  $\mu$ M) on day 6 for 24 hr. On day 7 all cultures were treated with LPS (10  $\mu$ g/ml for 4 hr) followed by flow cytometry to determine the percentages macrophage cells (CD11b<sup>+</sup>, F4/80<sup>+</sup>) that were immunopositive for Annexin V (apoptosis marker) and/or 7-AAD (necrosis marker). The ratio of Annexin V positive cells to 7-AAD positive cells were used to calculate Apoptotic Necrotic Index (ANI) values using the simple formula [ANI = (Annexin V<sup>+</sup> cells/7-AAD<sup>+</sup> cells) -1]. Positive ANI values indicated predominant apoptotic cell death while negative values represented chiefly necrotic cell death. Under mild M1 or M2 polarizing conditions, LCL161 did not significantly alter the ANIs relative to vehicle-treated BMDMs (Figure 23). However, there were non-significant statistical trends towards reduced apoptosis and increased necrosis (lower or negative ANIs) for BMDMs treated with LCL161 (mild M1, 0.41; mild M2, -0.19) compared to vehicle-treated BMDMs [mild M1, 0.75 ( $p = 0.08$ ); mild M2, 0.02 ( $p = 0.09$ )]. In contrast to mildly polarizing conditions, under strong M1 and M2 polarizing conditions, BMDMs treated with LCL161 were mostly necrotic (strong M1, -0.19; strong M2, -0.14) while vehicle-treated BMDMs were mainly apoptotic (strong M1, 0.41; strong M2, 0.70). These findings suggest that cIAP1/2 suppression induces a shift of LPS-induced death from apoptosis to necrosis.

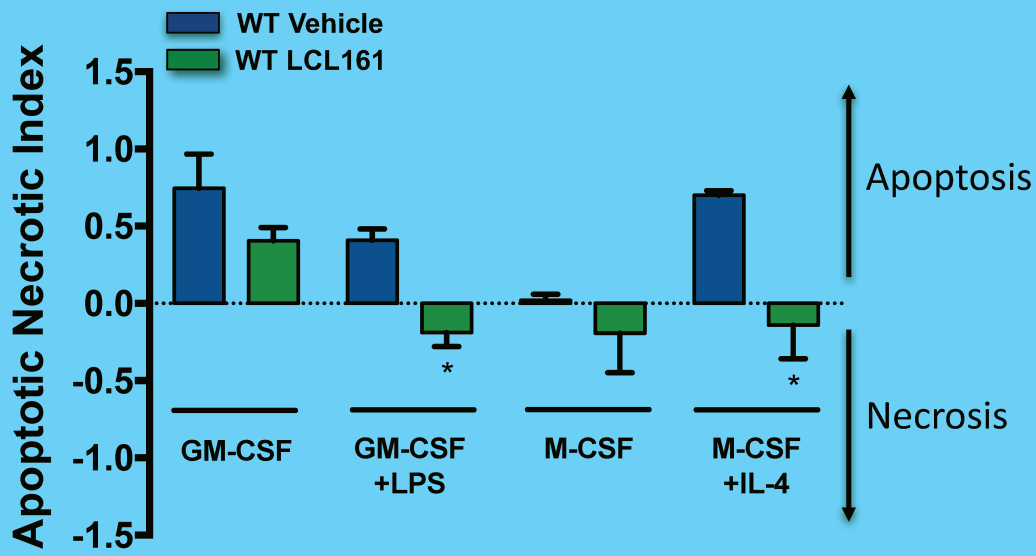


**Figure 23:** Effects of exposure to a lethal concentration of LPS (10  $\mu\text{g/ml}$ ) for 4 hr on the apoptosis and necrosis of BMDMs cultured under mild M1, strong M1, mild M2 or strong M2 polarizing conditions that were treated with vehicle or LCL161. After gating for double-positive macrophage cells ( $\text{CD11b}^+$ ,  $\text{F4/80}^+$ ) the percentages of Annexin (apoptosis marker) and 7AAD (necrosis) positive cells were determined. The Apoptotic Necrotic Index Values for each of the 8 culture conditions are shown. \* $p < 0.05$ , Mann-Whitney U test ( $n=3$ ).

## CHAPTER 4: DISCUSSION

### 4.1 Determining the effects of cIAP2 suppression on M1 and M2 macrophage polarization

It is well established that monocyte-derived macrophages (resident microglia and infiltrating macrophages) are the predominant inflammatory cells in active and chronic demyelinating MS plaques<sup>55,72</sup>. Based on experimentation with the EAE model, M1 macrophages are thought to promote CNS damage in MS by releasing pro-inflammatory mediators such as nitric oxide, TNF- $\alpha$  and IL- $\beta$ <sup>55-58</sup>. By contrast, M2 macrophages release anti-inflammatory cytokines (IL-4, IL-10, IL-13) that resolve CNS inflammation and stimulate myelin repair resulting in the recovery of neurological function in EAE mice<sup>56-58,60,61</sup>. Since macrophages are plastic, capable of shifting their polarization state within an M1-to-M2 spectrum, altering macrophage polarization towards an M2 state may have therapeutic potential for the treatment of MS<sup>55,72</sup>. The anti-apoptotic proteins cIAP1 and cIAP2 (cIAP1/2) promote innate immunity by protecting macrophages from FAS-, Toll-4- and TNF- $\alpha$ -induced cell death<sup>23,32,73</sup>. These findings suggest that treatments which suppress cIAP1/2 levels may impact MS disease course by promoting the apoptotic elimination of macrophages<sup>74,75</sup>. However, the relative effects of cIAP1/2 suppression on the polarization of M1 and M2 macrophages are not known. I therefore determined whether genetic ablation of cIAP2 or pharmacological suppression of cIAP1/2 levels altered M1 and M2 polarization and EAE disease severity.

#### **4.2 cIAP2 deficiency impaired the generation of macrophages in BMDMs cultured under mild M1 or strong M2 polarizing conditions**

First, the production of macrophages in BMDMs derived from WT and cIAP2 null mice cultured under mild M1 or M2 macrophage polarizing conditions were compared. While cIAP2 ablation did not alter the generation of macrophages under mild M2 (M-CSF) polarization, cIAP2 loss reduced the generation of macrophages from BMDMs cultured under mild M1 (GM-CSF) polarizing conditions (Figure 4). cIAP2 expression is not induced by GM-CSF in innate immune cells<sup>76</sup>. Furthermore, cIAP2 deletion did not promote the apoptosis of BMDMs cultured under mild M1 polarizing conditions (Figure 6). These findings suggest that the impaired differentiation of hematopoietic stem cells (HSCs), rather than increased macrophage apoptosis, reduced M1 polarization in cIAP2 null BMDMs. However, under strong M1 polarizing (GM-CSF+LPS) conditions, no difference was found between the percentages macrophages generated in WT and cIAP2 null BMDMs (Figure 5). The percentages of apoptotic macrophages were also similar in WT and cIAP2 null BMDMs (Figure 6). This result is consistent with evidence that the concentration of LPS (10 ng/ml) used in my studies to induce strong M1 polarization conditions does not trigger the death of peritoneal macrophages isolated from cIAP2 null mice<sup>23</sup>. However, the ablation of cIAP2 did decrease the production of macrophage in BMDMs cultured under strong M2 (M-CSF+IL-4) polarizing conditions (Figure 5). Unlike mild M1 polarization conditions, apoptotic macrophages were more prevalent in cIAP2 null than WT BMDMs cultured under strong M2 polarizing conditions. This finding indicates that cIAP2 deficiency impaired the survival of macrophages in BMDMs cultured under strong M2 polarizing conditions. Although the effect of cIAP2 deletion on

the survival of macrophages exposed to IL-4 has not been previously reported, IL-4 is known to increase the resistance of colon rectal cancer cells by elevating levels of the IAP family member survivin<sup>77</sup>.

### **4.3 Ablation of cIAP2 biases the polarization of BMDMs to an M2-like state**

I next employed qRT-PCR to measure levels of M1 and M2 mRNA markers in WT and cIAP2 null BMDMs cultured under strong M1 or M2 polarizing conditions. These studies indicated that cIAP2 deficiency altered BMDM differentiation by either strong M1 or strong M2 polarizing conditions. Under strong M1 polarizing conditions, cIAP2 null BMDMs displayed reduced M1 marker mRNA levels and enhanced M2 marker mRNA levels compared to WT BMDMs (Figure 7). These results suggest that under strong M1 conditions, cIAP2 null BMDMs adopted an M2-like state. Interestingly, under strong M2 polarizing conditions, cIAP2 null BMDMs showed suppressed mRNA levels for both M1 and M2 markers relative to WT cultures. This suggests a failure of both M1 and M2 polarization. My flow cytometry studies indicated that the increased susceptibility of cIAP2 null BMDMs to apoptotic elimination may have contributed to these findings (Figure 6). However, potential effects of cIAP2 loss on the differentiation of HSCs in BMDM cultures cannot be ruled out. In summary, cIAP2 loss impaired the ability of BMDMs to respond appropriately to both M1 and M2 polarizing conditions.

### **4.4 Immunopanning of BMDM cultures to isolate macrophages**

Bone marrow primarily consists of HSCs which can differentiate into a variety of cell types. HSCs cultured with GM-CSF differentiate not only into M1-like macrophages but

also bone marrow-derived dendritic cells<sup>6,8,78</sup>. Addition of LPS increased the generation of double-positive CD11b, F4/80 macrophages from ~22-25% (Figure 4A, GM-CSF) to ~64-65% (Figure 5A, GM-CSF+LPS). This was accompanied by a reduction in single positive CD11b cells (dendritic cells) from ~71-72% (Figure 4A, GM-CSF) to ~23-27% (Figure 5A, GM-CSF+LPS). Since dendritic cells (DCs) also express M1 and M2 markers (TNF- $\alpha$ , IL-10, CD86, CD206) and depend on cIAP1/2 for apoptotic resistance, DCs are an additional source of M1 and M2 marker mRNAs in BMDMs<sup>79-81</sup>. To ensure macrophages were the primary source of M1 and M2 mRNA marker expression, BMDM cultures were immunopanned using the F4/80 antibody to select macrophages. Flow cytometry was used to assess the efficiency of immunopanning by comparing the percentages of macrophages and DCs in the supernatants of non-immunopanned and immunopanned BMDM cultures. Immunopanning reduced the percentage of double-positive CD11b and F4/80 cells (macrophages) and increased the percentages of single-positive CD11b cells (DCs) in the supernatants of BMDMs (Figure 9). These findings provide indirect evidence that macrophages, and not DCs, were isolated by immunopanning. These macrophage-purified BMDMs were termed mpBMDMs.

#### **4.5 Strong M1 or M2 polarizing conditions have distinct effects on M1 and M2 mRNA expression profiles in non-immunopanned and immunopanned BMDMs**

Unlike non-immunopanned cIAP2 null BMDMs that displayed enhanced M2 marker mRNA levels under strong M1 conditions (Figure 7B, D and E), M1 marker mRNA levels were similar for WT and cIAP2 null mpBMDMs (Figure 10B, D and F).

Macrophage enrichment by immunopanning thus indicated that cIAP2 deletion did not

disrupt the strong M1 polarization of these immune cells by GM-CSF+LPS. In stark contrast, cIAP2 null mpBMDMs displayed profoundly impaired polarization by strong M2 (M-CSF+IL-4) conditions. Both M1 and M2 marker mRNA levels were elevated in cIAP2 null compared to WT mpBMDMs (Figure 10A-F). By comparison, non-immunopanned cIAP2 null BMDMs showed reduced M2 marker expression under strong M2 polarizing conditions. Although both M1 and M2 mRNA markers were elevated in cIAP2 null mpBMDMs, the overall increase in mRNA levels was higher for M1 than M2 markers suggesting cIAP2 null cells adopted a more M1 than M2 state under strong M2 polarization conditions. This enhanced generation of pro-inflammatory M1 macrophages in cIAP2 null mpBMDMs aligns with the elevated EAE disease severity of cIAP2 null relative to WT mice (Figure 15A and B). cIAP2 deletion therefore appears to promote M1 macrophage polarization under conditions that normally favour M2 polarization. However, the concurrent induction of M2 polarization produced by cIAP2 loss suggests that an imbalance between M1 and M2 macrophage function may have further contributed to increased EAE disease severity in cIAP2 null animals. The mRNA levels for cIAP2 in WT cells were also measured in mpBMDMs cultured under strong M1 and M2 polarizing conditions. WT mpBMDMs displayed higher cIAP2 levels when cultured under strong M1 than M2 polarizing conditions (Figure 10G). This finding is consistent with evidence that LPS activates cIAP2 expression in peritoneal macrophages<sup>23</sup>.

#### **4.6 Suppression of cIAP1/2 protein levels in BMDMs with the SMAC mimetic LCL161 induced an M1 macrophage polarization bias**

The next set of experiments aimed to determine if treatment of BMDMs with a SMAC mimetic yielded the same results produced by genetic ablation of cIAP2. cIAP1/2 both have E3 ligase activity that is stimulated by the SMAC mimetic LCL161, resulting in auto-ubiquitination of these proteins that targets them for degradation by the proteasome<sup>25</sup>. Western blot analysis showed that cIAP1/2 protein levels were reduced in WT BMDMs treated with LCL161 for 24 hr (Figure 11). To ensure that LCL161 treatment did not interfere with the immunopanning process, the supernatants of non-immunopanned and immunopanned BMDMs were collected and analyzed by flow cytometry as previously described. As was the case for BMDMs not treated with a SMAC mimetic (Figure 9), immunopanning successfully reduced macrophage and increased single-immunopositive CD11b cells (DCs) percentages in the supernatants of cultures grown under either mild or strong M1 or M2 polarizing conditions and then treated with LCL161 (Figure 12). Following immunopanning, the adherent macrophage cells were analyzed by qRT-PCR as previously discussed. Under strong M1 culture conditions, acute suppression of cIAP1/2 levels with LCL161 selectively increased the expression of M1 markers (TNF- $\alpha$  and c-Myc) in mpBMDMs indicating a bias towards M1 polarization (Figure 13A and B). These results differ from those obtained with cIAP2 null mpBMDMs in which strong M1 polarization was unaltered (Figure 10A-C). However, these findings are consistent with a previous report showing that suppression of cIAP1/2 by a chemically-related SMAC mimetic blocked M2 polarization in favour of M1 polarization<sup>82</sup>. Additionally, treatment of peripheral blood mononuclear cells with

LCL161 has been shown to enhance the production of pro-inflammatory Th1 cytokines thus supporting the upregulation of M1 markers seen in LCL161-treated BMDM cultures<sup>20,83</sup>.

#### **4.7 LCL161 massively increased the apoptosis of macrophages in BMDMs cultured under strong M2 polarizing conditions**

Following treatment with LCL161, it was not possible to detect mRNAs encoding M1 and M2 markers as well as cIAP2 by qRT-PCR in mpBMDMs isolated from BMDMs cultured under strong M2 polarizing conditions (Figure 13A-G). Subsequent flow cytometry revealed that LCL161 treatment promoted a massive increase in the apoptotic death of macrophages (80% Annexin V-positive) detected in BMDMs cultured under strong M2 polarizing conditions (Figure 14). Relative to macrophages in cIAP2 null BMDM cultures (Figure 6), the percentages of apoptotic macrophages were increased by LCL161 for WT BMDMs cultured under mild or strong M1 and M2 polarizing conditions (Figure 14). The loss of cIAP1/2 thus dramatically reduced the resistance of macrophages to apoptotic death. In the future, it will be important to determine the effects of lower concentrations of LCL161 (<10  $\mu$ M) that modestly reduce apoptotic resistance on M1 and M2 macrophage polarization. In summary, these data support a pivotal role for cIAP1/2 in M2 polarization by showing that loss of these anti-apoptotic proteins shifts macrophage polarization towards an M1 state by promoting the apoptotic elimination of M2 macrophages.

#### **4.8 Oral administration of LCL161 increased EAE disease severity**

Mice subjected to EAE were dosed orally with LCL161 to determine the effects of reduced cIAP1/2 levels on disease progression. In a first experiment, EAE mice were sacrificed at DPI 15 to allow the harvesting of blood, liver and spinal cords at peak disease. EAE severity was elevated by LCL161 from DPI 12-15 (Figure 15A). In a second experiment, mice were dosed with LCL161 till DPI 30 to examine disease severity at later time points. LCL161-treated mice in this experiment also exhibited increased EAE disease severity characterized by earlier disease onset and impaired recovery at DPI 30 relative to vehicle-treated EAE mice (Figure 15B). Western blot analysis confirmed that cIAP1/2 protein levels in the liver were reduced for LCL161-EAE relative to vehicle-EAE mice (Figure 15C). Suppression of cIAP1/2 levels therefore enhanced paralysis and motor deficits in this mouse model of MS.

#### **4.9 LCL161 increased CD38 expression in the spinal cords and suppressed plasma Th1 and Th2 cytokine concentrations for EAE mice**

Oral administration of LCL161 enhanced expression of CD38 (M1 marker) in the spinal cords of EAE mice at DPI 15 (Figure 16A). There was also a non-significant trend towards increased expression of the M1 marker Fpr2 in LCL161-treated, relative to vehicle-treated, EAE mice ( $p=0.08$ ; Figure 16C). These findings suggest that LCL161 increased M1 macrophage-mediated spinal cord inflammation may have contributed to increased EAE disease severity. LCL141 also modestly impacted M1 marker expression in the spinal cords of MOG<sub>35-55</sub> antigen controls (CFA mice). However, the inconsistent effects of LCL161 on M1 marker mRNA levels (reduced TNF- $\alpha$  and elevated Gpr18;

Figure 16B and F) in CFA mice rendered clear interpretation of these results difficult. In addition, M2 marker (Egr2 and c-Myc) mRNA levels were elevated in the spinal cords of LCL161-CFA, relative to vehicle-CFA, mice (Figure 17A and B). These results were unexpected because for mpBMDMs, LCL161 promoted M1 rather than M2 macrophage polarization (Figure 13A and E). Nevertheless, these findings are consistent with altered innate immune function in healthy mice treated with LCL161<sup>20</sup>. Although LCL161 increased M1 macrophage polarization *in vitro* and promoted M1-mediated inflammation in the spinal cords of EAE mice, oral administration of this SMAC mimetic reduced the plasma concentrations in EAE mice for both pro- and anti-inflammatory cytokines, termed Th1 and Th2 cytokines. Relative to vehicle-treated EAE mice, LCL161-treated mice showed decreased plasma concentrations of both Th1 [TNF- $\alpha$ , IFN- $\gamma$ , IL-1 $\beta$  and IL-12p70 (Figure 18A, B, D and F); IL-6 (Figure 20A)] and Th2 [IL-10, IL-13 and IL-5 (Figure 19A-C); IL-3 (Figure 20B)] cytokines. In addition, LCL161 reduced plasma levels of the chemoattractants CXCL1 (KC) and CCL-4 (MIP-1b; Figure 21A and D). Despite increased EAE severity at DPI 15, LCL161 therefore produced an unexpected reduction of overall immune function at this peak disease time point.

These findings indicate the limitations of *in vitro* experimentation for predicting the complex effects of systemically administered LCL161 on the immune function of EAE mice. Macrophages are only a subset of the various immune cell populations implicated in EAE and MS<sup>84</sup>. The complex effects of cIAP2 on M1 and M2 polarization are supported by the differing effects of cIAP2 deletion on M1 and M2 marker mRNA levels in non-immunopanned and immunopanned cIAP2 null BMDMs (Figures 7 and 10). The

presence of DCs in BMDMs and their absence in mpBMDMs may have contributed to these disparate findings. Since cIAP1/2 regulate the survival of many other immune cell types such as DCs, natural killer cells, neutrophils, T and B lymphocytes, the altered function of these various immune cell subtypes may have contributed to the suppression of both Th1 and Th2 cytokines by LCL161 in EAE mice<sup>12,81,85</sup>. Future studies should therefore address the effects of LCL161 on the function of these immune cells populations in EAE mice.

#### **4.10 LCL161 treatment did not alter levels of Ly6C<sup>Hi</sup> monocytes but increased Ly6C<sup>Lo</sup> monocytes in EAE mice**

Monocyte derived macrophages are generated from two distinct population subsets which originate in the bone marrow<sup>55</sup>. The first are Ly6C<sup>Hi</sup> (classical) monocytes which become tissue resident macrophages during inflammation. In EAE, the production of Ly6C<sup>Hi</sup> monocytes is key to disease development because depletion of these monocytes leads to EAE resistance<sup>55,71</sup>. Though Ly6C<sup>Hi</sup> monocytes are primarily inflammatory cells, this monocyte subtype can also promote the resolution of inflammation<sup>78</sup>. In the context of EAE, the internalization of myelin by differentiated Ly6C<sup>Hi</sup> monocytes promotes their polarization to an anti-inflammatory state<sup>50,55,56</sup>. Furthermore, in spinal cord injury models, Ly6C<sup>Hi</sup> monocytes differentiate into M2 macrophages that are necessary for the resolution of inflammation and tissue repair<sup>59</sup>. Ly6C<sup>Hi</sup> monocytes may therefore activate or dampen the immune response, depending on the polarization cues that are present<sup>78</sup>. Flow cytometry analysis indicated that there was no difference between the percentage of Ly6C<sup>Hi</sup> cells in vehicle-EAE and LCL161-EAE mice (Figure 22B). This suggests that

treatment with LCL161 does not influence Ly6C<sup>Hi</sup> monocytes generation. The other main subset of monocytes is Ly6C<sup>Lo</sup> (non-classical) monocytes which monitor the vascular endothelium and are typically considered precursors to M2 macrophages<sup>55,70,78</sup>. However, Ly6C<sup>Lo</sup> monocytes have been shown to activate the innate immune system by responding to local danger signals and initiating the recruitment of inflammatory cells<sup>55,71,78</sup>. This was the case in a mouse model of autoimmune arthritis where Ly6C<sup>Lo</sup> monocyte infiltration is responsible for disease progression<sup>70</sup>. Unlike Ly6C<sup>Hi</sup> monocytes, LCL161-treated EAE mice showed an increased percentage of Ly6C<sup>Lo</sup> monocytes (Figure 22B). Therefore, it is possible that an elevation of Ly6C<sup>Lo</sup> monocytes by LCL161 contributes to enhanced EAE disease severity. Future flow cytometry studies should use additional antibodies (i.e. CXCL3, CCL2, and MHCII) to determine if treatment with LCL161 alters the polarization of Ly6C<sup>Hi</sup> and Ly6C<sup>Lo</sup> monocytes.

#### **4.11 Suppression of cIAP1/2 levels with LCL161 converted the mode of cell death for LPS-treated BMDMs from apoptosis to necrosis**

The suppression of cIAP1/2 may also exacerbate EAE disease by altering the mode of macrophage cell death. Apoptosis results in the removal of cells by preserving the cell membrane while necrosis ruptures the plasma membrane resulting in the release of intracellular contents that promote inflammation<sup>18</sup>. Results from this study, as well as the findings of other laboratories, indicate that cIAP2 loss, induced either genetically or pharmacologically, reduces blood monocyte viability, especially under strong M2 polarizing conditions<sup>23,36,37</sup>. A reduction in cIAP2 levels promotes the clean elimination of cells by apoptosis<sup>38</sup>. However, the suppression of cIAP1/2 in macrophages may shift

their mode of cellular death from apoptosis to necrosis resulting in inflammatory damage<sup>32,37</sup>. To determine if treatment with LCL161 enhanced macrophage necrosis, BMDMs were treated with either vehicle or LCL161 and exposed to a lethal concentration of LPS (10 µg/ml). Compared to vehicle-treated BMDMs cultured under mild M1 or M2 polarizing conditions BMDMs treated, LCL161 did not alter the mode of cell death (positive ANIs indicating apoptosis, Figure 23). However, BMDMs cultured under strong M1 and M2 polarizing conditions and treated with LCL161 were significantly more necrotic than vehicle-treated BMDMs (Figure 23). Intercellular contents (DNA, mitochondria) released from necrotic cells activate pattern recognition receptors on immune cells including macrophages, DCs and neutrophils cells resulting in an injurious inflammatory response<sup>65</sup>. These findings suggest that the induction of necrosis within the spinal cord by LCL161 may have contributed to enhanced neuroinflammation and elevated disease severity for EAE mice treated with LCL161. Future studies employing histological markers that detect necrotic immune cells in the spinal cords of vehicle-EAE and LCL161-EAE mice will be required to test this hypothesis.

#### **4.12 NF-κB pathway involvement in macrophage polarization and survival**

Activation of the TNF-α receptor 1 (TNFR1) and Toll-4 receptor promote the polarization of M1-like macrophages by initiating the canonical NF-κB pathway<sup>86</sup>. The canonical NF-κB pathway is activated by a large receptor complex that triggers the ubiquitin-mediated degradation of the inhibitor of NF-κB (IκB) which releases the p50/p65 subunits of NF-κB<sup>87</sup>. These NF-κB subunits then migrate to the nucleus and

activate target genes such as TNF- $\alpha$ <sup>88</sup>. This creates a feedforward cycle of enhanced TNF- $\alpha$  synthesis and TNFR1 activation necessary for M1 macrophage polarization. cIAP1/2 are required for NF- $\kappa$ B signaling to promote survival via the transcription of anti-apoptotic genes such as c-FLIP<sup>89</sup>. These signaling pathways also modulate the transcription of cytokines and chemokines. In the absence of cIAP1/2, TNFR1 stimulates the formation and subsequent activation of the death inducing complex (complex II/riposome) that triggers caspase-mediated apoptosis<sup>89</sup>. The development of transgenic mice enabling the depletion of either cIAP1 or cIAP2 or cIAP1/2 has enabled studies that have shown that cIAP1 is most important in permitting activation of the canonical NF- $\kappa$ B pathway<sup>31</sup>. Unlike cIAP1 that is generated at constant levels, cIAP2 has low constitutive expression and is upregulated by TNFR1 and Toll-4-mediated activation of the canonical (p50/p65) NF- $\kappa$ B pathway<sup>12,40</sup>. This enables cIAP2 to further support activation of the canonical NF- $\kappa$ B pathway by suppressing apoptosis<sup>12</sup>. Consistent with my findings, loss of cIAP2 has been shown to promote the apoptosis of macrophages by TLR-4 and TNFR1 activation<sup>23</sup>.

cIAP1/2 also modulate activity of the non-canonical NF- $\kappa$ B pathway. In addition to TNFR1, macrophages have a second class of TNF- $\alpha$  receptors known as TNFR2<sup>90</sup>. TNFR2 activation stimulates the non-canonical NF- $\kappa$ B pathway by triggering proteolytic processing of the inactive p100/RelB dimers into active p52/RelB NF- $\kappa$ B complexes<sup>91</sup>. TNFR2-induced non-canonical NF- $\kappa$ B signalling is enhanced by TNFR1-mediated induction of the canonical NF- $\kappa$ B pathway<sup>91</sup>. SMAC mimetics increase TNFR2-induced activation of the non-canonical NF- $\kappa$ B pathway in macrophages maintained under mild

M1 polarizing conditions<sup>92</sup>. Using a selective ligand for TNFR2 (TNC-sc(mu) TNF80), suppression of cIAP1/2 was found to promote mild cell death that was enhanced by caspase inhibition with zVAD-fmk<sup>92</sup>. Caspase inhibition with zVAD-fmk enhanced TNFR2-induced cell death by promoting a form of necrosis called necroptosis<sup>92</sup>. Since LPS-induces TNF- $\alpha$  synthesis, these findings suggest that activation of the non-canonical NF- $\kappa$ B pathway may have contributed to the increase of LPS-induced macrophage cell death in LCL161-treated BMDMs by inducing necroptosis. My findings further suggest that TNFR2-mediated macrophage necroptosis in LCL161-treated BMDMs is enhanced by exposure to strong M1 or M2 polarizing conditions (Figure 23). Future studies that employ necrostatin, a small molecule inhibitor of necroptosis, will be required to test this hypothesis<sup>93</sup>.

#### **4.13 Regulation of dendritic cell and neutrophil cell function by cIAP1/2**

Dendritic cells (DCs) are an important class of antigen-presenting cells that play a key role in the activation of pro-inflammatory immune cells<sup>84</sup>. It has been observed that DCs accumulate in the spinal cords of EAE mice that results in the activation of T-cells<sup>84</sup>. As with macrophages, progenitors in the bone marrow give rise to DCs that release pro-inflammatory cytokines necessary for immune activation<sup>94</sup>. The survival of these progenitor cells, necessary for the generation of DCs, is also supported by cIAP1/2<sup>81</sup>. The suppression of cIAP1/2 levels by treatment with LCL161 may thus have reduced plasma pro-inflammatory cytokines levels by prohibiting DC survival. Furthermore, their elimination by necroptosis rather than apoptosis in the presence of LCL161 may have exacerbated inflammatory damage in the spinal cord.

During early to peak EAE disease, increased neutrophil colony expansion and infiltration within demyelination lesions are observed<sup>95,96</sup>. Neutrophil infiltration has been linked to neuroinflammation that is resolved by the apoptotic removal of these cells. These processes are regulated by cIAP1/2 in neutrophils<sup>97</sup>. Therefore, suppression of cIAP1/2 levels in LCL161-treated EAE may have reduced neutrophil survival and thus reduced their ability to produce pro-inflammatory cytokines. Additionally, phagocytosis of apoptotic neutrophils by macrophages is required to prevent the secondary necrosis of apoptotic neutrophils. This not only prevents the release of pro-inflammatory intracellular contents during necrosis but also shifts macrophage polarization to an anti-inflammatory M2 state<sup>98</sup>. However, if macrophage polarization and function are impaired by cIAP1/2 loss, as suggested by my *in vitro* studies, it is possible that macrophages were unable to properly phagocytosis neutrophils resulting in elevated spinal cord damage.

#### **4.14 The potential role of cIAP1/2 in oligodendrocyte cell survival**

MS and EAE are characterized by the autoimmune-mediated destruction of myelin-producing oligodendrocytes that insulate axons in the brain and spinal cord resulting in the impaired propagation of action potentials and neurological deficits<sup>42</sup>. Remyelination is therefore essential for functional recovery in both MS and EAE<sup>99,100</sup>. The proliferation, differentiation, migration and survival of oligodendrocyte progenitor cells (OPCs) required for remyelination are highly influenced by the inflammatory status of their local microenvironment. For example, cytokines released by M2 macrophages promote OPC proliferation, maturation and survival<sup>62,101</sup> while M2 macrophage depletion impairs OPC differentiation<sup>101</sup>. Disrupted M2 macrophage polarization by LCL161 may thus have

exacerbated EAE severity by blocking remyelination. DCs and neutrophils also regulate OPC function and survival providing a further mechanism for the deleterious effects of LCL161 on disease severity in EAE mice<sup>102</sup>. TNF- $\alpha$  signaling via TNFR2 stimulates OPC differentiation required for remyelination in EAE mice<sup>103</sup>. Since cIAP1/2 block necroptosis by TNFR2-mediated activation of the non-canonical NF- $\kappa$ B pathway<sup>92</sup>, LCL161-induced cIAP1/2 suppression may have inhibited remyelination by inducing OPC necroptosis. It would therefore be worthwhile to test the effects LCL161 on OPC differentiation and survival to determine if this mechanism may contribute to increased EAE severity. Future studies should also examine the relative roles cIAP1 and cIAP2 in the regulation of OPC and oligodendrocyte cell survival. The recent development of cIAP1<sup>lox/lox</sup>/cIAP2<sup>Frt/Frt</sup> mice allows the cell-specific deletion of either cIAP1 and/or cIAP2 by crossing these mice with transgenic lines that express the Cre and/or Flippase recombinase(s) under control of a cell-specific promoter<sup>20</sup>. Use of these experimental approaches would make it possible to study the relative roles played by cIAP1/2 in the survival of macrophages, DCs, neutrophils and oligodendrocytes in EAE.

#### **4.15 Conclusions**

Genetic ablation of cIAP2 has been found to increase disease severity in models of inflammatory bowel disease<sup>104,105</sup>. My study is the first to show that cIAP1/2 suppression also elevates EAE disease severity. Genetic deletion of cIAP2 or pharmacological suppression of cIAP1/2 disrupted M1 and M2 macrophage polarization and survival *in vitro*. However, it is unclear how impaired M1 and M2 macrophage polarization may have contributed to the effects of LCL161 on EAE mice. For instance, genetic ablation of

cIAP2 and suppression of cIAP1/2 with LCL161 both biased the polarization of mpBMDMs to an M1-like state. However, LCL161 treatment only elevated mRNA levels for the M1 marker CD38 with a non-significant trend toward increased Fpr2 mRNA levels and failed to increase the expression of M1 markers such as TNF- $\alpha$ , CD86, NOS2 and Gpr18, in the spinal cords of EAE mice (Figure 16). Furthermore, plasma concentration of both Th1 and Th2 cytokines as well as several chemoattractants were reduced by LCL161 in EAE mice at peak disease (Figures 18-21). These findings suggest that in the context of EAE, LCL161 treatment caused a general suppression of immune function. This was unexpected because elevated plasma pro-inflammatory cytokines levels are correlated with increased EAE severity at peak disease<sup>106</sup>. The discrepancies between my *in vitro* and *in vivo* data may therefore be explained by the reductive nature of cell culture studies that are unable to model *in vivo* events.

The regulation of cellular events responsible for autoimmune-mediate demyelination EAE are highly-complex, involving interactions between multiple immune cell subtypes, pro-inflammatory and anti-inflammatory mediators, OPCs and oligodendrocytes<sup>55</sup>. Since cIAP1/2 are ubiquitous regulators of cell survival, the effects of LCL161 on EAE mice may therefore represent the effects of cIAP1/2 suppression on many cell types. Though my studies only showed that cIAP1/2 suppression interfered with macrophage polarization and promoted their apoptotic and necrotic cell death, it is possible that other immune cell subtypes such as DCs, neutrophils and lymphocytes in EAE mice may have suffered similar fates following treatment with LCL161. The death of these cells could potentially explain the general suppression of both pro- and anti-inflammatory immune

cytokine plasma concentrations despite increased EAE disease severity. Within the spinal cord, enhanced necrosis of resident and infiltrating immune cells may have increased EAE disease severity by promoting inflammatory damage. cIAP1/2 inhibition may have also impaired the differentiation and survival of OPCs necessary for remyelination and functional recovery. Lastly, protection of oligodendrocytes by the systemic administration of leukemia inhibitory factor in a model of spinal cord injury is accompanied by the induction of cIAP2 in these cells<sup>102</sup>. Assuming that LCL161 reaches efficacious concentrations in the spinal cord following oral administration, LCL161 may therefore have increase EAE severity by inhibiting the pro-survival effects of cIAP2 on oligodendrocytes. Additional studies described in the previous sections are thus warranted to examine the effects of SMAC mimetics on the viability status of immune cells, OPCs and oligodendrocytes in EAE mice.

SMAC mimetics have shown early promise in the treatment of patients with sarcomas, carcinomas and lymphomas<sup>107,108</sup>. These compounds may be particularly useful in the management of cancers resistant to traditional chemotherapeutics<sup>109</sup>. However, my findings suggest that SMAC mimetics may exacerbate neurological deficits in patients with MS. It is therefore critical that the precise mechanisms by which SMAC mimetics worsen autoimmune-immune demyelination be established.

## REFERENCES

1. Mosser, D. M. & Edwards, J. P. Exploring the full spectrum of macrophage activation. *Nat. Rev. Immunol.* **8**, 958–969 (2008).
2. Sica, A. & Mantovani, A. Macrophage plasticity and polarization: in vivo veritas. *J. Clin. Invest.* **122**, 787–795 (2012).
3. Liu, G. & Yang, H. Modulation of macrophage activation and programming in immunity. *J. Cell. Physiol.* **228**, 502–512 (2013).
4. Sica, A., Schioppa, T., Mantovani, A. & Allavena, P. Tumour-associated macrophages are a distinct M2 polarised population promoting tumour progression: Potential targets of anti-cancer therapy. *Eur. J. Cancer* **42**, 717–727 (2006).
5. Qian, B.-Z. & Pollard, J. W. Macrophage Diversity Enhances Tumor Progression and Metastasis. *Cell* **141**, 39–51 (2010).
6. Martinez, F. O. & Gordon, S. The M1 and M2 paradigm of macrophage activation: time for reassessment. *F1000Prime Rep.* **6**, 6–13 (2014).
7. Murray, P. J. *et al.* Macrophage Activation and Polarization: Nomenclature and Experimental Guidelines. *Immunity* **41**, 14–20 (2014).
8. Fleetwood, A. J., Dinh, H., Cook, A. D., Hertzog, P. J. & Hamilton, J. A. GM-CSF- and M-CSF-dependent macrophage phenotypes display differential dependence on Type I interferon signaling. *J. Leukoc. Biol.* **86**, 411–421 (2009).
9. Josephs, D. H., Bax, H. J. & Karagiannis, S. N. Tumour-associated macrophage polarisation and re-education with immunotherapy. *Front. Biosci. (Elite Ed)*. **7**, 293–308 (2015).
10. Kobayashi, K. *et al.* Minocycline selectively inhibits M1 polarization of microglia. *Cell Death Dis.* **4**, e525 (2013).
11. Jablonski, K. A. *et al.* Novel Markers to Delineate Murine M1 and M2 Macrophages. *PLoS One* **10**, e0145342 (2015).
12. LaCasse, E. C. *et al.* IAP-targeted therapies for cancer. *Oncogene* **27**, 6252–6275 (2008).
13. Crook, N. E., Clem, R. J. & Miller, L. K. An apoptosis-inhibiting baculovirus gene with a zinc finger-like motif. *J. Virol.* **67**, 2168–2174 (1993).

14. Liston, P. *et al.* Suppression of apoptosis in mammalian cells by NAIP and a related family of IAP genes. *Nature* **379**, 349–353 (1996).
15. Ambrosini, G., Adida, C. & Altieri, D. C. A novel anti-apoptosis gene, survivin, expressed in cancer and lymphoma. *Nat. Med.* **3**, 917–921 (1997).
16. Richter, B. W. *et al.* Molecular cloning of ILP-2, a novel member of the inhibitor of apoptosis protein family. *Mol. Cell. Biol.* **21**, 4292–301 (2001).
17. Hauser, H. P., Bardroff, M., Pyrowolakis, G. & Jentsch, S. A giant ubiquitin-conjugating enzyme related to IAP apoptosis inhibitors. *J. Cell Biol.* **141**, 1415–1422 (1998).
18. Robertson, G. S., Crocker, S. J., Nicholson, D. W. & Schulz, J. B. Neuroprotection by the inhibition of apoptosis. *Brain Pathol.* **10**, 283–292 (2000).
19. Broemer, M. & Meier, P. Ubiquitin-mediated regulation of apoptosis. *Trends Cell Biol.* **19**, 130–140 (2009).
20. Silke, J. & Vaux, D. L. IAP gene deletion and conditional knockout models. *Semin. Cell Dev. Biol.* **39**, 97–105 (2015).
21. Verhagen, A. M., Coulson, E. J. & Vaux, D. L. Inhibitor of apoptosis proteins and their relatives: IAPs and other BIRPs. *Genome Biol.* **2**, REVIEWS3009 (2001).
22. Mahoney, D. J. *et al.* Both cIAP1 and cIAP2 regulate TNF $\alpha$ -mediated NF- $\kappa$ B activation. *Proc. Natl. Acad. Sci. U. S. A.* **105**, 11778–11783 (2008).
23. Conte, D. *et al.* Inhibitor of Apoptosis Protein cIAP2 Is Essential for Lipopolysaccharide-Induced Macrophage Survival Inhibitor of Apoptosis Protein cIAP2 Is Essential for Lipopolysaccharide-Induced Macrophage Survival. *Mol. Cell. Biol.* **26**, 699 (2006).
24. Martorell, L. *et al.* The hypoxia-inducible factor 1/NOR-1 axis regulates the survival response of endothelial cells to hypoxia. *Mol. Cell. Biol.* **29**, 5828–542 (2009).
25. Fulda, S. Smac mimetics as IAP antagonists. *Semin. Cell Dev. Biol.* **39**, 132–138 (2015).
26. Martinez-Ruiz, G., Maldonado, V., Ceballos-Cancino, G., Grajeda, J. P. R. & Melendez-Zajgla, J. Role of Smac/DIABLO in cancer progression. *J. Exp. Clin. Cancer Res.* **27**, 48 (2008).
27. van Loo, G. *et al.* The role of mitochondrial factors in apoptosis: a Russian roulette with more than one bullet. *Cell Death Differ.* **9**, 1031–1042 (2002).

28. Hunter, A. M., LaCasse, E. C. & Korneluk, R. G. The inhibitors of apoptosis (IAPs) as cancer targets. *Apoptosis* **12**, 1543–1568 (2007).
29. Liston, P., Lefebvre, C., Fong, W. G., Xuan, J. Y. & Korneluk, R. G. Genomic characterization of the mouse inhibitor of apoptosis protein 1 and 2 genes. *Genomics* **46**, 495–503 (1997).
30. Moulin, M. *et al.* IAPs limit activation of RIP kinases by TNF receptor 1 during development. *EMBO J.* **31**, 1679–1691 (2012).
31. Wong, W. W.-L. *et al.* cIAPs and XIAP regulate myelopoiesis through cytokine production in an RIPK1- and RIPK3-dependent manner. *Blood* **123**, 2562–2572 (2014).
32. McComb, S. *et al.* cIAP1 and cIAP2 limit macrophage necroptosis by inhibiting Rip1 and Rip3 activation. *Cell Death Differ.* **19**, 1791–1801 (2012).
33. Beug, S. T. *et al.* Smac mimetics and innate immune stimuli synergize to promote tumor death. *Nat. Biotechnol.* **32**, 182–190 (2014).
34. Billack, B. Macrophage activation: role of toll-like receptors, nitric oxide, and nuclear factor kappa B. *Am. J. Pharm. Educ.* **70**, 102 (2006).
35. Liu, H. *et al.* TNF- $\alpha$ -Induced Apoptosis of Macrophages Following Inhibition of NF- $\kappa$ B: A Central Role for Disruption of Mitochondria. *J. Immunol.* **172**, 1907–1915 (2004).
36. Fulda, S. Targeting inhibitor of apoptosis proteins for cancer therapy: A double-edge sword? *J. Clin. Oncol.* **32**, 3190–3191 (2014).
37. Müller-Sienerth, N. *et al.* SMAC Mimetic BV6 Induces Cell Death in Monocytes and Maturation of Monocyte-Derived Dendritic Cells. *PLoS One* **6**, e21556 (2011).
38. Bai, L., Smith, D. C. & Wang, S. Small-molecule SMAC mimetics as new cancer therapeutics. *Pharmacol. Ther.* **144**, 82–95 (2014).
39. Probst, B. L. *et al.* Smac mimetics increase cancer cell response to chemotherapeutics in a TNF- $\alpha$ -dependent manner. *Cell Death Differ* **17**, 1645–1654 (2010).
40. Zarnegar, B. J. *et al.* Noncanonical NF- $\kappa$ B activation requires coordinated assembly of a regulatory complex of the adaptors cIAP1, cIAP2, TRAF2 and TRAF3 and the kinase NIK. *Nat. Immunol.* **9**, 1371–1378 (2008).

41. Tchoghandjian, A., Jennewein, C., Eckhardt, I., Rajalingam, K. & Fulda, S. Identification of non-canonical NF- $\kappa$ B signaling as a critical mediator of Smac mimetic-stimulated migration and invasion of glioblastoma cells. *Cell Death Dis.* **4**, (2013).
42. Compston, A. & Coles, A. Multiple sclerosis. *Lancet* **359**, 1221–1231 (2002).
43. Franklin, R. J. M. Why does remyelination fail in multiple sclerosis? *Nat. Rev. Neurosci.* **3**, 705–714 (2002).
44. Plemel, J. R., Liu, W.-Q. & Yong, V. W. Remyelination therapies: a new direction and challenge in multiple sclerosis. *Nat. Rev. Drug Discov.* (2017).
45. Lassmann, H., Brück, W. & Lucchinetti, C. F. The Immunopathology of Multiple Sclerosis: An Overview. *Brain Pathol.* **17**, 210–218 (2007).
46. Qi, X., Lewin, A. S., Sun, L., Hauswirth, W. W. & Guy, J. Mitochondrial protein nitration primes neurodegeneration in experimental autoimmune encephalomyelitis. *J. Biol. Chem.* **281**, 31950–31962 (2006).
47. Moore, C. S. *et al.* Direct and indirect effects of immune and central nervous system-resident cells on human oligodendrocyte progenitor cell differentiation. *J. Immunol.* **194**, 761–772 (2015).
48. Rawji, K. S. & Yong, V. W. The benefits and detriments of macrophages/microglia in models of multiple sclerosis. *Clin. Dev. Immunol.* **2013**, 948976 (2013).
49. Rawji, K. S., Mishra, M. K. & Yong, V. W. Regenerative Capacity of Macrophages for Remyelination. *Front. cell Dev. Biol.* **4**, 47 (2016).
50. Constantinescu, C. S., Farooqi, N., O'Brien, K. & Gran, B. Experimental autoimmune encephalomyelitis (EAE) as a model for multiple sclerosis (MS). *Br. J. Pharmacol.* **164**, 1079–1106 (2011).
51. Steinman, L. & Zamvil, S. S. How to successfully apply animal studies in experimental allergic encephalomyelitis to research on multiple sclerosis. *Ann. Neurol.* **60**, 12–21 (2006).
52. Miller, S. D., Karpus, W. J. & Davidson, T. S. Experimental Autoimmune Encephalomyelitis in the Mouse. *Curr. Protoc. Immunol.* 1–26 (2007).
53. Hemmer, B., Kerschensteiner, M. & Korn, T. Role of the innate and adaptive immune responses in the course of multiple sclerosis. *Lancet Neurol.* **14**, 406–419 (2015).

54. Mikita, J. *et al.* Altered M1/M2 activation patterns of monocytes in severe relapsing experimental rat model of multiple sclerosis. Amelioration of clinical status by M2 activated monocyte administration. *Mult. Scler.* **17**, 2–15 (2011).
55. Bogie, J. F. J., Stinissen, P. & Hendriks, J. J. A. Macrophage subsets and microglia in multiple sclerosis. *Acta Neuropathol.* **128**, 191–213 (2014).
56. Kroner, A. *et al.* TNF and Increased Intracellular Iron Alter Macrophage Polarization to a Detrimental M1 Phenotype in the Injured Spinal Cord. *Neuron* **83**, 1098–1116 (2014).
57. Duffy, S. S., Lees, J. G. & Moalem-Taylor, G. The Contribution of Immune and Glial Cell Types in Experimental Autoimmune Encephalomyelitis and Multiple Sclerosis. *Mult. Scler. Int.* **2014**, 1–17 (2014).
58. Greenhalgh, A. D. & David, S. Differences in the Phagocytic Response of Microglia and Peripheral Macrophages after Spinal Cord Injury and Its Effects on Cell Death. *J. Neurosci.* **34**, (2014).
59. Liu, C. *et al.* Targeting the Shift from M1 to M2 Macrophages in Experimental Autoimmune Encephalomyelitis Mice Treated with Fasudil. *PLoS One* **8**, (2013).
60. Brosnan, C. F., Bornstein, M. B. & Bloom, B. R. The effects of macrophage depletion on the clinical and pathologic expression of experimental allergic encephalomyelitis. *J. Immunol.* **126**, 614–620 (1981).
61. McQualter, J. L. *et al.* Granulocyte macrophage colony-stimulating factor: a new putative therapeutic target in multiple sclerosis. *J. Exp. Med.* **194**, 873–882 (2001).
62. Liu, C. Y. *et al.* Fasudil mediates cell therapy of EAE by immunomodulating encephalomyelitic T cells and macrophages. *Eur. J. Immunol.* **45**, 142–152 (2015).
63. Tseng, P.-H. *et al.* Different modes of ubiquitination of the adaptor TRAF3 selectively activate the expression of type I interferons and proinflammatory cytokines. *Nat. Immunol.* **11**, 70–75 (2010).
64. Benveniste, E. N. Role of macrophages / microglia in multiple sclerosis and experimental allergic encephalomyelitis. *J. Clin. Invest.* **75**, 165–173 (1997).
65. Labbé, K., McIntire, C. R., Doiron, K., Leblanc, P. M. & Saleh, M. Cellular Inhibitors of Apoptosis Proteins cIAP1 and cIAP2 Are Required for Efficient Caspase-1 Activation by the Inflammasome. *Immunity* **35**, 897–907 (2011).
66. Bustin, S. A. *et al.* The MIQE Guidelines: Minimum Information for Publication of Quantitative Real-Time PCR Experiments. *Clin. Chem.* **55**, 611–622 (2009).

67. Fiander, M. D. J., Stifani, N., Nichols, M., Akay, T. & Robertson, G. S. Kinematic gait parameters are highly sensitive measures of motor deficits and spinal cord injury in mice subjected to experimental autoimmune encephalomyelitis. *Behav. Brain Res.* **317**, 95–108 (2017).
68. Yu, Y.-R. A. *et al.* A Protocol for the Comprehensive Flow Cytometric Analysis of Immune Cells in Normal and Inflamed Murine Non-Lymphoid Tissues. *PLoS One* **11**, e0150606 (2016).
69. Gately, M. K. *et al.* The interleukin-12/interleukin-12-receptor system: role in normal and pathologic immune responses. *Annu. Rev. Immunol.* **16**, 495–521 (1998).
70. Misharin, A. V. V *et al.* Nonclassical Ly6C<sup>−</sup> Monocytes Drive the Development of Inflammatory Arthritis in Mice. *Cell Rep.* **9**, 591–604 (2014).
71. Ginhoux, F. & Jung, S. Monocytes and macrophages: developmental pathways and tissue homeostasis TL - 14. *Nat. Rev. Immunol.* **14**, 392–404 (2014).
72. Mishra, M. K. & Yong, V. W. Myeloid cells - targets of medication in multiple sclerosis. *Nat. Rev. Neurol.* **12**, 539–551 (2016).
73. Hartwig, T. *et al.* The TRAIL-Induced Cancer Secretome Promotes a Tumor-Supportive Immune Microenvironment via CCR2. *Mol. Cell* **65**, 730–742.e5 (2017).
74. Hebb, A. L. O., Moore, C. S., Bhan, V. & Robertson, G. S. Targeting apoptosis to treat multiple sclerosis. *Curr. Drug Discov. Technol.* **5**, 75–77 (2008).
75. Warford, J. & Robertson, G. S. New methods for multiple sclerosis drug discovery. *Expert Opin. Drug Discov.* **6**, 689–699 (2011).
76. Hasegawa, T. *et al.* Expression of the inhibitor of apoptosis (IAP) family members in human neutrophils: up-regulation of cIAP2 by granulocyte colony-stimulating factor and overexpression of cIAP2 in chronic neutrophilic leukemia. *Blood* **101**, 1164–1171 (2003).
77. Di Stefano, A. B. *et al.* Survivin is regulated by interleukin-4 in colon cancer stem cells. *J. Cell. Physiol.* **225**, 555–561 (2010).
78. Geissmann, F., Manz, M. G., Jung, S., Sieweke, M. H. & Ley, K. Development of monocytes, macrophages and dendritic cells. *Science (80-. )*. **327**, 656–661 (2010).
79. Merad, M., Sathe, P., Helft, J., Miller, J. & Mortha, A. The Dendritic Cell Lineage: Ontogeny and Function of Dendritic Cells and Their Subsets in the Steady State and the Inflamed Setting. *Annu. Rev. Immunol.* **31**, 563–604 (2013).

80. Worbs, T., Hammerschmidt, S. I. & Förster, R. Dendritic cell migration in health and disease. *Nat. Rev. Immunol.* **17**, 30–48 (2016).
81. Park, Y., Lee, S. W. & Sung, Y. C. Cutting Edge: CpG DNA inhibits dendritic cell apoptosis by up-regulating cellular inhibitor of apoptosis proteins through the phosphatidylinositol-3'-OH kinase pathway. *J. Immunol.* **168**, 5–8 (2002).
82. Lecis, D. *et al.* Smac mimetics induce inflammation and necrotic tumour cell death by modulating macrophage activity. *Cell Death Dis.* **4**, e920 (2013).
83. Pinzon-Ortiz, M. *et al.* Abstract 2343: The immune modulatory roles of IAP inhibitor, LCL161, and its connection to immune-checkpoint molecules. *Cancer Res.* **76**, (2016).
84. Gandhi, R., Laroni, a & Weiner, H. Role of the innate immune system in the pathogenesis of multiple sclerosis. *J neuroimmunol* **221**, 7–14 (2010).
85. Dougan, M. *et al.* IAP inhibitors enhance co-stimulation to promote tumor immunity. *J. Exp. Med.* **207**, 2195–2206 (2010).
86. Wang, N., Liang, H. & Zen, K. Molecular mechanisms that influence the macrophage M1-M2 polarization balance. *Front. Immunol.* **5**, 1–9 (2014).
87. Li, Q. & Verma, I. M. NF- $\kappa$ B regulation in the immune system. *Nat. Rev. Immunol.* **2**, 725–734 (2002).
88. Bonizzi, G. & Karin, M. The two NF- $\kappa$ B activation pathways and their role in innate and adaptive immunity. *Trends Immunol.* **25**, 280–288 (2004).
89. Vasilikos, L., Spilgies, L. M., Knop, J. & Wong, W. W.-L. Regulating the balance between necroptosis, apoptosis and inflammation by inhibitors of apoptosis proteins. *Immunol. Cell Biol.* **95**, 160–165 (2017).
90. Wajant, H., Pfizenmaier, K. & Scheurich, P. Tumor necrosis factor signaling. *Cell Death Differ.* **10**, 45–65 (2003).
91. Rauert, H. *et al.* Membrane Tumor Necrosis Factor (TNF) Induces p100 Processing via TNF Receptor-2 (TNFR2). *J. Biol. Chem.* **285**, 7394–7404 (2010).
92. Siegmund, D., Kums, J., Ehrenschwender, M. & Wajant, H. Activation of TNFR2 sensitizes macrophages for TNFR1-mediated necroptosis. *Cell Death Dis.* **7**, e2375 (2016).
93. Degterev, A. *et al.* Chemical inhibitor of nonapoptotic cell death with therapeutic potential for ischemic brain injury. *Nat. Chem. Biol.* **1**, 112–119 (2005).

94. Banchereau, J. *et al.* Immunobiology of Dendritic Cells. *Annu. Rev. Immunol.* **18**, 767–811 (2000).
95. Rumble, J. M. *et al.* Neutrophil-related factors as biomarkers in EAE and MS. *J. Exp. Med.* **212**, 23–35 (2015).
96. Wu, F., Cao, W., Yang, Y. & Liu, A. Extensive infiltration of neutrophils in the acute phase of experimental autoimmune encephalomyelitis in C57BL/6 mice. *Histochem. Cell Biol.* **133**, 313–322 (2010).
97. O’Neill, A. J. *et al.* Gene Expression Profile of Inflammatory Neutrophils: Alterations in the Inhibitors of Apoptosis Proteins During Spontaneous and Delayed Apoptosis. *Shock* **21**, 512–518 (2004).
98. Gabelloni, M. L., Trevani, A. S., Sabatté, J. & Geffner, J. Mechanisms regulating neutrophil survival and cell death. *Semin. Immunopathol.* **35**, 423–437 (2013).
99. Franklin, R. J. M., Ffrench-Constant, C., Edgar, J. M. & Smith, K. J. Neuroprotection and repair in multiple sclerosis. *Nat. Rev. Neurol.* **8**, 624–634 (2012).
100. Franklin, R. J. M. & Ffrench-Constant, C. Remyelination in the CNS: from biology to therapy. *Nat. Rev. Neurosci.* **9**, 839–55 (2008).
101. Miron, V. E. *et al.* M2 microglia and macrophages drive oligodendrocyte differentiation during CNS remyelination. *Nat. Neurosci.* **16**, 1211–1218 (2013).
102. Azari, M. F. *et al.* Leukemia inhibitory factor arrests oligodendrocyte death and demyelination in spinal cord injury. *J. Neuropathol. Exp. Neurol.* **65**, 914–929 (2006).
103. Madsen, P. M. *et al.* Oligodendroglial TNFR2 Mediates Membrane TNF-Dependent Repair in Experimental Autoimmune Encephalomyelitis by Promoting Oligodendrocyte Differentiation and Remyelination. *J. Neurosci.* **36**, 5128–5143 (2016).
104. Pedersen, J., LaCasse, E. C., Seidelin, J. B., Coskun, M. & Nielsen, O. H. Inhibitors of apoptosis (IAPs) regulate intestinal immunity and inflammatory bowel disease (IBD) inflammation. *Trends Mol. Med.* **20**, 652–665 (2014).
105. Dagenais, M. *et al.* A critical role for cellular inhibitor of protein 2 (cIAP2) in colitis-associated colorectal cancer and intestinal homeostasis mediated by the inflammasome and survival pathways. *Mucosal Immunol.* **9**, 146–158 (2016).

106. Warford, J. *et al.* The flavonoid-enriched fraction AF4 suppresses neuroinflammation and promotes restorative gene expression in a mouse model of experimental autoimmune encephalomyelitis. *J. Neuroimmunol.* **268**, 71–83 (2014).
107. Amaravadi, R. K. *et al.* A Phase I Study of the SMAC-Mimetic Birinapant in Adults with Refractory Solid Tumors or Lymphoma. *Mol. Cancer Ther.* **14**, 2569–2575 (2015).
108. Noonan, A. M. *et al.* Pharmacodynamic markers and clinical results from the phase 2 study of the SMAC mimetic birinapant in women with relapsed platinum-resistant or -refractory epithelial ovarian cancer. *Cancer* **122**, 588–597 (2016).
109. Mizobuchi, K. & Tanizaki, H. On estimation of almost ideal demand system using moving blocks bootstrap and pairs bootstrap methods. *Empir. Econ.* **47**, 1221–1250 (2014).